Molecular Mechanisms of Tumor Promoting Breast Fibroblasts

A dissertation

submitted by

Jenny Ann Rudnick

In partial fulfillment of the requirements

for the degree of

Doctor of Philosophy

in

Cell, Molecular & Developmental Biology

TUFTS UNIVERSITY

Sackler School of Graduate Biomedical Sciences

September, 2011

Advisor: Dr. Charlotte Kuperwasser

List of Abbreviations

Ago2: argonaute-2

AML: acute myeloid leukemia

BCSCs: breast cancer stem-like cells ($CD44^+/CD24^-/EpCAM^+$)

BMI: body mass index

BMPRII: bone morphogenetic protein receptor type II

CAF: cancer associated fibroblast

CK: cytokeratin

CM: conditioned medium

CSCs: cancer stem cells

Cox-2: cyclooxygenase-2

E10: embryonic day 10

ECM: extracellular matrix

ELISA: enzyme-linked immunosorbent assay

EMT: epithelial-mesenchymal transition

EPCs: endothelial progenitor cells

ERα: estrogen receptor alpha

EtOH: ethanol

FACS: fluorescence activated cell sorting

FAP: fibroblast activation protein

FGF10: fibroblast growth factor 10

FGFR2b: fibroblast growth factor receptor 2b

FISH: fluorescence in situ hybridization

FSH: follicle stimulating hormone

FSP: fibroblast surface protein

HMECs: human mammary epithelial cells ($CD49f^{+}/EpCAM^{+}$)

HSC: hematopoeitic stem cell

HRT: hormone replacement therapy

IF: immunofluorescence

IHC: immunohistochemistry

IL-1β: interleukin 1 beta

IL-6: interleukin 6

IPF: idiopathic pulmonary fibrosis

IPH: idiopathic pulmonary hypertension

IRB: institutional review board

kDa: kilodalton

LH: luteinizing hormone

Ma-CFCs: mammary colony forming cells ($CD24^{hi}/CD49f^{lo}$)

MaSCs: mouse mammary stem cells ($CD29^{+}/CD24^{+}$ and/or $CD24^{med}/CD49f^{hi}$)

MCP-1: monocyte chemoattractant protein 1

MECs: mouse mammary epithelial cells

miRs: microRNAs

MMPs: matrix metalloproteinases

MMTV: mouse mammary tumor virus

MRI: magnetic resonance imaging

MRU: mammary repopulating unit

MSCs: mesenchymal stem cells

Mass Spec: liquid chromatography tandem mass spectrometry

NFκB: nuclear factor kappa B

NOD/SCID: non-obese diabetic severe combined immunodeficient

NSAIDs: non-steroidal anti-inflammatory drugs

Oligo: oligonucleotide

PACT: protein kinase R- activating protein

PDCD4: programmed cell death gene 4

PGE2: prostaglandin E2

P4H: prolyl-4-hydroxylase

PI-MECs: parity induced mammary epithelial cells

PR: progesterone receptor

Pre-miR: precursor microRNA

PRF-DMEM: phenol red free Dulbecco's Modified Eagle's Medium

Pri-miR: primary microRNA

PTEN: phosphatase and tensin homolog

PyMT: polyoma middle T antigen

qRT-PCR: quantitative reverse transcription polymerase chain reaction

RHA: RNA helicase A

RMFs: reduction mammoplasty fibroblasts

RISC: RNA induced silencing complex

SAGE: serial analysis of gene expression

SATB2: special AT-rich sequence binding protein

SDF1α: stromal derived factor 1 alpha

SEM: standard error of the mean

SMARCD1: SWI/SNF related, matrix associated, actin dependent regulator of chromatin, subfamily d, member-1

αSMA: alpha smooth muscle actin

SNP: single nucleotide polymorphism

TAM: tumor associated macrophage

TDLU: terminal ductal lobular unit

TEB: terminal end bud

TGFβ: transforming growth factor beta

TIMP3: tissue inhibitor of metalloproteinases 3

TNFα: tumor necrosis factor alpha

TRBP: TAR RNA binding protein

UTR: untranslated region

VSMCs: vascular smooth muscle cells

WAP: whey acidic protein

WT: wildtype

WHR: waist hip ratio

Abstract

Breast cancer is a heterogeneous, multi-factorial disease of aberrant breast development whose etiology relies upon several microenvironmental changes within the tissue. As cancerous cells accumulate within the breast epithelium, fibroblasts within the connective tissue stroma become activated, thereby inducing inflammation, matrix remodeling, and bone marrow derived cell recruitment, which collectively promote tumor growth. Fibroblasts within breast tumor tissues are heterogeneous, and cell surface markers or functional characteristics of the most tumor promoting fibroblasts within the cell population remain ill-defined. Moreover, the molecular mechanisms governing the gene expression of tumor promoting fibroblasts, in comparison to fibroblasts from disease free breast tissues, remain largely unknown. Here, I demonstrate that tumor promoting fibroblasts are distinguished from those that are non-tumor promoting based on their high secretion of the pro-inflammatory hormone prostaglandin E2 (PGE2) and their response to PGE2 signaling. PGE2 signaling enhances fibroblast secretion of interleukin 6 (IL-6), which is required for the expansion of breast cancer stem-like cells (BCSCs). Secondly, I demonstrate that fibroblasts isolated from stroma of breast carcinomas, referred to as cancer associated fibroblasts (CAFs), are distinguished from fibroblasts isolated from disease free reduction mammoplasty tissues (RMFs) based on their ability to induce the expression of mature microRNA21 (miR21) in response to TGFβ. Collectively, these data may provide foundations for discovery of adjuvant breast

cancer therapies targeting tumor associated stroma and insight into patients who may benefit best from this additional treatment option.

Personal Acknowledgements

This thesis is written with utmost gratitude for Charlotte Kuperwasser: thank you for your teachings, guidance, and unwaivering faith in me. You are inspirational, brilliant, considerate and modest no matter the circumstance. Thank you for showing me these qualities are attainable with success. Thank you for making my dream come true.

I would not have the opportunity to write this thesis if it weren't for my generous, supportive, proud parents: Barbara and Bob Rudnick. Thank you for encouraging me, validating me and assisting me every step of the way through this long journey. My dreams have come true because of your love and support.

Thank you Christopher Rudnick for growing up to be the most wonderful, considerate and thoughtful man I have ever known (aside from Dad!). Thank you for always supporting me. You are an amazing "little" brother. I wish you all the best with your future endeavors.

This work would not be possible without the generous help and support from all past and present members of the Kuperwasser laboratory. We make a wonderful Team. Thank you all for becoming a surrogate family over the last few years.

Thank you to the tissue culture room, for your ability to reveal even the most repressed secrets!

And to all the wonderful friends and colleagues I have met along the way:

"What a long, strange trip it's been!" Come visit me in San Francisco!

Dedication

This thesis is dedicated to my late grandfather, John Corssino, who gave me the gift of education and believed I could do great things with it.

Table of Contents

List of Figures

List of Tables

List of Supplemental Figures

List of Supplemental Tables

Molecular Mechanisms of Tumor Promoting Breast Fibroblasts

A dissertation

submitted by

Jenny Ann Rudnick

In partial fulfillment of the requirements

for the degree of

Doctor of Philosophy

in

Cell, Molecular & Developmental Biology

TUFTS UNIVERSITY

Sackler School of Graduate Biomedical Sciences

September, 2011

Advisor: Dr. Charlotte Kuperwasser

CHAPTER I:

Introduction

1.1 Anatomy of the human breast

The breast is organized into 15-25 independent glandular units called breast lobes, each consisting of a tubulo-acinar gland. The lobes are embedded in both connective and adipose tissue and subdivided by collagenous septa. The lobes are arranged radially around the nipple. Each lobe contains a single large duct, the lactiferous duct, which drains each lobe via a separate opening on the surface of the nipple. The nipple contains bands of smooth muscle oriented parallel to the lactiferous ducts and circularly near the nipple base; contraction of this smooth muscle causes nipple erection.

Each breast lobe is divided into a variable number of breast lobules, each lobule consisting of a system of ducts. Large numbers of secretory alveoli will develop from these ducts during pregnancy. The lobules are separated by dense collagenous interlobular tissue; the ducts are supported by a less collagenous and more adipose rich highly vascular intralobular tissue (H. George Burkitt, 1993).

The duct system is composed of an epithelial bilayer containing two distinct types of mammary epithelial cells. These cells can be distinguished histologically based on their position within the duct and immunohistochemically based on the differential proteins they express. Luminal epithelial cells face the lumen of the ducts and express cytokeratins (CK) 8, 18, and 19. Myoepithelial cells sit basally to luminal epithelial cells and reside on a basement membrane forming a barrier

between the mammary parenchyma and the stroma (Fig. 1.1A,B); they express CK14, CK5, CALLA/CD10 and smooth muscle alpha actin (αSMA).

1.2 Development of the human breast

Breast tissue develops in a distinct fashion compared to other human vertebrate organs. Unlike most vertebrate organs that are patterned during embryogenesis and fully developed before birth, the breast undergoes the majority of its development post-natally and throughout the lifetime of the female. The onset of breast development occurs when the embryo measures 4.5 to 6 mm; newly specified breast epithelial cells become indented at the epithelial-stromal border, sprouting and separating into 10-15 branches of epithelial ducts that open separately onto the epidermal surface at the nipple. Development of the breast occurs isometrically with the rest of the body until the onset of puberty. With the surge of ovarian and pituitary hormones at puberty, the networks of ducts leading from the nipple grow and divide into bundles of primary and secondary ducts, terminating with end buds (Anderson and Clarke, 2004; Wiseman and Werb, 2002).

The end buds are the sites of active breast epithelial cell proliferation. Continuous branching leads to the formation of increasingly smaller ducts and ductules. The terminal ductules eventually give rise to terminal ductal lobulo-aveolar units (TDLUs), which are the functional and principle milk-producing units of the breast (Fig. 1.1C). These TDLUs initially exist as alveolar buds that mature upon menarche due to hormonal changes within the woman's menstrual cycle,

A

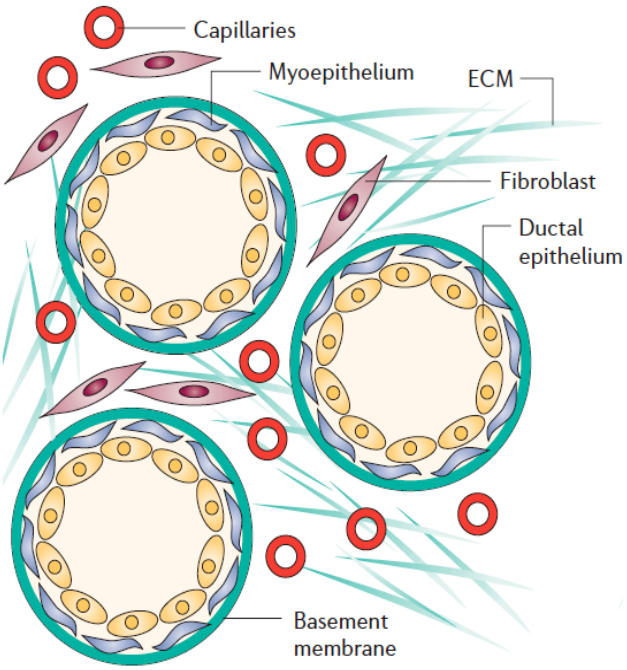
Capillaries
Myoepithelium
ECM
Fibroblast
Ductal epithelium
Basement membrane

B

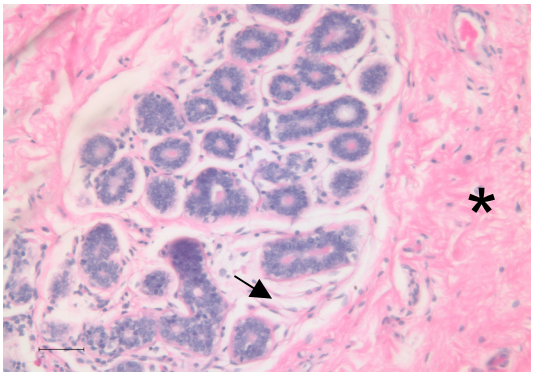
*

C

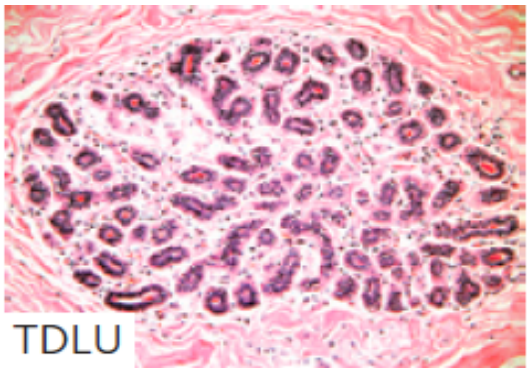
TDLU

Figure 1.1: Cell types within the human breast.

(A) Schematic of a cross section of a duct, showing luminal cells facing the ductal lumen and myoepithelial cells resting on a basement membrane. Adipocytes are also present but are not pictured here. From Kalluri & Zeisberg, *Nat Rev Cancer*, 2007. **(B)** H&E staining of the human breast, showing cross sections of ducts within an adipose and fibrous stroma (arrow) embedded in a dense ECM (*). Scale bar, 50 μm. Histology performed by Tufts Medical Center Histology Core. **(C)** H&E staining of a terminal ductal lobular unit (TDLU), the functional unit of the breast, showing a bilayered epithelium. From Vargo-Gogola and Rosen, *Nat Rev Cancer*, 2007.

and are then referred to as more highly developed acini or alveoli (Russo and Russo, 2004).

The human menstrual cycle begins with the follicular phase, characterized by follicle stimulating hormone (FSH) induced maturation of ovarian follicles and high estrogen secretion. The luteinizing hormone (LH) surge at mid cycle triggers release of the egg whereas the remnant follicle will become the corpus luteum and secrete increasing amounts of progesterone, characteristic of the post ovulatory, luteal phase of the cycle. In the adult, non-pregnant, non-lactating breast, epithelial proliferation is maximal during this time, when estrogen and progesterone are being secreted by the corpus luteum; these hormones drive ductal elongation and side branching, respectively (Brisken and Duss, 2007; Clarke, 2006). Also during the luteal phase of the menstrual cycle, the TDLUs develop into secretory sacs known as alveoli, which open into the intra-lobular duct. The TDLUs become more elaborate in terms of the number of alveoli they contain with each successive ovulatory cycle (Clarke, 2006; Labarge et al., 2007).

Given the essential roles of estrogen and progesterone in breast epithelial cell proliferation, it is surprising to learn that proliferating cells in the normal human breast do not contain estrogen receptor alpha (ERα) nor progresterone receptor (PR), ligand dependent transcription factors that mediate the signaling responses driven by these hormones. Elegant studies by Brisken and colleagues have demonstrated that paracrine mechanisms are responsible for the roles of

estrogen and progesterone in orchestrating breast epithelial cell proliferation and morphogenesis (Brisken et al., 1998; Mallepell et al., 2006).

Breast development achieves full maturity and function during pregnancy and lactation. The full development of the TDLUs is accelerated during pregnancy due to the secretion of progesterone and the pituitary hormone prolactin. During this time, the breast lobules expand in terms of the number of epithelial cells and alveoli they contain in preparation for lactation. Progesterone withdrawal at this stage prepares the breast epithelium for lactation. The mammary lobules are enlarged and the alveoli have a dilated lumen. Prolactin drives the expression of milk-producing genes; milk is synthesized and then released into the mammary alveoli and ductal system. As long as milk is removed regularly within a 48 hour period from the gland, the alveolar cells will continually make milk (Russo and Russo, 2004). At the termination of lactation, the lobules involute to resemble those present in the non-pregnant gland.

1.3 Development of the mouse mammary gland

Mouse mammary gland development is dependent upon epithelial-mesenchymal crosstalk. Development commences at embryonic day 10 (E10) to birth at around E19. Visible placodes arrive from a lateral ectodermal thickening, called the milk line, around E11. These placodes are the first specification of mammary cell fate; mice have 5 pairs of placodes to initiate the development of 5 sets of mammary glands. Fibroblast growth factor-10 (FGF10) secretion by the underlying mesenchyme is essential for placode formation, as embryos null for

FGF10 or its receptor, FGF receptor 2b (FGFR2b), lack all mammary placodes except placode 4 (Mailleux et al., 2002). Thus, the first stages of mammary gland development require mesenchymal cues.

During E12 and E13, the placodes increase in size and invaginate the underlying dermis to form small buds that are connected to the epidermis by a narrow stalk. The primary mammary mesenchyme surrounds these immature mammary buds. The epithelial cells within the buds begin to proliferate and elongate at the tip, pushing through a dense mesenchymal layer towards deeper layers of dermal mesenchyme. This will eventually give rise to the mammary fat pad. At the leading tips of the newly formed ducts, further proliferation and bifurcation results in a primitive mammary tree present in the neonate (Robinson, 2007). This rudimentary tree remains quiescent until approximately 3 weeks of age. During these early stages of development, the stromal compartment of the gland is filled with large adipocytes, interspersed fibroblasts, blood vessels and lymphatic vessels (Fig. 1.2A).

Approximately 3 weeks of age marks the onset of ovarian hormone secretion. At this time, the gland undergoes two major phases of growth: ductal growth, initiated at puberty, and alveolar differentiation, initiated at pregnancy. During ductal growth, the terminal end buds (TEBs) appear (Fig. 1.2B); these are the sites of ductal elongation and branching and represent the site of highest proliferation in the gland. The outer layer of cells remains undifferentiated (cap cells) and have bipotent cell fate (both luminal and myoepithelial cells). During this ductal growth phase, proliferation and cell migration of the cells at the edge

of the TEB causes invasion into the fat pad and elongation of the duct. As cells differentiate at the trailing edge the myoepithelial cells lay down basement membrane, and the stroma is formed by fibroblasts surrounding the ducts. When the TEBs reach the edge of the fat pad, they regress to form terminal ducts. Established ducts are hollowed to form a bilayer epithelium of luminal epithelial cells surrounded by basally-oriented myoepithelial cells resting on a basement membrane and encased in stroma. This continues until 10-12 weeks of age, when the majority of the TEBs have given rise to terminal ducts.

With the onset of the estrous cycle at puberty, the gland begins to branch and form alveolar buds. Similar to human breast development, these alveolar buds differentiate completely only during pregnancy in order to secrete milk for lactation (Fig. 1.2C). Initial pregnancy induced mammary growth involves massive proliferation of ductal branches and formation of alveolar buds. During the second half of pregnancy, lobulo-alveolar development occurs: the immature alveolar buds undergo full differentiation into individual alveoli that will become the milk secreting lobules during lactation. By late pregnancy, the fat pad is mostly composed of alveoli with a significant reduction in stromal content (Richert et al., 2000).

At the onset of lactation, the alveoli are filled with milk secretions and approximately 30% of the gland is filled with adipocytes. Myoepithelial cells surround the alveolus and respond to the hormone oxytocin by contracting to force the milk out of the alveolus and drain into the ducts. The process of lactation continues for approximately 3 weeks until the pups are weaned. Upon

A

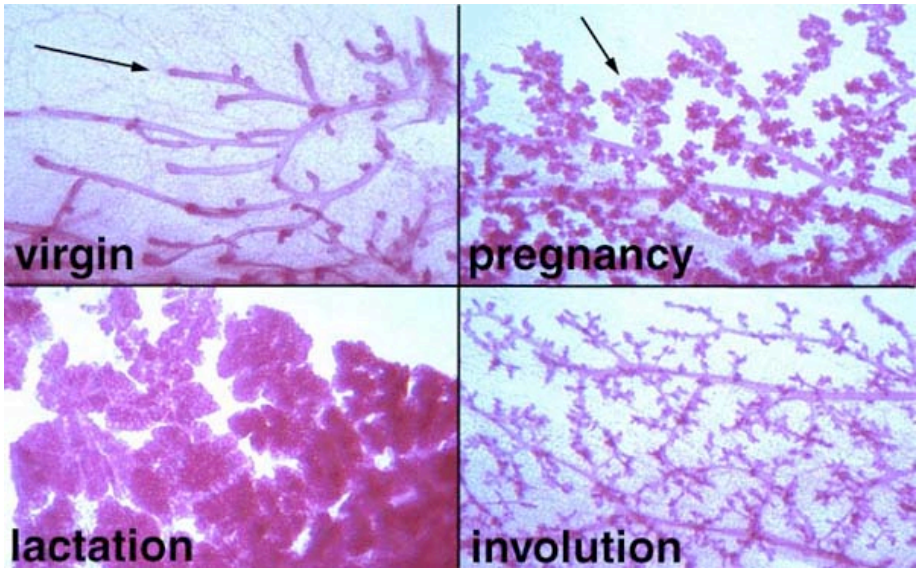
virgin
pregnancy
lactation
involution

B

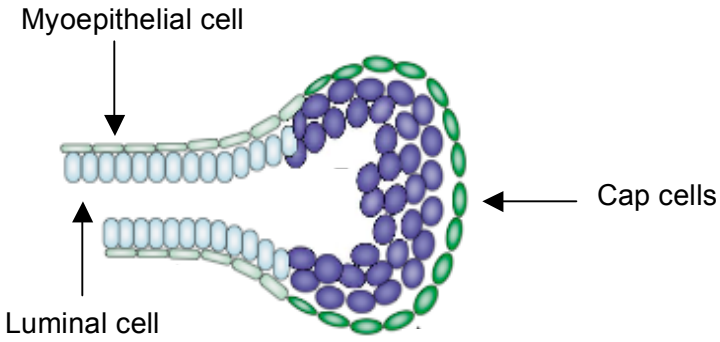
Myoepithelial cell
Cap cells
Luminal cell

C

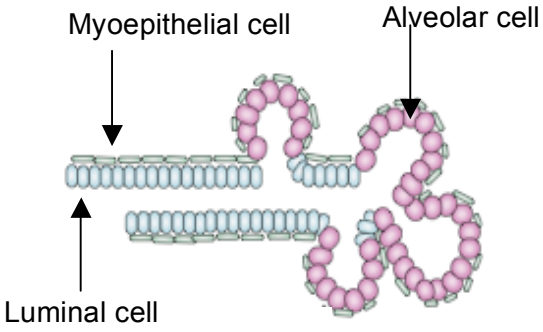
Myoepithelial cell
Alveolar cell
Luminal cell

<u>Figure 1.2:</u> Ductal and lobulo-alveolar differentiation of the mouse mammary gland.

(A) The 4 stages of mouse mammary gland development. Arrows indicate terminal end buds (TEBs) present during ductal elongation (in the virgin) and alveolar differentiation (during pregnancy). Whole mounts from Lothar Hennighausen, NIH. **(B)** Schematic representations of the TEB. Cap cells are bipotent mammary stem cells. From Woodward & Rosen, *J Cell Sci*, 2007. **(C)** Schematic representation of ductal and alveolar cells during mid pregnancy. From Woodward & Rosen, *J Cell Sci*, 2007.

weaning, the gland begins to involute; mammary epithelial cells undergo apoptosis and are cleared by infiltrating macrophages, and the stroma undergoes extensive remodeling. The process of involution takes approximately 2 weeks to complete, and the gland is then regressed to the nearly non-pregnant state. At this time, the gland is ready to initiate another round of pregnancy, lactation and involution (McDaniel et al., 2006; Richert et al., 2000). This developmental cycle is maintained by a population of mammary stem cells, functionally defined as cells able to reconstitute an epithelium-divested mammary fat pad, using a technique developed by DeOme *et al*. (Deome et al., 1959).

While development of the mouse mammary gland is a simplified parallel to development of the human breast, there exists one striking difference between the human and mouse mammary stromal microenvironments. The rodent mammary gland is primarily composed of an adipose rich stroma with an epithelial parenchyma, while the human breast is largely a more fibrous-adipose stroma with an epithelial parenchyma (Medina, 2004). Investigators utilizing the standard mouse xenograft technique to model human breast cancer in mice overlook this discrepancy in microenvironment, as it is largely not an issue for engraftment of (immortalized) human breast cancer cell lines. However, this discrepancy in microenvironment poses large problems to study human mammary epithelial cell development and malignancy in the mouse host, as these cells have very poor engrafting efficiency in the mouse mammary fat pad (Medina, 2004; Sheffield and Welsch, 1988). To circumvent this issue, Kuperwasser *et al.* developed a technique to “humanize” the gland after

removing the rudimentary tree from the mouse mammary fat pad. Fibroblasts isolated from reduction mammoplasty tissues (RMFs) were immortalized and irradiated, and ad-mixed with immortalized, non-irradiated RMFs, and inoculated into cleared mouse mammary fat pads. The RMFs were allowed to engraft and proliferate, upon which dissociated human mammary epithelial cells from ostensibly disease-free breast tissues were injected and allowed to engraft in the humanized microenvironment, permitting normal mammary morphogenesis and differentiation (Kuperwasser et al., 2004; Proia and Kuperwasser, 2006). These studies allude to the importance of heterotypic interactions between mammary epithelium and mammary stroma for proper development, differentiation and function of the mouse and human gland.

1.4 Mouse mammary stem cells

Mammary epithelium taken from any area of the mouse mammary gland is able to fully reconstitute a ductal tree in a cleared mammary fat pad (Daniel et al., 1968; Kordon and Smith, 1998), utilizing the technique by DeOme *et al*. (Deome et al., 1959). These data suggest mouse mammary stem cells (MaSCs) are dispersed throughout the gland and activated upon transplantation.

Several investigators have interrogated the MaSC cell surface markers utilizing the cleared fat pad technique in conjunction with genetic labeling and fluorescence activated cell sorting (FACS). Significant evidence suggests that the MaSCs are ERα negative; this is surprising given that ovarectomized mice cannot undergo pubertal ductal elongation, and ERα null mammary glands only

develop rudimentary mammary trees. However, elegant recombination experiments have demonstrated that mammary epithelial cells from ERα null mammary glands and mammary epithelial cells from ERα WT mammary glands can both contribute to reconstituting a cleared mammary fat pad, and both cell types equally contribute to ductal elongation (Mallepell et al., 2006). These data suggest that the MaSC is indeed ERα negative, and moreover, that ERα null mammary epithelia contain MaSCs but require ERα positive cells for their activation. ERα positive cells are thus referred to as niche "sensor cells," whose role is to respond to systemic estrogen signals by secreting growth factors that result in MaSC activation and thus, mammary gland development. This mechanism is only one of myriad complex paracrine interactions between cells of the mammary epithelium that are essential for its proper growth and differentiation. Recent evidence suggests that similar paracrine mechanisms within the mammary epithelia may be important in promoting the growth of breast tumors (Fillmore et al., 2010).

Using genetic labeling and FACS techniques, single cell suspensions of mouse mammary epithelial cells have been analyzed for the marker profile of a very small percentage of putative mammary stem cells. First, it was shown that one single mammary epithelial cell marked with LacZ was capable of reconstituting a full mammary gland *in vivo*, contributing to both luminal and myoepithelial lineages and generating functional lobuloalveolar units. This cell had the surface marker profile of $CD29^{hi}CD24^{+}$, and for semantics purposes, was irrefutably termed "the mammary repopulating unit" (MRU) (Shackleton et al.,

2006). Interestingly, it was shown that this subpopulation of cells is indeed ERα negative (Asselin-Labat et al., 2006), but is highly responsive to estrogen and progesterone, since ovariectomy significantly diminishes MaSC number and transplantation ability (Asselin-Labat et al., 2010).

Using a more stringent FACS gating technique, a following report identified the MRUs to be enriched in a fraction of $CD24^{med}/CD49f^{hi}$ cells, whereas the $CD24^{hi}CD49f^{low}$ cells had functional characteristics of more differentiated progenitor cells, and thus were termed “mammary colony-forming cells” (Ma-CFCs). Both of these marker sets have passed the gold standard technique of allowing for full reconstitution of the mammary tree in a cleared fat pad and have been further validated by other investigators (Asselin-Labat et al., 2006; Sleeman et al., 2007).

To add complication to the mouse MaSC hierarchy, mammary epithelial cell limiting dilution transplantation studies in both rats and mice demonstrated the existence of ductal-limited and lobule-limited progenitors, likely derived from a bipotent stem cell (Kordon and Smith, 1998; Smith, 1996). Lobule-limited progenitors are unable to produce cap cells, which are required for the penetration of the mammary fat pad at the tips of the growing terminal end buds; Ductal-limited progenitors fail to produce progeny capable of sustaining alveolar development and growth during pregnancy (Boulanger and Smith, 2009). It is unclear at present how the population of $CD24^{med}/CD49f^{hi}$ or $CD24^{+}/CD29^{+}$ MaSCs delineate these two mammary fates.

The discovery of distinct ductal- and lobular-limited progenitors in the mouse mammary gland let to the discovery of third distinct population of MaSCs, termed parity-induced mammary stem cells (PI-MECs). This cell population is present in the nulliparous female but becomes activated upon pregnancy. PI-MECs possess self-renewal capacity, multi-potency, and the ability to contribute to the formation of secretory alveoli upon subsequent pregnancies (Boulanger et al., 2005; Wagner et al., 2002).

1.5 Human breast stem cells

The characterization of bona-fide, functional markers for human breast stem cells has been much more challenging, largely due to the difficulties of obtaining sufficient amounts of primary tissue, difficulties in culturing these cells, and moreover, the lack of an *in vivo* stem cell transplantation model for human cells that has the same technical ease as that pioneered by DeOme *et al.* To circumvent these issues, investigators can use *in vitro* assays to enrich and propagate populations of human mammary epithelial cells (HMECs) enriched in stem and progenitor activity, such as the mammosphere assay (Dontu et al., 2003). However, the act of culturing HMECs may cause inadvertent selection of certain subpopulations, skewing the results of subsequent functional assays. In fact, it has yet to be definitively proven that human breast stem cells can be isolated from primary tissues without propagation in culture, split between cleared-fat pad stem cell transplantation assays and mammosphere culture, and later investigated to show that the cells contributing to both assays are indeed

identical (Molyneux et al., 2007). Nevertheless, frequently used markers for human breast stem cells are CD49f and EpCAM, based on pioneering work in the mouse. To demonstrate the stem cell activity in subpopulations of HMECs, cells are typically isolated and removed of stromal content by lineage depleting endothelial, fibroblastic, lymphocytic and monocytic lineages using an immunomagetic bead sorting strategy (referred to as Lin^-) (Proia et al., 2011; Villadsen et al., 2007). The remaining population, enriched in HMECs, is subjected to FACS analysis based on expression of CD49f and EpCAM. This yields a FACS plot with four distinct clouds (or subpopulations), with the $CD49f^{hi}/EpCAM^{hi}$ population containing stem cell and multipotent progenitor activity, based on mammosphere forming ability, and the capacity to generate TDLU-like structures in laminin-rich extracellular matrix (ECM) (Villadsen et al., 2007).

There exists evidence to suggest that ductal and lobular luminal cells derive from distinct lineage restricted progenitors in mice (Smith, 1996), although experiments performed with HMECs have yet to show this definitively in the human breast. Also, it remains unknown if PI-MECs exist in the human breast and play a role in subsequent pregnancies, as has been demonstrated in mouse mammary gland development. Furthermore, it remains unknown if $CD49f^+/EpCAM^+$ human MaSCs contain all three populations of stem cells whose existence has been documented within the mouse mammary gland.

A stem cell niche may be localized within the terminal ducts, as cells within this region stain positive for both cell lineage markers CK14 and CK19, and cells

dissected from terminal ducts can give rise to cells capable of mammosphere formation, multipotent colony formation and formation of bilayered, TDLU-like structures in three dimensional culture conditions. In contrast, cells dissected from lobules did not display these functional characteristics suggestive of stemness (Labarge et al., 2007; Villadsen et al., 2007).

1.6 Stromal influences in mammary stem cell fate and behavior

Elegant recombination studies demonstrated the potent influences of the mammary stromal microenvironment on MaSC fate and tumorigenic potential. The discovery of a distinct population of MaSCs that are activated upon pregnancy (PI-MECs) allowed for their lineage marking using the pregnancy activated mammary specific promoter whey acidic protein (WAP) driving Cre expression in Rosa26 LacZ mice. Adult testicular cells isolated from these mice were ad-mixed with limiting dilutions of MECs, inoculated into cleared mammary fat pads, impregnated and examined at the end of involution. Adult testicular cells interacted with the MECs and the mammary stroma to contribute outgrowths of normal mammary trees, suggesting that signals from the mammary epithelium and stroma were sufficient to alter spermatogenic cell fate (Boulanger et al., 2007). A similar experiment was conducted with neural stem cells isolated from fetal and adult WAP-Cre/Rosa26R mice ad-mixed with MECs; neural stem cells contributed to normal outgrowths in cleared fat pads (Booth et al., 2008).

MaSCs and progenitor cells have been implicated as the possible cells of origin for many human breast cancers (for more detailed discussion, see

Sections 1.8 and 1.9). Understanding how these cells read signals from their local microenvironment is essential to understanding the mechanisms governing breast cancer initiation and progression. Intriguingly, mouse mammary tumor cells can be temporarily normalized, incorporated into normal mammary outgrowths, and differentiated into functional mammary cell types, when admixed with non-transformed MECs at a respective ratio of 1:50 and inoculated into wild-type (WT) cleared fat pads (Booth et al., 2011). Collectively, these data demonstrate the potency of the mammary microenvironment in governing cell fate and behavior, and highlight the importance of studying epithelial-stromal interactions for a larger understanding of breast cancer origin and maintenance.

1.7 Epidemiology and heterogeneity of breast cancer

Breast cancer is the most common cancer among women in the US and is the second leading cause of cancer-related deaths (Jemal et al., 2007). More than 120,000 estimated deaths due to breast cancer are expected annually in the US and Europe combined (Jemal et al., 2009). While most of these breast cancers are sporadic, it is estimated that 5-10% of all breast cancers arise in individuals that have highly penetrant mutations in the breast cancer susceptibility genes, *BRCA1* and *BRCA2.* Individuals carrying mutations in these two genes have a 40-80% chance of developing breast cancer, making these mutations that strongest predictors of breast cancer known to date (Easton et al., 1995; Fackenthal and Olopade, 2007). Because of this, patients who have a familial history of breast cancer can opt for genetic testing and potentially life-

saving prevention strategies such as early onset annual mammograms, magnetic resonance imaging (MRI), chemoprevention, and risk-reducing bilateral mastectomy (Jemal et al., 2007).

Within the last decade, it has become widely appreciated that sporadic breast cancers are not one disease but exceptionally heterogeneous, making uniform, successful treatment for all sporadic breast cancers particularly challenging. However, these individual breast cancers can be categorized based on their gene expression signatures and typically fall within five distinct subtypes, referred to as "the intrinsic subtypes of breast cancer" (Fig. 1.3): luminal A, luminal B, HER2-like, basal-like, and normal-like. Luminal A comprises the largest group of breast tumors; these tumors express markers of differentiated luminal epithelial cells such as ERα, PR, and GATA3, among others. Luminal B tumors have less expression of luminal epithelial cell markers and express a novel set of genes from that of Luminal A. Her2-like tumors overexpress the Her2 amplicon at 17q22.24 including *ERBB2*, *GRB7*, and *TRAP100*. Basal-like tumors are largely distinct from luminal tumors in that they express basal cytokeratins CK5, CK14 and CK17, completely lack expression of luminal genes, and have a worse clinical outcome than that of luminal tumors. Hereditary breast cancers from *BRCA1* carriers fall within this basal-like category. Lastly, the normal-like subtype of breast tumors are poorly defined but seem to express genes characteristic of adipose tissue and other non-epithelial cell types; "normal-like" may in fact be a misnomer (Sorlie, 2004).

The Carolina Breast Cancer Study sought to identify risk factors for the

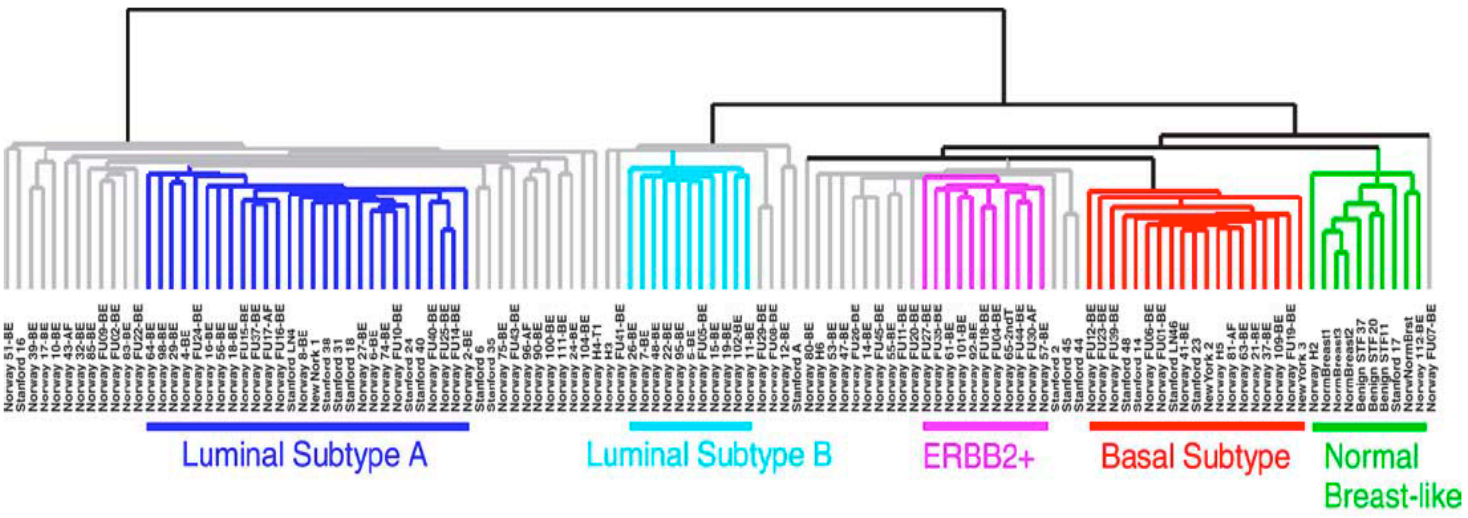

<u>Figure 1.3</u>: The 5 intrinsic subtypes of breast cancer.

Hierarchical clustering of 115 tumor tissues and seven non-malignant tissues using the intrinsic gene set. Experimental dendogram showing the clustering of the tumors into 5 subgroups. Branches corresponding to tumors with low correlation to any subtype are shown in grey. From Sorlie *et al.,* 2001. Note that the discovery of a 6th possible intrinsic subtype, the "claudin-low subtype," is not pictured here (Herschkowitz et al., 2007).

intrinsic subtypes of breast cancer. This population based, case-controlled study incorporated both African American and Caucasian women with invasive and *in situ* breast cancers compared to controls. The tumor sections from these women were subtyped using immunohistochemistry (IHC) for characteristic markers and then correlated with several breast cancer risk factors such as onset of menarche, age at first full term pregnancy, onset of menopause, lack of breastfeeding, use of lactation suppressants, environmental exposures (smoking, alcohol use), use of hormone replacement therapy (HRT), waste-hip ratio (WHR), and body mass index (BMI), among others. Consistent with literature demonstrating the racial disparities among breast cancer incidence and subtype (Ademuyiwa et al., 2011), postmenopausal white women showed the highest prevalence of luminal A breast tumors, while premenopausal African-American women exhibited the highest prevalence of basal-like breast cancers. Surprisingly, this study revealed that several risk factor associations for luminal A type breast cancer were in opposition to those associated with basal-like type breast cancer; increased parity, lack of breastfeeding, use of lactation suppressants, elevated WHR in pre-and postmenopausal women, and younger age at first full term pregnancy were strong risk factors for developing basal-like, but not luminal A-type breast cancers (Millikan et al., 2008).

In 2007, the speculation of a sixth intrinsic subtype of human breast cancer emerged, called the “claudin-low subtype” (Herschkowitz et al., 2007). This subtype correlated with poor prognosis invasive ductal carcinomas, typically “triple negative” (ER, PR, and HER2 negative; limiting adjuvant therapy options),

and enriched with a gene expression signature characteristic of MaSCs and of an epithelial-mesenchymal transition (EMT). Further characterization of this subtype suggested features of cancer stem-like cells (CSCs, discussed in detail in Section 1.8) (Prat and Perou, 2011). This subtype may become pronounced in breast tumors that have undergone endocrine therapy or chemotherapy, which may enrich for CSCs that have survival advantages over the majority of cells within the tumor bulk (Creighton et al., 2009).

1.8 Speculation of breast cancer cell of origin & cancer stem cell theory

The "cancer stem cell theory" originated from research on leukemia and other blood cancers, in conjunction with a thorough understanding of the hematopoietic stem cell (HSC) hierarchy. Bonnet *et al.* showed that human acute myeloid leukemia (AML) stem cells could be prospectively sorted from other cells within the tumor bulk based on the surface marker profile $CD34^{+}/CD38^{-}$. Using this sorted population, it was shown that these cells were the only cells capable of transferring AML from human patients onto non-obese diabetic/severe combined immunodeficient (NOD/SCID) mice (Bonnet, 2005; Bonnet and Dick, 1997).

Further support for the cancer stem cell theory in the context of breast tumors arose from a further characterization of breast cancer heterogeneity and the five intrinsic subtypes of breast cancer. It was hypothesized the human breast stem cell hierarchy may be reflected in the differentiation state of the cancer cell of origin, which would ultimately dictate the breast cancer subtype: luminal A tumors, which express markers of luminal cell differentiation, may derive from a luminal progenitor cell, whereas basal-like tumors, which express markers of

basal/myoepithelial cell differentiation, may derive from basal/myoepithelial progenitor cells (Fig. 1.4). In 2003, Clarke and colleagues lent further support for this hypothesis upon their discovery of breast cancer stem-like cells (BCSCs). In this landmark publication, human breast cancer cells were isolated from tumors, lineage depleted, and sorted for different populations based on any phenotypic combination of the cell surface markers $CD44^{+}$, $CD24^{-/lo}$, and $EpCAM^{+}$. Various dilutions of these cell populations were transplanted into the mammary fat pad of NOD/SCID mice. As few as one hundred $CD44^{+}/CD24^{-/lo}$ cells were capable of forming breast tumors in these mice compared to tens of thousands of cells with alternate phenotypic combinations of these markers, suggesting that the tumorigenic, aggressive potential of the breast cancer cells was not uniform. Moreover, the inoculation of one hundred $CD44^{+}/CD24^{-/lo}$ human breast cancer cells into mouse mammary fat pads was serially transplantable; each passage of one hundred $CD44^{+}/CD24^{-/lo}$ cells rendered tumors comprised of this particular cell population in addition to the alternate phenotypic combinations of these markers (Al-Hajj et al., 2003). This self renewal property of $CD44^{+}/CD24^{-/lo}$ breast cancer cells invoked the applicability of the cancer stem cell theory to human breast tumors. The stem-like properties of these cells were further supported upon the finding that breast cancer cells grown under mammosphere forming conditions (referred to as tumorspheres) are enriched in $CD44^{+}/CD24^{-/lo}$ cells (Fillmore and Kuperwasser, 2008; Ponti et al., 2005). Given the difficulties in isolating these populations from human breast tissues, Kuperwasser and colleagues showed that $CD44^{+}/CD24^{-/lo}/EpCAM^{+}$ cells are retained within

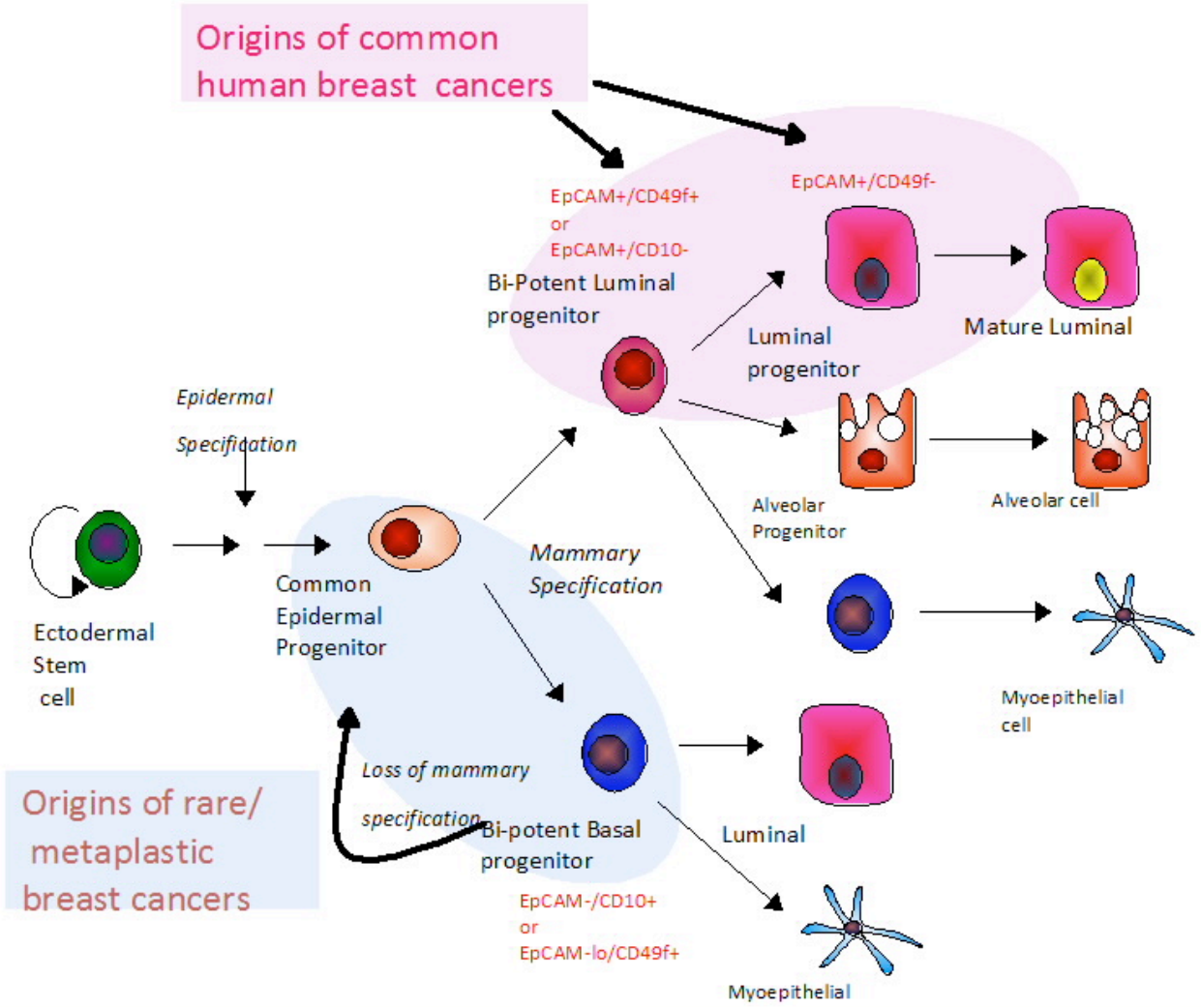
Origins of common human breast cancers
EpCAM+/CD49f+
or
EpCAM+/CD10-
Bi-Potent Luminal progenitor
EpCAM+/CD49f-
Luminal progenitor
Mature Luminal
Epidermal Specification
Alveolar Progenitor
Alveolar cell
Ectodermal Stem cell
Common Epidermal Progenitor
Mammary Specification
Myoepithelial cell
Loss of mammary specification
Origins of rare/ metaplastic breast cancers
Bi-potent Basal progenitor
Luminal
EpCAM-/CD10+
or
EpCAM-lo/CD49f+
Myoepithelial

<u>Figure 1.4:</u> The human breast stem cell hierarchy and likely origin of human breast cancers.

The human breast stem cell hierarchy, depicting both ductal and lobulo-alveolar differentiation as well as the origin of luminal, myoepithelial, and alveolar cells. Schematic kindly provided by Patricia Keller and Charlotte Kuperwasser, Tufts University School of Medicine.

commonly used breast cancer cell lines and the tumorgenicity of the cell line *in vivo* correlated with the basal percentage of $CD44^+/CD24^-/EpCAM^+$ cells within the line (Fillmore and Kuperwasser, 2008; Keller et al., 2010). This finding greatly simplifies the experimental challenges associated with studying the self-renewal and tumorigenic pathways of this cell population using primary breast tumor tissue (Fig. 1.5).

The term “cancer stem cell” is quite ambiguous, because it implies the transformed cell of origin is indeed a tissue specific stem cell. At present, this has yet to be definitively proven in the context of breast cancer. An equally plausible hypothesis is that the cancer stem cell is a more differentiated cell type within the tissue that has acquired self-renewal capability. Interestingly, either of these interpretations of the cancer stem cell definition would render insight into the hypothesis for transformed stem and progenitor cells serving as the basis for the molecular heterogeneity among human breast tumors. However, the identification of luminal progenitor cells as the candidate transformed cell population and likely cells of origin for mutant *BRCA1* driven breast cancers may suggest that progenitor cell populations are likely the origin of BCSCs (Lim et al., 2009).

1.9 Microenvironmental influences on cancer cell fate & behavior

Over an entire lifespan, individual cells incur several detrimental genetic insults due to environmental exposures and physiologically induced reactive oxygen species. Every cell within the body is susceptible to these carcinogens,

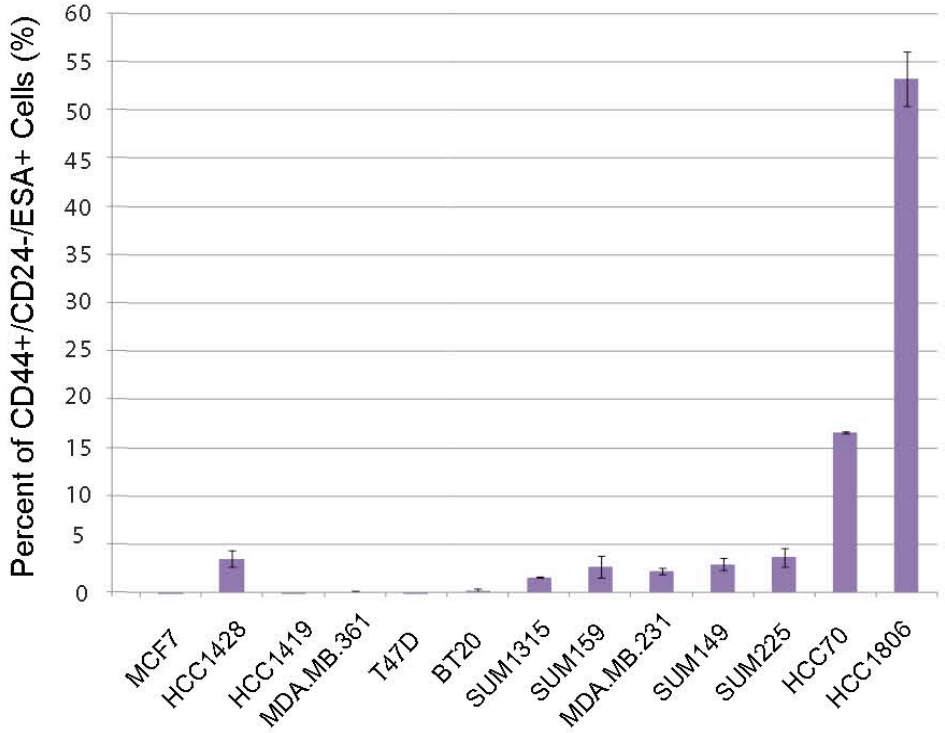
Percent of CD44+/CD24-/ESA+ Cells (%)
60
55
50
45
40
35
30
25
20
15
10
5
0
MCF7
HCC1428
HCC1419
MDA.MB.361
T47D
BT20
SUM1315
SUM159
MDA.MB.231
SUM149
SUM225
HCC70
HCC1806

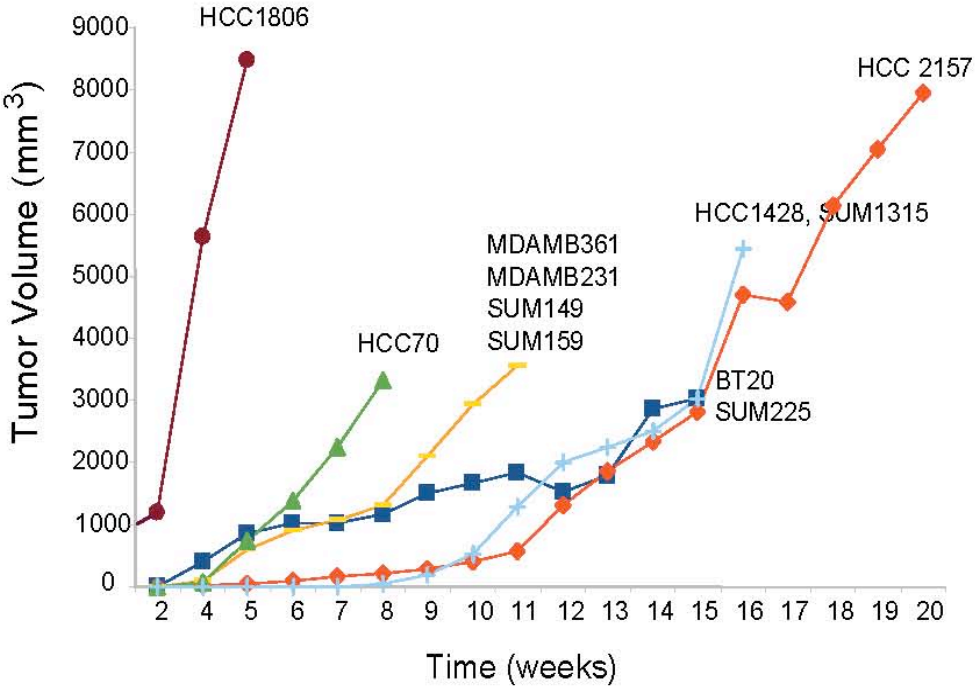
Tumor Volume (mm3)
9000
8000
7000
6000
5000
4000
3000
2000
1000
0
2 4 5 6 7 8 9 10 11 12 13 14 15 16 17 18 19 20
Time (weeks)
HCC1806
HCC 2157
HCC1428, SUM1315
MDAMB361
MDAMB231
SUM149
SUM159
HCC70
BT20
SUM225

<u>Figure 1.5:</u> The basal percentage of $CD44^+/CD24^-/EpCAM^+$ breast cancer stem-like cells (BCSCs) correlates with tumorgenicity *in vivo.*

Top, the basal percentage of $CD44^+/CD24^-/ESA^+$ BCSCs in commonly used breast cancer cell lines. To clarify, ESA is also called EpCAM. Note the basal percentage of BCSCs in the MCF7 cell line is 0.03%. Data provided by Amy Lin. Bottom, tumor volume from various breast cancer cells inoculated into the 4^{th} inguinal mouse mammary fat pad, measured over 20 weeks. Note highly tumorigenic breast cancer cell lines (i.e. HCC 1806) have high percentages of BCSCs. Data provided by Ina Klebba.

but each cell does not necessarily turn cancerous. Moreover, heritable cancer syndromes (such as those driven by inherited mutant *BRCA1* alleles) only predispose to breast and ovarian cancers, despite every cell within the body harboring this deleterious mutation. Based on these general observations, it is apparent that genetic alterations alone are not sufficient to drive cancer progression in tissues.

Several decages ago, Mintz and Illmensee demonstrated the potent tumor suppressive functions of a homeostatic tissue microenvironment. Embryonic carcinoma cells were injected either subcutaneously or into the mouse blastocyst. The subcutaneously injected tumor cells formed teratocarcinomas, while the blastocyst injected tumor cells gave rise to normal, chimeric mice (Mintz and Illmensee, 1975). These observations posed the possibility of tumor cells being “re-educated” by certain microenvironments to become cells that support proper tissue differentiation and homeostasis.

These findings led to an explosion in the last decade on “microenvironmental influences in cancer” research, as investigators began to appreciate that genetic mutation alone could not explain the origins of cancer (Bissell and Labarge, 2005). In a similar fashion to Mintz and Illmensee, Stoker *et al.* showed that Rous sarcoma virus infection of fibroblasts in culture results in rapid cell transformation and anchorage independent growth, while viral infection into chick embryos was non-tumorigenic despite widespread expression (Stoker et al., 1990). In the context of breast cancer, the mammary microenvironment may possess tumor suppressive function (similar to embryonic

microenvironments) unless “activated”. Combining the HIM model (described in Section 1.3) with lentiviral transduction of breast cancer relevant oncogenes into resected human breast organoids revealed an important role the mammary stroma in creating a “tumor-permissive” microenvironment. Specifically, tumors were efficiently generated from tissue recombinants containing a co-mix of the oncogene-expressing organoids with immortalized human breast fibroblasts overexpressing HGF; tumor development was rarely observed when the oncogene-expressing organoids were co-mixed with primary breast fibroblasts (Wu et al., 2009). Experiments in mice also revealed the important role of mammary stroma in permitting or inhibiting tumor development. Mouse mammary fat pads cleared of endogenous epithelium were exposed to high doses of irradiation followed by inoculation with unirradiated, nonmalignant mouse mammary epithelial cells. Aggressive mammary tumors formed within the irradiated mouse stroma, but not in the sham-irradiated cleared fats (Barcellos-Hoff and Ravani, 2000). Interestingly, irradiation of the mouse stroma increases the number and repopulating activity of MaSCs (Nguyen et al., 2011), suggesting that stromal activation may exert influence over stem cell number and activity, and this may be a required step in the induction of tumorigenesis.

Mammary stroma is a collection of various connective tissue cell types and ECM. Several studies have dissected these stromal components to investigate the individual contribution of each to tumorigenesis. It is known that ECM attachment regulates growth, differentiation and the tumorigenic capacity of breast epithelial cells in culture, likely by modulating biochemical and

biomechanical signaling events. For example, transformed human mammary epithelial cells treated with a β1 integrin blocking antibody form significantly smaller tumors *in vivo* and re-assemble normal mammary gland architecture in a 3D culture model (Weaver et al., 1997). It is known that breast tumors have significantly different ECM content and organization compared to disease-free breast tissue. In particular, the ECM remodeling that occurs during post-lactational involution of the breast is associated with high matrix metalloproteinase activity, fibrillar collagen deposition, and the release of bioactive fibronectin and laminin fragments that initiate biochemical signaling. Because of this switch to a more inflammatory mammary microenvironment, involuting matrix promotes the invasion and metastasis of breast cancer cells *in vitro* and *in vivo* (McDaniel et al., 2006). These data may lend insight into the "pregnancy associated breast cancer" phenomenon, where there is a heightened risk of developing breast cancer within the first 5 years following pregnancy. The consequences of ECM remodeling on breast tumor progression and metastasis remain an active area of breast cancer research (Levental et al., 2009). Collectively, these data highlight the role of the microenvironment serving a dominant role over cellular genotype.

1.10 Stromal reaction in breast cancer & parallels to wound healing

It is well established that stroma associated with normal mammary gland development is strikingly different from that associated with breast carcinomas (Bissell and Radisky, 2001; Kalluri and Zeisberg, 2006). When compared to

normal tissues, the stroma accompanying breast tumors contains an increased number of fibroblasts and immune cell infiltrates, enhanced capillary density, increased collagen I and fibrin deposition, all which collectively alter the structure and stiffness of the ECM and induce changes in signaling within the adjacent epithelium (Bissell et al., 2002; Dvorak, 1986). Compared to normal mammary gland stroma, breast tumor-associated stroma shows elevated expression of αSMA, collagen IV, prolyl-4-hydroxylase (P4H), fibroblast activated protein (FAP), tenascin, desmin, calponin, caldesmon and others (Degen et al., 2007; Orimo et al., 2005; Ronnov-Jessen et al., 1995).

Several reports have used transcriptome-wide analyses to report the changes in stromal gene expression associated with tumor development (Allinen et al., 2004; Casey et al., 2009; Finak et al., 2008; Ma et al., 2009). The most prominent upregulated genes include components of the ECM and matrix metalloproteases (MMPs) responsible for stromal remodeling as well as secreted and cell surface proteins. In fact, based on serial analysis of gene expression (SAGE) and single nucleotide polymorphism (SNP) analyses, the most dramatic and consistent modifications in gene expression occurred within the fibroblast and myoepithelial fractions sorted from primary human breast tumors (Allinen et al., 2004). Whether these stromal changes in gene expression are the result of genetic alterations remains controversial (Campbell et al., 2009; Eng et al., 2009; Hu et al., 2005). However, it is generally accepted that epigenetic reprogramming, mediated by histone modifications, DNA methyltransferases,

chromatin modifying factors, and microRNAs (miRs), is at least in part responsible (Enkelmann et al., 2011; Fiegl et al., 2006; Hu et al., 2005).

The majority of human breast cancers are associated with a strong desmoplastic stroma and inflammatory response that strikingly resembles the stromal response during chronic wound healing (Bissell and Radisky, 2001; Dvorak, 1986; TIsty and Coussens, 2006). Both tumors and wounds elicit stromal reactions that are characterized by ECM remodeling, growth factor secretion, cell migration, and angiogenesis. During normal wound healing, this stromal response is initiated by bone marrow-derived hematopoietic cells and is accompanied by a marked increase in vascular permeability, plasma extravasation, fibrin deposition, platelet activation and inflammatory cell infiltration, which together result in the release of numerous of cytokines and growth factors (Dvorak, 1986; Mori et al., 2005). This response leads to the generation of granulation tissue, which is characterized by angiogenesis, activation of fibroblasts into αSMA positive myofibroblasts, and matrix remodeling (Wixler et al., 2007). In breast tumor pathogenesis, rupture of the basement membrane and loss of the myoepithelial layer may initiate this desmoplastic response (Hu et al., 2009; Hu et al., 2008; Vargo-Gogola and Rosen, 2007) (Fig. 1.6).

Given the striking parallel between tumor progression and wound healing, it is not surprising that chronically inflamed/wounded tissues are more likely to instigate the development of carcinomas, as demonstrated by H. pylori induced gastritis (Houghton and Wang, 2005), inflammatory bowel diseases such

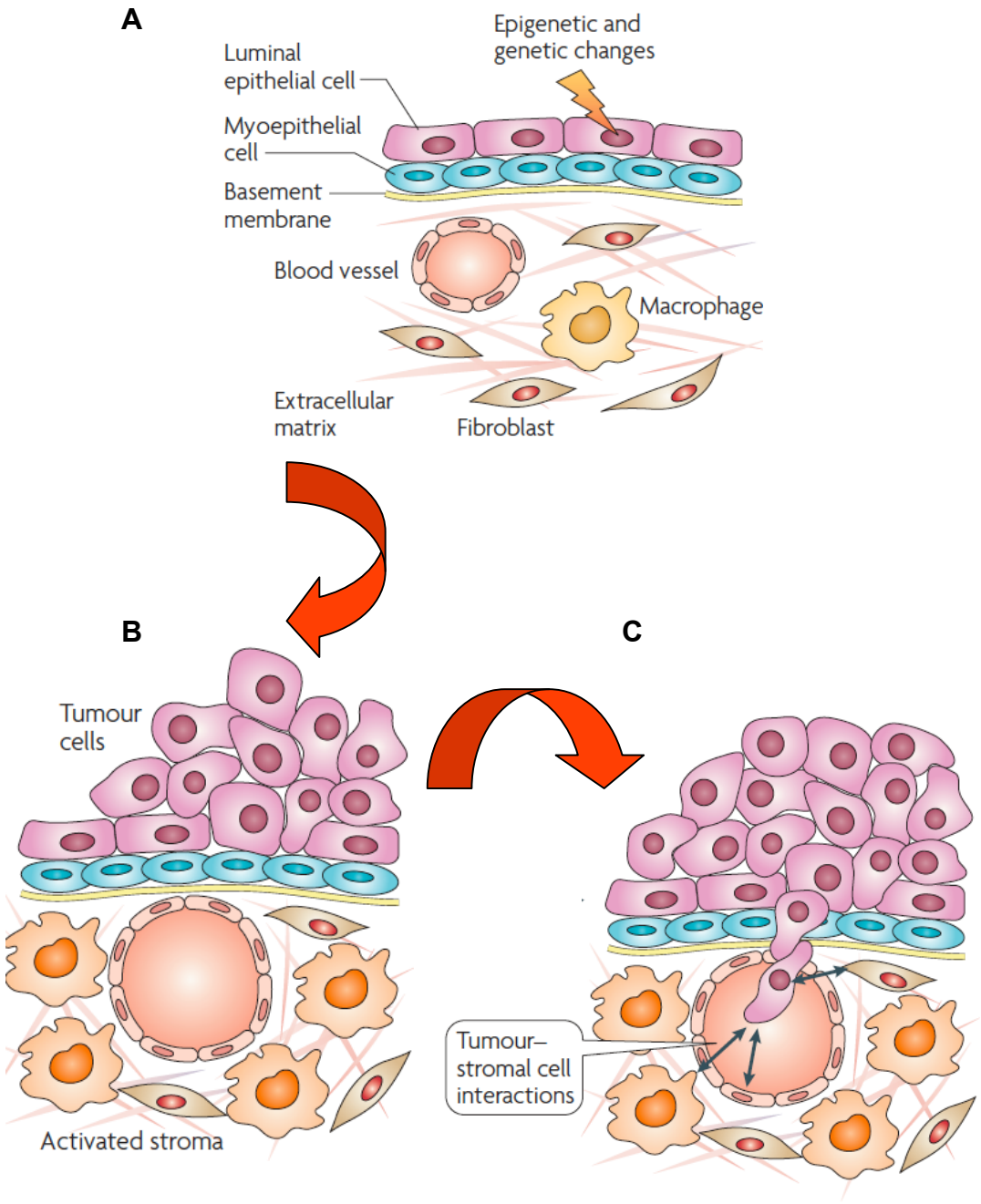
A
Epigenetic and genetic changes
Luminal epithelial cell
Myoepithelial cell
Basement membrane
Blood vessel
Macrophage
Extracellular matrix
Fibroblast
B
Tumour cells
Activated stroma
C
Tumour–stromal cell interactions

Figure 1.6. Schematic representation of breast cancer progression. **(A)** The acquisition of both epigenetic and genetic changes to cells within mammary epithelial cells, as well as changes within the stromal microenvironment, initiate breast cancer development. **(B)** As tumor cells proliferate and tissue integrity is lost, the ductal lumens fill with cells, fibroblasts become activated, and inflammatory cells are recruited. **(C)** The overgrowth of cancer cells within the ductal lumen causes basement membrane breakdown and invasion into the stroma. Tumor cells interact with activated fibroblasts (CAFs) and intravasate through the blood vessels to begin the final steps of metastasis (colonization within a different organ from that of the primary tumor). Metastasis is the main cause of morbidity and mortality associated with this disease. From Vargo-Gogola and Rosen, *Nat Rev Cancer*, 2007.

ulcerative colitis and Crohn's disease (Grivennikov et al., 2009), and obesity-induced hepatoseatosis (Park et al., 2010). Interestingly, adaptive immunity may not only initiate the formation of carcinomas (de Visser et al., 2005; Greten et al., 2004; Okayasu et al., 1996), but can also drive their progression to more invasive, poorly differentiated phenotypes. In fact, recent studies have demonstrated that inflammation can drive the progression of breast tumors despite any known breast specific inflammatory conditions that predispose this tissue to tumorigenesis. These inflammatory tumor promoting mechanisms driving breast cancer progression result from the stromal recruitment of $CD4^+$ cells (DeNardo et al., 2009), regulatory T cells (Tan et al., 2011), $Gr1^+CD11b^+$ myeloid cells (Yang et al., 2008), and type II macrophages (Doedens et al., 2010); these cells cultivate an activated microenvironment that supports cancer cell proliferation, growth, survival and even metastatic capability. For example, mice expressing polyoma middle T antigen (PyMT) under control of the mouse mammary tumor virus (MMTV) promoter develop aggressive mammary adenocarcinomas and lung metastases in a macrophage dependent manner, and this is in part due to macrophage mediated induction of the angiogenic switch (Lin et al., 2006). Stromal derived molecules such as monocyte chemoattractant protein 1 (MCP-1) recruit tumor-associated macrophages (TAMs), and MCP-1 blocking antibodies can significantly decrease macrophage infiltration, angiogenesis and mammary tumor growth in mice (Fujimoto et al., 2009). In addition to macrophages, $CD11b^+$ $Gr1^+$ myeloid cells (referred to as myeloid-derived suppressor cells (MDSCs)) are known to be significantly

increased in tumor bearing mice, with increased numbers found in the spleen, blood and lymph nodes (Gabrilovich and Nagaraj, 2009). These recruited cells suppress the activation of $CD4^+$ and $CD8^+$ T cells, block the activation of natural killer cells and limit dendritic cell maturation (Ostrand-Rosenberg and Sinha, 2009), allowing a favorable microenvironment for tumor cells to flourish and evade host immunosurveillance. It is possible that MDSCs may differentiate into activated TAMs when encountering factors secreted by tumor cells or other stromal cells in the microenvironment (Sica and Bronte, 2007). The inflammatory cytokine interleukin-1 beta (IL-1β) promotes the accumulation of MDSCs within the tumor microenvironment and accelerates tumor progression (Tu et al., 2008), suggesting that inflammatory molecules may promote tumor progression, in part, by mediating immunosurveillance through the recruitment of MDSCs. Like IL-1β, other pro-inflammatory mediators such as interleukin-6 (IL-6) and prostaglandin E2 (PGE2) are known to increase the numbers of MDSCs within the circulation, and have profound affects on tumor progression in mice (Bunt et al., 2007; Chang et al., 2005; Sinha et al., 2007; Winslow et al., 2006). Anti-inflammatory therapies such as monoclonal antibodies to tumor necrosis factor alpha (TNFα) (Peyrin-Biroulet, 2010), IL-6 (Febbraio et al., 2010), and cyclooxygenase 2 (Cox-2) inhibitors (which block the biosynthesis of the pro-inflammatory hormone PGE2) (Jacoby et al., 2000; Vane et al., 1994) have been successful in attenuating inflammation-driven carcinomas, and may decrease the risk of developing breast cancer (Ulrich et al., 2006).

1.11 The heterogeneity of fibroblasts

Fibroblasts are flat, spindle shaped cells with multiple emanating processes and a major cell type present within all connective tissues of the body; they provide structural support, matrix deposition, and organization of adjacent epithelia. Fibroblasts in cell cultures or tissue sections are usually identified based on their morphological, proliferative and phenotypic characteristics, which is hardly definitive, because several cell types in 2D culture will acquire fibroblast characteristics. Moreover, aside from assaying matrix production and deposition, there are no key features or bona fide markers of fibroblasts to distinguish them from other cell types in culture (Krenning et al., 2010) (Table 1.1). Thus, the question of "what makes a fibroblast a fibroblast?" has long been overlooked.

Similarly, the distinction between fibroblasts and myofibroblasts is usually based on the latter's expression of αSMA and other contractile proteins, which is hardly a bona fide distinction, given that fibroblasts placed in standard cell culture conditions will acquire myofibroblast phenotype (i.e. stress fiber formation) and the expression of myofibroblast- associated proteins (i.e. αSMA) (Ronnov-Jessen et al., 1995; Ronnov-Jessen et al., 1990). Since smooth muscle cells, pericytes and myoepithelial cells also express αSMA, identifying myofibroblasts based on αSMA expression even in human breast tumor tissues is open to interpretation.

Perhaps the lack of specific markers for fibroblast/myofibroblast is a reflection of the marked heterogeneity among these cells with respect to proliferation, collagen production, and cytokine secretion (Fries et al., 1994; Jelaska et al., 1999). It is known that fibroblasts have tissue specific properties;

Table. 1-11: Commonly used markers of fibroblasts and myofibroblasts.
From Krenning *et al., J Cell Physiol*, 2010.

Protein	Function	Expressed by other cell type	Refs.
α-Smooth muscle actin (αSMA)	Intermediate-filament associated protein	Smooth muscle cells, pericytes, myoepithelial cells	Akpolat et al. (2005); Azuma et al. (2009)
Cadherin-9	Ca-dependent adhesion molecule	Neurons; tumor vasculature	Thedieck et al. (2007); Hirano et al. (2003)
CD40	TNFα receptor family member	Various antigen presenting cells	Smith (2004)
CD248 (TEM1)	Collagen receptor	Pericytes, endothelial cells	Bagley et al. (2008); MacFadyen et al. (2005)
Col1a1	Collagen type I biosynthesis	Osteoblasts, chondroblasts	Liska et al. (1994)
Discoidin domain receptor 2 (DDR2)	Collagen-binding tyrosine kinase receptor	Smooth muscle cells, hepatic stellate cells, endothelial cells	Vogel et al. (2006); Olaso et al. (2001); Mohan et al. (2001)
Fibroblast activation protein-1 (FAP1)	Serine protease (gelatinase)	Activated melanocytes	Rettig et al. (1993); Ramirez-Montagut et al. (2004)
Fibroblast-specific protein-1 (FSP1/S100A4)	Intermediate-filament associated Ca-binding protein	Smooth muscle cells, invasive carcinoma cells	Strutz et al. (1995); Sugimoto et al. (2006)
Fibroblast surface antigen (FSA)	Fibronectin-binding molecule	Monocytes/macrophages	Wartiovaara et al. (1974)
Heat shock protein-47 (HSP47)	Collagen-binding serpin chaperone	Monocytes/macrophages, various collagen-producing cells	Shioshita et al. (2000); Sauk et al. (2005)
Platelet-derived growth factor receptor-β (PDGFRb)	Receptor tyrosine kinase	Smooth muscle cells, pericytes	Lindahl et al. (1997); Kaur et al. (2009)
Prolyl-4-hydroxylase	Collagen biosynthesis	Endothelial cells, epithelial cells	Mussini et al. (1967); Langness and Udenfriend (1974)
Thymus cell antigen-1 (THY1/CD90)	Cell adhesion molecule	Leukocytes, endothelial cells, various progenitor cells	Wetzel et al. (2006); Dezso et al. (2007)
Vimentin	Intermediate-filament associated protein	Endothelial cells, smooth muscle cells, pericytes, myoepithelial cells	Franke et al. (1979); Mork et al. (1990)

fibroblasts from skin tissue differ in their morphology, proliferation and matrix deposition compared to fibroblasts from lung tissue (Fries et al., 1994). Interestingly, fibroblasts within the same tissue can exhibit heterogeneity. For example, in a population of human gingival fibroblasts, approximately 50% were responsive to PGE2 treatment, and this population had reduced membrane transport and proliferation rate compared to the unresponsive population (Ko et al., 1977). Similarly, human dermal fibroblasts differentially produced PGE2 upon exposure to monocyte conditioned media or IL-1 (Korn et al., 1984). However, the differences observed within these populations could also be attributed to the inability to sort highly pure populations of fibroblasts from other connective tissue cell types that grow well in 2D culture. Nevertheless, these data invoke the hypothesis that certain fibroblast populations within certain tissues are more inflammatory and activated than others, and these fibroblasts in particular may be responsible for mediating wound healing, fibrotic diseases, and the stromal reactions accompanying the growth of solid tumors.

Fibroblast heterogeneity is also apparent in populations of cancer associated fibroblasts (CAFs); these are myofibroblasts found within the vicinity of solid tumors and distinguished from myofibroblasts within the stroma of wounded tissues based on the latter's co-evolvement with tumor cells and the ability to support tumor growth in mice (Erez et al., 2010; Kojima et al., 2010; Olumi et al., 1999; Orimo et al., 2005). Like myofibroblasts in wounded tissues, these CAFs are frequently marked based on expression of αSMA, which is heterogeneously expressed in the stroma of different patient derived tumors

(Micke and Ostman, 2005; Sugimoto et al., 2006) (Fig. 1.7). Moreover, the tumor promoting ability of CAFs (as demonstrated by co-mixing these cells with a breast cancer cell line and comparing tumor growth in mice to injection of breast cancer cells alone) can vary dramatically among different patient derived CAF populations. Interestingly, there lacks a correlation between tumor subtype and the tumor promoting potential of CAFs isolated from these tumors, and the heterogeneity in CAF phenotype has been largely understudied. Characterizing the heterogeneity of CAFs is important to understanding the mechanisms governing breast cancer progression, because these cells, like recruited bone marrow derived cells (discussed in Section 1-10), also mediate tumor associated inflammation and desmoplasia (Erez et al., 2010; Radisky and Radisky, 2007; Silzle et al., 2004).

The heterogeneity in CAF phenotype may largely be a reflection of several possible cells of origin. One such origin may be from the conversion of certain populations of resident tissue fibroblasts exposed to chronic transforming growth factor beta-1 (TGFβ), a cytokine highly secreted during wound healing and tumor progression. TGFβ has been implicated based on its ability to mediate the conversion of fibroblasts into myofibroblasts and promote the assembly of stress fibers and fibronectin-containing fibrils, which generate the contractile forces characteristic of these cells (Kojima et al., 2010; Tomasek et al., 2006; Vaughan et al., 2000). Moreover, TGFβ is a major instigator of tissue fibrosis, a collection of diseases largely mediated by activated fibroblasts. Interestingly, fibrotic fibroblasts, which harbor several characteristics of myofibroblasts and CAFs,

A

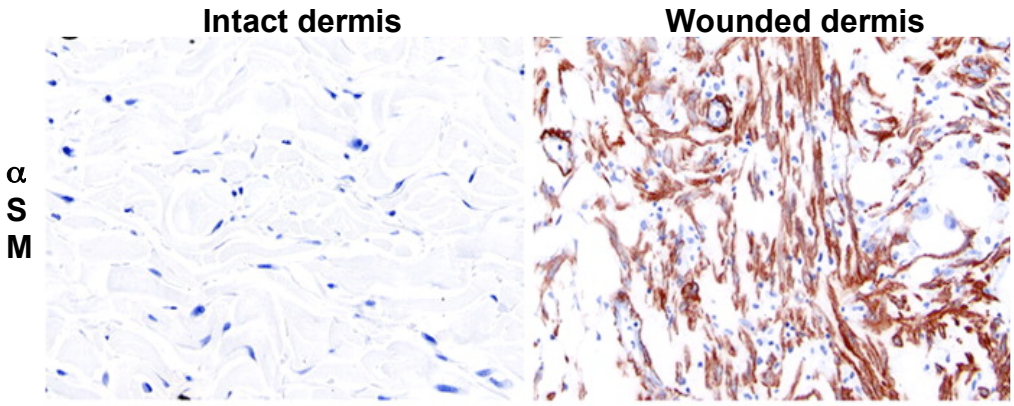
Intact dermis
Wounded dermis
α
S
M

B

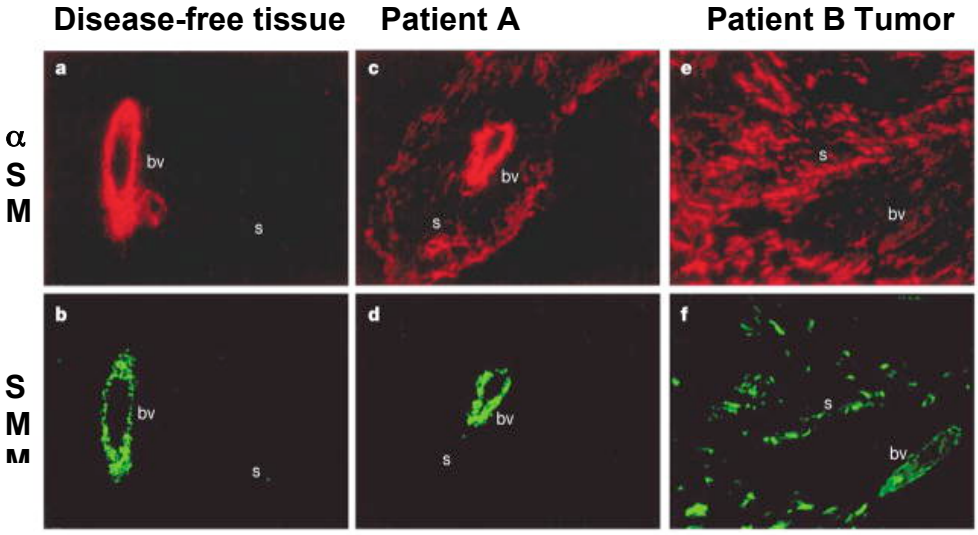
Disease-free tissue
Patient A
Patient B Tumor
α
S
M
S
M
M
a
b
c
d
e
f
bv
s

Figure 1.7: Presence of activated fibroblasts during wound healing and cancer.

(A) Immunohistochemistry (IHC) for αSMA expression in intact human dermis or wounded dermis. αSMA+ cells appear mesenchymal in morphology suggesting they are myofibroblasts. From Wixler *et al., J Cell Biol*, 2007. **(B)** Comparison of disease free versus tumor associated stroma (s). *a,b*: disease-free breast tissue lacks stromal expression of αSMA and smooth muscle myosin (SMM) except within blood vessels (bv); *c,d:* tumor tissue from patient A showing robust expression of αSMA, but not SMM, in the stroma; *e,f:* tumor tissue from patient B showing robust expression of both αSMA and SMM in the stroma, demonstrating fibroblast patient heterogeneity. From Bissell & Radisky, *Nat Rev Cancer*, 2001.

respond to chronic TGFβ exposure by hypermethylating specific gene(s) required to main the fibrotic fibroblast state. Transient TGFβ exposure is sufficient to briefly reduce expression of these particular genes, but chronic TGFβ exposure is required to maintain the fibrotic fibroblast phenotype and perpetuate disease (Bechtel et al., 2010). These data lend speculation to the idea that CAFs are epigenetically modified fibroblasts from the resident tissue, consequently from chronic exposure to TGFβ within the tumor microenvironment. In fact, both TGFβ and stromal derived factor 1 apha (SDF1α) have been implicated in promoting a positive feedback loop that is dependent on tumor and stromal cell crosstalk and is required to maintain a CAF-like state in a breast tumor xenograft model (Kojima et al., 2010). These results are consistent with those from early 1990s, where it was shown that tumor cells are sufficient to induce a myofibroblast phenotype in cultured resident tissue fibroblasts using a 3D co-culture system; however only a fraction of the fibroblasts, those in closest contact with the tumor cells, responded in this fashion (Ronnov-Jessen et al., 1995). Notably, it remains unknown if the myofibroblast phenotype is a permanent state of fibroblast differentiation or a de-differentiation to a more primitive cell state, and whether CAFs derive from resident fibroblasts within human connective tissues that accompany epithelia.

CAFs, like myofibroblasts associated with wound healing, may also be derived from recruited bone marrow derived cells. Both may be derived from circulating fibrocytes, cells that express hematopoietic stem cell markers as well as monocyte lineage and fibroblast markers (Bellini and Mattoli, 2007).

Fibrocytes are known to differentiate into myofibroblasts and have been identified within invasive ductal carcinomas and DCIS lesions of the breast (Barth et al., 2002; Direkze et al., 2004; Kisseleva et al., 2006; Mori et al., 2005; Phillips et al., 2004; Schmidt et al., 2003). In addition, bone marrow derived mesenchymal stem cells (MSCs) have also been shown to differentiate into αSMA positive cells with CAF-like characteristics (Mishra et al., 2008; Spaeth et al., 2009).

The transdifferentiation of a variety of cell types has also been proposed as a source of CAFs. For example, the endothelial mesenchymal transition has been shown to produce myofibroblast-like cells upon exposure to TGFβ. Tumors formed from endothelial cell-specific LacZ reporter mice contain LacZ-positive fibroblasts (Zeisberg et al., 2007), suggesting that endothelial transdifferentiation can contribute to the CAF content of the microenvironment. The epithelial-mesenchymal transition (EMT) has long been regarded as a necessary step in the progression to invasive tumors. Interestingly, there is some evidence to suggest that tumor cells undergoing an EMT may transdifferentiate into myofibroblasts (Kim et al., 2006; Petersen et al., 2003; Radisky et al., 2007), although this fails to reconcile the lack of profound genetic mutations within tumor associated stroma.

Within the last few years, more research has been dedicated to understanding the molecular mechanisms that govern CAF phenotype and tumor promoting ability rather than attempting to identify the particular CAF cell(s) of origin (of which there are likely many). Using xenograft mouse models, CAFs have been shown to support the growth of human breast cancer cells through

SDF1α mediated recruitment of endothelial progenitor cells (EPCs) and tumor angiogenesis (Orimo et al., 2005). In a stepwise xenograft mouse model of squamous cell carcinoma, CAFs promote the growth of cancer cells through an NFκB and IL-1β dependent signaling pathway (Erez et al., 2010), demonstrating that CAFs have pro-inflammatory properties. Indeed, CAFs have a highly pro-inflammatory secretome (Erez et al., 2010). In addition, CAFs may also support tumor associated inflammation indirectly, by secreting chemoattractant factors which recruit TAMS, MDSCs, T regulatory cells, and other myeloid derived cells to the tumor microenvironment. A small amount of literature suggests that CAFs may also influence the percentage of BCSCs through their secretion of SDF1 (Huang et al., 2010). Importantly, the heterogeneity of different CAF populations in mediating these tumor promoting functions were not addressed in these studies.

In summary, while the CAF cell of origin remains elusive, the inherent tumor promoting properties of this particular cell type validate its contribution to breast tumor progression and warrant further investigation into the heterogeneity and molecular makeup of these cells. Identifying molecular characteristics and markers of activated and tumor promoting fibroblast populations could validate their ability to serve as a target adjuvant therapy in the treatment of breast cancer.

1.12 Significance of the project

Despite recent advances in the treatment of breast cancer largely due to early detection screenings, there lacks a specific treatment option that addresses both the heterogeneity and marked stromal response characteristic of this disease. The stromal contribution to the initiation and progression of breast tumors has been highly substantiated within the last decade. Stromal gene expression signatures can predict patient prognosis and response to neoadjuvent chemotherapy (Farmer et al., 2009; Finak et al., 2008), and tumor associated stroma serves as a potential drug target (LeBeau et al., 2009; Loeffler et al., 2006; Ostermann et al., 2008). CAFs are a particular cell type within the tumor associated stroma known to promote the growth and survival of breast cancer cells. They serve as an attractive drug targeting option because they are only found in breast tumors and not within disease-free breast tissue, and are the most prominent stromal cell type associated with carcinomas (Silzle et al., 2004). Understanding the heterogeneity among various patient derived CAFs is essential to elucidating which patients may benefit from an adjuvant therapy targeting the tumor associated stroma. We hypothesize that breast tissue derived fibroblasts, from both resected tumor specimens (CAFs) and disease-free reduction mammoplasty tissues (RMFs) are a heterogeneous with respect to tumor promoting ability, and that the most tumor promoting fibroblast populations are highly pro-inflammatory. We hypothesize that CAFs support breast tumor growth by expanding the number of highly tumorigenic BCSCs present within the tumor. Lastly, we hypothesize that CAFs are epigenetically distinct from RMFs

and respond to growth factor signaling (such as TGFβ) through distinct pathways.

1.13 Specific Aims

Specific Aim 1

a. **To determine distinguishing features of tumor promoting and non-tumor promoting breast fibroblasts.**
b. **To determine the mechanism by which certain fibroblast populations promote mammary tumor growth.**

We will isolate CAFs from resected breast tumor specimens and disease-free fibroblasts from reduction mammoplasty tissues (RMFs). We will characterize these CAF and RMF samples for expression of activated fibroblast markers (using IF and quantitative reverse transcription PCR (qRT-PCR)), for differential tumor promoting ability (using functional assays with MCF7 breast cancer cells), and for differential secretion of pro-inflammatory molecules (using human specific enzyme linked immunoassays (ELISAs) and cytokine arrays). Lastly, we will attempt to correlate fibroblast tumor promoting ability with any of our identified characteristics.

Specific Aim 2

a. **To characterize the differences in the epigenetic response to TGFβ between CAFs and RMFs.**
b. **To determine if miR21 regulates CAF phenotype.**

We will isolate CAFs and RMFs as described in Aim 1. We will characterize

the relative levels of the primary, precursor, and mature forms of miR21, miR199a, miR100 and miR25 in CAFs and RMFs upon treatment with either TGFβ or vehicle by miR specific qPCR. We will characterize the relative levels of miR processing proteins and the sensitivity to TGFβ signaling between these two cell types by qPCR and western blot. We will utilize a previously established pull down assay (Heo et al., 2009) to see what proteins associate with miR21 in a TGFβ dependent manner. To determine if miR21 regulates CAF phenotype, we will transfect antisense miR oligonucleotides and collect CM from CAFs and RMFs to use for MCF7 tumorsphere assays.

CHAPTER II

Functional heterogeneity of breast fibroblasts is defined by a prostaglandin secretory phenotype that promotes expansion of cancer-stem like cells

2.1 Abstract

Fibroblasts are important in orchestrating various functions necessary for maintaining normal tissue homeostasis as well as promoting malignant tumor growth. Significant evidence indicates that fibroblasts are functionally heterogeneous with respect to their ability to promote tumor growth, but markers that can be used to distinguish growth promoting from growth suppressing fibroblasts remain ill-defined. While the expression of alpha smooth muscle actin (αSMA) is presumed to identify activated myofibroblasts, fibroblasts can readily acquire αSMA expression under many different conditions. Thus, whether the expression of αSMA is associated with a functionally distinct population of tumor-promoting fibroblasts remains unclear. Here we show that human breast fibroblasts are functionally heterogeneous with respect to tumor-promoting activity regardless of whether they were isolated from normal or cancerous breast tissues and regardless of αSMA expression. Rather, we show that fibroblasts which secrete abundant levels of prostaglandin (PGE2) when isolated from either reduction mammoplasty or carcinoma tissues were both capable of enhancing tumor growth *in vivo* and could increase the number of cancer stem-like cells. PGE2 further enhanced the tumor promoting properties of fibroblasts by increasing secretion of IL-6, which was necessary, but not sufficient, for expansion of breast cancer stem-like cells. These findings identify a population of

fibroblasts which both produce and respond to PGE2, and that are functionally distinct from other types of fibroblasts. Identifying markers of these cells could allow for the targeted ablation of tumor-promoting and inflammatory fibroblasts in human breast cancers.

2.2 Introduction

Fibroblasts were first described in the late 19th century by the pathologist Rudolph Virchow based on their residence within connective tissues and their elongated, spindle-like shape (Kalluri and Zeisberg, 2006). As the most prominent cell type within connective tissues, these mesenchymal cells function to deposit and remodel extracellular matrix (ECM), specify epithelial fate and maturation of tissues, facilitate granulation of tissues post wounding and promote re-epithelialization (Baglole et al., 2006; Bellini and Mattoli, 2007; Desmouliere et al., 2005; Dvorak, 1986; Silzle et al., 2004). Fibroblasts are required for mammary gland development, as signals from the underlying primary mesenchyme are required to induce mammary placode elongation and invasion to form the primitive mammary ductal tree (Arendt et al., 2010).

In addition to regulating and maintaining tissue homeostasis, fibroblasts are well established mediators of tissue fibrosis following injury and promoters of epithelial tumor growth. During fibrosis, the acquisition of epigenetic alterations (Bechtel et al., 2010) results in fibroblasts with altered gene expression, conferring an increase in growth factor production, ECM deposition, and proliferation (Krenning et al., 2010). During carcinoma progression, the

associated desmoplastic stroma includes an abundance of αSMA+ expressing fibroblasts, collectively referred to as cancer associated fibroblasts (CAFs). These cells are also found in connective tissues during wound healing and are frequently termed “myofibroblasts”. These αSMA+ fibroblasts isolated from the stroma of solid tumors can significantly promote the growth of breast (Orimo et al., 2005; Orimo and Weinberg, 2006; Shimoda et al., 2010), prostate (Olumi et al., 1999), pancreas (Hwang et al., 2008), and skin cancer cells in mice (Erez et al., 2010). Some of these CAF mediated tumor promoting mechanisms have been established, such as increasing tumor angiogenesis and mediating macrophage recruitment, both of which serve as a prominent sources of growth factors and cytokines for the growth of tumor cells (Liao et al., 2009). Recently, αSMA+ myofibroblasts have also been shown to possess a pro-inflammatory phenotype (Erez et al., 2010), suggesting that these cells may contribute to the tumor associated inflammation that accompanies the progression of tumors.

Despite the established functions of fibroblasts in tissue homeostasis and disease, the molecular mechanisms contributing to the phenotypic and functional heterogeneity among fibroblasts remains largely unknown. It has been reported that the gene expression of fibroblasts derived from disease- free breast tissue harbors a greater heterogeneity than those derived from breast carcinomas, even within the same patient (Bauer et al., 2010). This is surprising, given that breast tumors are heterogeneous and there exists significant heterogeneity among the expression of αSMA within the tumor associated stroma (Micke and Ostman, 2005). While αSMA is a common marker routinely used to identify CAFs, these

cells may vary in the levels of αSMA expression (Sugimoto et al., 2006), and it remains unknown if robust expression of αSMA marks the most tumor promoting fibroblasts within a given fibroblast population. It also should be noted that several cell types in the tumor microenvironment, in addition to fibroblasts, will express αSMA (Bissell and Radisky, 2001; Radisky et al., 2001; Radisky et al., 2007), and it is not a unique marker of CAFs or myofibroblasts. Moreover, it is well established that fibroblasts isolated from homeostatic tissues will acquire αSMA expression and stress fibers, resembling the phenotype of myofibroblasts when explanted in culture, exposed to TGFβ, or exposed to tumor cell conditioned media (Ronnov-Jessen et al., 1995; Ronnov-Jessen et al., 1990; Webber et al., 2010). Because of this, maintaining the phenotypic and functional discrepancy of fibroblasts from homeostatic versus diseased tissues in culture has been extremely difficult.

Intriguingly, αSMA+ fibroblasts isolated from tumor associated stroma are not the only source of fibroblasts that harbor the capacity to support epithelial tumor growth. Fibroblasts isolated from arthritic synovium can promote growth of co-mixed human breast cancer cells in a xenograft mouse model of breast cancer (Hu et al., 2009). However, there are numerous examples to demonstrate the tumor suppressive function of fibroblasts as well. For example, ras-transformed mouse keratinocytes are unable to form tumors in syngeneic animals when they are co-mixed with dermal fibroblasts isolated from disease-free mouse skin (Dotto et al., 1988); initiated primary human prostate epithelial cells do not form tumors under the renal capsule when co-mixed with fibroblasts

from disease free human prostate tissues, unlike their CAF counterparts (Olumi et al., 1999). These functional discrepancies among fibroblast populations remain to be reconciled.

In this manuscript, we sought to understand the properties of breast fibroblasts that contribute to a tumor promoting phenotype. Using fibroblast populations isolated from both disease-free and breast tumor tissues, we demonstrate for the first time that the ability of fibroblasts to promote tumor growth is irrespective of αSMA expression or tissue source, but correlates with the ability of these cells to secrete PGE2 and respond to PGE2 signaling. These data may lend insight into the dichotomy among the tumor promoting or tumor suppressive functions of various fibroblast populations, and warrants the investigation of novel markers for these cells among heterogeneous fibroblast populations. Discovery of such markers may elucidate which patients in the clinic would largely benefit from an adjuvant therapy targeting both the eradication of tumor cells and the tumor promoting fibroblasts within the tumor stroma.

2.3 Results

2.3.a. Isolation and characterization of fibroblasts from human breast tissues.

We obtained fibroblasts from a variety of resected breast tissue samples (Table 2.1): those derived from breast tumor specimens of varying hormone receptor and HER2 status, and those derived from disease-free reduction mammoplasty tissues. Given the inability to prospectively sort for different

Table 2.1: Summary of tissue derived fibroblasts used for this study.

Patient ID	Tissue Source	αSMA Expression	Basal IL-6 Secretion	PGE2 Secretion
A	Mastectomy; ER+/HER2-/BRCA1 carrier	Medium	Low	Medium
C	Mastectomy; ER-/HER2-	Low	Low	High
D	Invasive lobular carcinoma; ND	ND	Low	ND
E	Invasive ductal carcinoma; ER-/PR-/HER2+	Medium	Medium	Medium
F	Lumpectomy; ND	ND	ND	Medium
G	Mastectomy; ER+/HER2-	ND	ND	ND
H	Phyllodes tumor	ND	ND	ND
I	Mammoplasty; disease free	High	Low	Low
J	Mammoplasty; disease free	ND	Medium	Medium
K	Mammoplasty; disease free	Low	Low	High
L	Mammoplasty; disease free	ND	Medium	ND
M	Mammoplasty; disease free	Low	Medium	Medium
N	Mammoplasty; disease free	Medium	ND	ND

SMA expression is defined as: low, <45% positive; medium, 45-55% positive; high, >55% positive. ND, not determined.

populations of fibroblasts due to the lack of established and unique cell surface markers for these cells, we used the ability of fibroblasts to preferentially adhere to and grow *ex-vivo* under defined conditions. qRT-PCR and IF were used to characterize and verify that the cells isolated from human breast tissues were indeed enriched in fibroblasts.

We first assayed for the expression of fibroblast and epithelial markers to ascertain the purity of the cultured stromal cells. Cells were largely negative for cytokeratin 18 (CK18) and cytokeratin 14 (CK14) expression (Fig. 2.1A, Supplemental Fig. 2.1B), indicating these cells were devoid of breast epithelial cells, and expressed robust vimentin and prolyl-4-hydroxylase (P4H) (Fig. 2.1B and Supplemental Fig. 2.1). In addition to these fibroblast markers, we also assayed for the expression of αSMA, a marker of myofibroblasts and cancer associated fibroblasts (CAFs). Consistent with previous reports, αSMA expression *in vivo* was only present within the stroma associated with breast tumors but not within the stroma of the normal human breast tissues (Fig. 2.1C). However, cultured fibroblasts isolated from all the different patient samples acquired αSMA expression as previously reported (Desmouliere et al., 1992; Ronnov-Jessen and Petersen, 1993; Ronnov-Jessen et al., 1990); expression was similar among patient derived fibroblasts despite differences in expression *in vivo*. Interestingly, none of the patient derived fibroblasts, regardless of the tissue source of origin, were more than 50% αSMA positive as measured by IF (Fig. 2.1B); there was no significant difference in αSMA expression among these patient samples (Fig. 2.1B, $p=0.1433$). We corroborated these IF results by

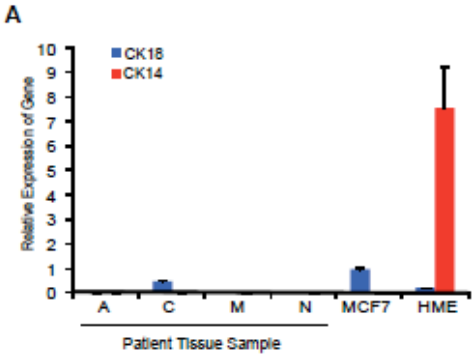
A
CK18
CK14
Relative Expression of Gene
10
9
8
7
6
5
4
3
2
1
0
A
C
M
N
MCF7
HME
Patient Tissue Sample

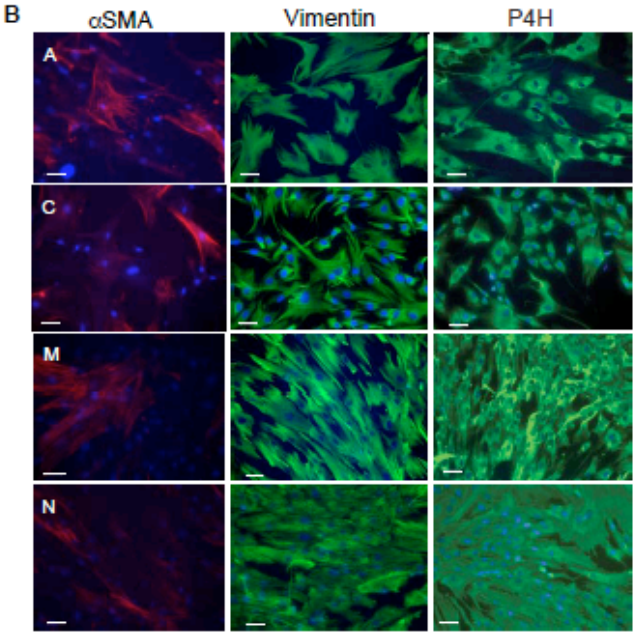
B
αSMA
Vimentin
P4H
A
C
M
N

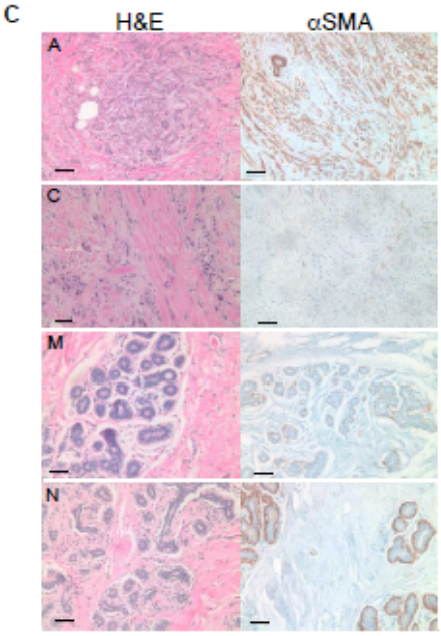
C
H&E
αSMA
A
C
M
N

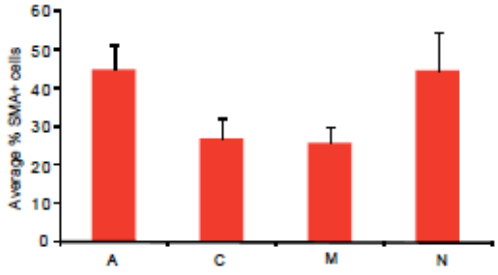
Average % SMA+ cells
60
50
40
30
20
10
0
A
C
M
N

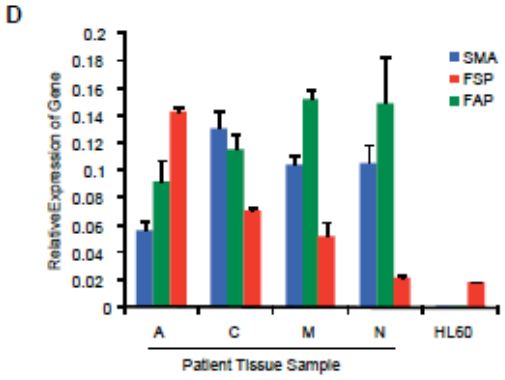
D
RelativeExpression of Gene
0.2
0.18
0.16
0.14
0.12
0.1
0.08
0.06
0.04
0.02
0
SMA
FSP
FAP
A
C
M
N
HL60
Patient Tissue Sample

<u>Figure 2.1:</u> Characterization of patient derived fibroblasts from human breast tumor tissues and reduction mammoplasty tissues.

(A) Quantitative RT-PCR for the relative levels of breast epithelial markers CK18 and CK14 transcripts in tissue derived fibroblasts from patient samples A, C, M and N. MCF7 and immortalized human mammary epithelial cells (HME) serve as positive controls for CK18 and CK14, respectively. **(B)**, Top, IF for the expression of mesenchymal markers vimentin and prolyl-4-hydroxylase (P4H) in tissue-derived fibroblasts from patient samples A, C, M and N. Nuclei are stained with DAPI. Scale bar, 50 μm. Bottom, quantification of the percentage of αSMA+ cells per total number of cells in a given field. **(C)**, H&E stains and αSMA immunohistochemistry of human breast tumor tissue sections (A, C) and human reduction mammoplasty tissue sections (M, N) from which fibroblasts were derived. Scale bar, 50 μm. **(D)** Quantitative RT-PCR for the relative levels of αSMA, FAP, and FSP transcripts in tissue-derived fibroblasts from patient samples A, C, M and N after propagating *in vitro*. HL60 cells are shown as a negative control. Statistics were performed with a single factor ANOVA, p=0.143).

quantitative RT-PCR (Fig. 2.1D). Moreover, to avoid the confounding effects of serum-induced αSMA expression in cultured cells, we serum starved patient derived fibroblasts for 96 hours. Even under serum starvation conditions for this extended period of time, the levels in αSMA expression between these patient samples did not change (data not shown).

Recently, fibroblast specific protein (FSP) and fibroblast activation protein (FAP) have been reported to distinguish different types of fibroblasts in tumor tissues. Therefore, we also examined FSP and FAP expression in breast tissue derived fibroblasts. Both CAFs and normal fibroblasts harvested from several different patient samples expressed high transcript levels of these two proteins (Fig. 2.1D).

Given that αSMA, FSP or FAP expression *in vitro* could not distinguish fibroblasts isolated from human breast tumor specimens versus fibroblasts isolated from disease-free human breast tissues, we sought to identify other proteins whose expression may be enriched in one tissue source or the other. Recently, expression of Caveolin-1 has been reported to be downregulated in CAFs compared to disease-free fibroblasts, and loss of Caveolin-1 in mammary stromal fibroblasts promotes a tumor promoting, CAF-like phenotype (Sotgia et al., 2009; Trimmer et al., 2011; Witkiewicz et al., 2009). However, we found robust expression of Caveolin-1 in fibroblasts from both breast tumor specimens and disease-free tissues, indicating that, similar to αSMA, this protein could not distinguish between these cell types *in vitro* (Supplemental Fig. 2.1).

2.3.b. An inflammatory phenotype correlates with fibroblast tumor promoting ability.

Given the lack of differences in marker expression between fibroblasts isolated from breast tumor tissues versus fibroblasts isolated from disease-free breast tissues, we sought to assay for functional differences in promoting mammary tumor growth *in vivo.* Accordingly, we co-mixed fibroblasts from 5 different tissue sources (patients A, C, E, I and K) with weakly tumorigenic, estrogen-dependent MCF7 cells, and inoculated ad-mixed cells into the inguinal mammary fat pad of female NOD/SCID mice. Fibroblasts derived from tissue samples C, K, and E co-mixed with MCF7 cells formed larger tumors than MCF7 cells injected alone, whereas fibroblasts derived from tissue sample I failed to support MCF7 tumor growth, and only supported tumor formation 50% of the time (Fig. 2.2A, 2.2B). Thus, tumor promoting ability of fibroblasts did not depend on their tissue source of origin (i.e. breast tumor or reduction mammoplasty, Table 2.1), nor did it associate with their extent of αSMA, FSP, FAP, or Caveolin-1 expression (Fig. 2.1 and Supplemental Fig. 2.1).

Based on these findings, we sought to identify characteristics of these tissue derived fibroblasts that could resolve the differences in their ability to support MCF7 tumor growth. Recent reports have indicated that CAFs express an NFκB mediated pro-inflammatory secretome that is required for their ability to support tumor growth (Erez et al., 2010). Thus, we hypothesized that fibroblasts differ in their inherent pro-inflammatory state, which might account for their tumor promoting capabilities *in vivo*. In fact, all tissue-derived fibroblasts *in vitro*,

A

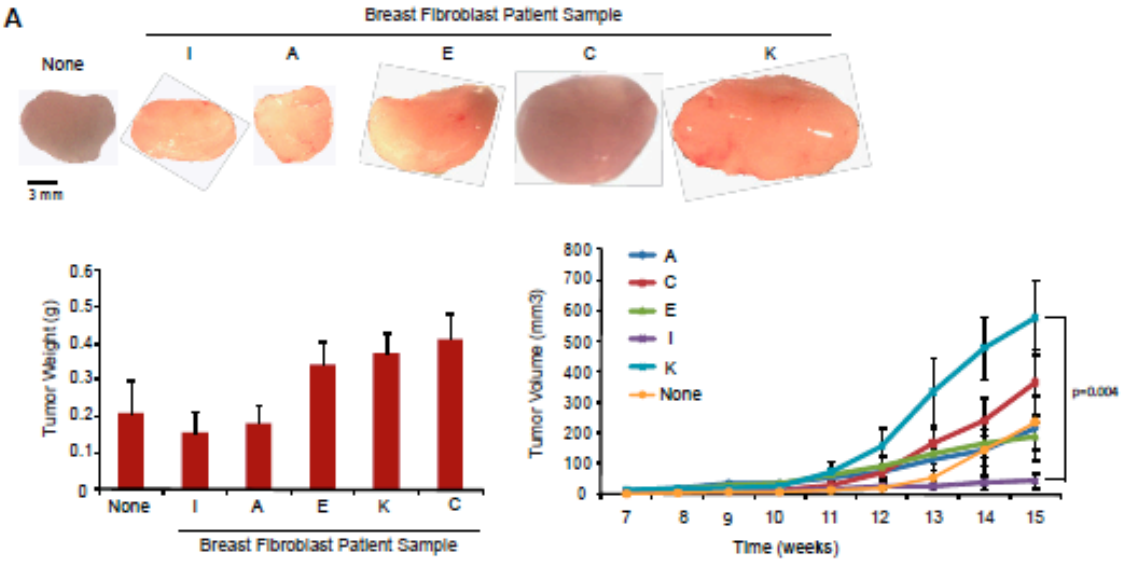

B

Fibroblast	Frequency	Tumor* Incidence
A	10/10	100%
C	8/8	100%
E	10/10	100%
I	4/8	50%
K	4/4	100%
none	2/4	50%

* Tumors are defined as palpable masses > 3mm in diameter

C

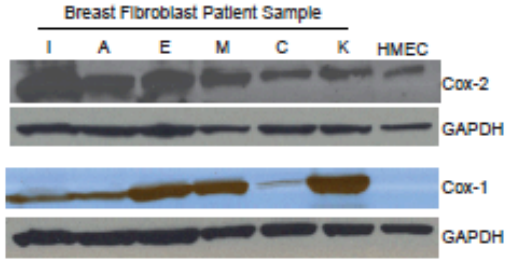

D

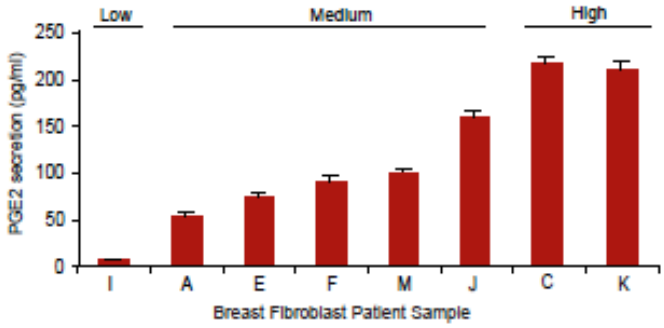

<u>Figure 2.2:</u> Fibroblast mediated tumor promotion *in vivo* correlates with PGE2 secretion *in vitro*.

(A) Resected tumors from mice inoculated with a co-mix of tissue-derived fibroblasts from 5 different patients (A, C, E, I, K) and MCF7 breast cancer cells, or MCF7 cells injected alone (none). Scale bar, 3 mm. Bottom left, tumor weights from mice inoculated with with a co-mix of tissue-derived fibroblasts from 5 different patients (A, C, E, I, K) and MCF7 breast cancer cells, or MCF7 cells injected alone (none). Statistics were performed using a single factor ANOVA, p=0.045). Bottom right, average tumor volume (mm^3) from mice inoculated with a co-mix of tissue-derived fibroblasts from 5 different patients (A, C, E, I, K) and MCF7 breast cancer cells, or MCF7 cells injected alone (none), assessed over 16 weeks. Statistics were performed using a Kruskal-Wallis nonparametric ANOVA (p=0.02) followed by a two-tailed t test of means, comparing the volume of tumors derived from MCF7s co-mixed with patient sample K to those derived from MCF7s co-mixed with patient sample I (p=0.004). Error bars, SEM. **(B)** Tumor incidence from mice inoculated with a co-mix of tissue-derived fibroblasts from 5 different patients (A, C, E, I, K) and MCF7 breast cancer cells, or MCF7 cells injected alone (none). **(C)** Cox-2 and Cox-1 western blots of lysates prepared from various tissue-derived fibroblasts. Human mammary epithelial cells (HMECs) are shown as a positive control for Cox-2. **(D)** PGE2- based immunoassay of CM from various tissue-derived fibroblasts. PGE2 concentrations are determined by a set of control standards of known

concentration, according to the manufacturer's instructions. Statistics were performed using a single factor ANOVA ($p=2.84 \times 10^{-12}$). Error bars, SEM.

regardless of their tissue of origin, expressed cyclooxygenase-2 (Cox-2), an enzyme upregulated during tissue inflammation and tumorigenesis (Meric et al., 2006), as well as its isoform Cox-1 (Fig. 2.2C and Supplemental Fig. 2.2). Both Cox-2 and Cox-1 catalyze the synthesis of the pro-inflammatory hormone prostaglandin E2 (PGE2), although Cox-1 is thought to be constitutively expressed in most tissues and likely responsible for producing the levels of prostaglandins required for normal tissue function (Ricciotti and Fitzgerald, 2010).

Given that these tissue-derived fibroblasts express Cox-1 and Cox-2, we assayed for the levels of PGE2 in the conditioned media (CM) from these cells. Fibroblasts from 8 different tissue samples were serum starved for 72 hrs in phenol-red free DMEM, upon which the CM was collected, filtered, and assayed for the concentration of the pro-inflammatory hormone PGE2 by a specific immunoassay. CM from several different tissue samples exhibited significant differences in PGE2 secretion ($p=2.84 \times 10^{-12}$): low (< 50 pg/ml; patient sample I), medium (50-150 pg/ml; tissue samples A, E, F, M, J) or high (>200 pg/ml; tissue samples C, K) (Fig. 2.2D). Intriguingly, we found a correlation between the ability to secrete high levels of PGE2 *in vitro* and the ability to promote MCF7 tumor growth *in vivo*. In fact, there was a statistically significant difference in the ability to support MCF7 tumor growth between high PGE2 secreting fibroblasts (K) compared to low PGE2 secreting fibroblasts (I) ($p=0.004$). These findings

suggest that unlike αSMA, FAP, FSP, or Caveolin-1 expression, the ability to secrete PGE2 may contribute to the tumor promoting phenotype of fibroblasts.

2.3.c. Secreted factors from tumor-promoting fibroblasts expand breast cancer stem-like cells.

It is known that breast tumors are comprised of cells with varying tumorigenic potential. Using primary human breast cancer tissues, it has been demonstrated that the $CD44^+/CD24^-/EpCAM^+$ population of cells can support tumor initiation with as few as 100 cells and have self-renewing, stem-like properties (Al-Hajj et al., 2003). These "aggressive" cell populations are retained within commonly used breast cancer cell lines, with MCF7 cells having a basal percentage of 0.03% (Fillmore et al., 2010; Keller et al., 2010). Because high PGE2-secreting fibroblasts support MCF7 tumor growth, we hypothesized that these fibroblasts may secrete factors that expand the most aggressive, tumorigenic cells within the tumor bulk. To determine if fibroblasts could expand this aggressive cell population, we treated MCF7 cells for 6 days with CM isolated from serum starved tissue derived fibroblasts exhibiting varying degrees of PGE2 secretion *in vitro*. We quantified the percentage of aggressive, $CD44^+/CD24^-/EpCAM^+$ stem-like cells by FACS following this 6-day treatment. CM from fibroblasts of varying tumor promoting potential and PGE2 secretion had significant differences in their ability to expand the percentage of aggressive MCF7 cells (Fig. 2.3A, $p=0.0007$). Interestingly, those fibroblasts exhibiting high levels of PGE2 secretion resulted in a significant increase in the proportion of

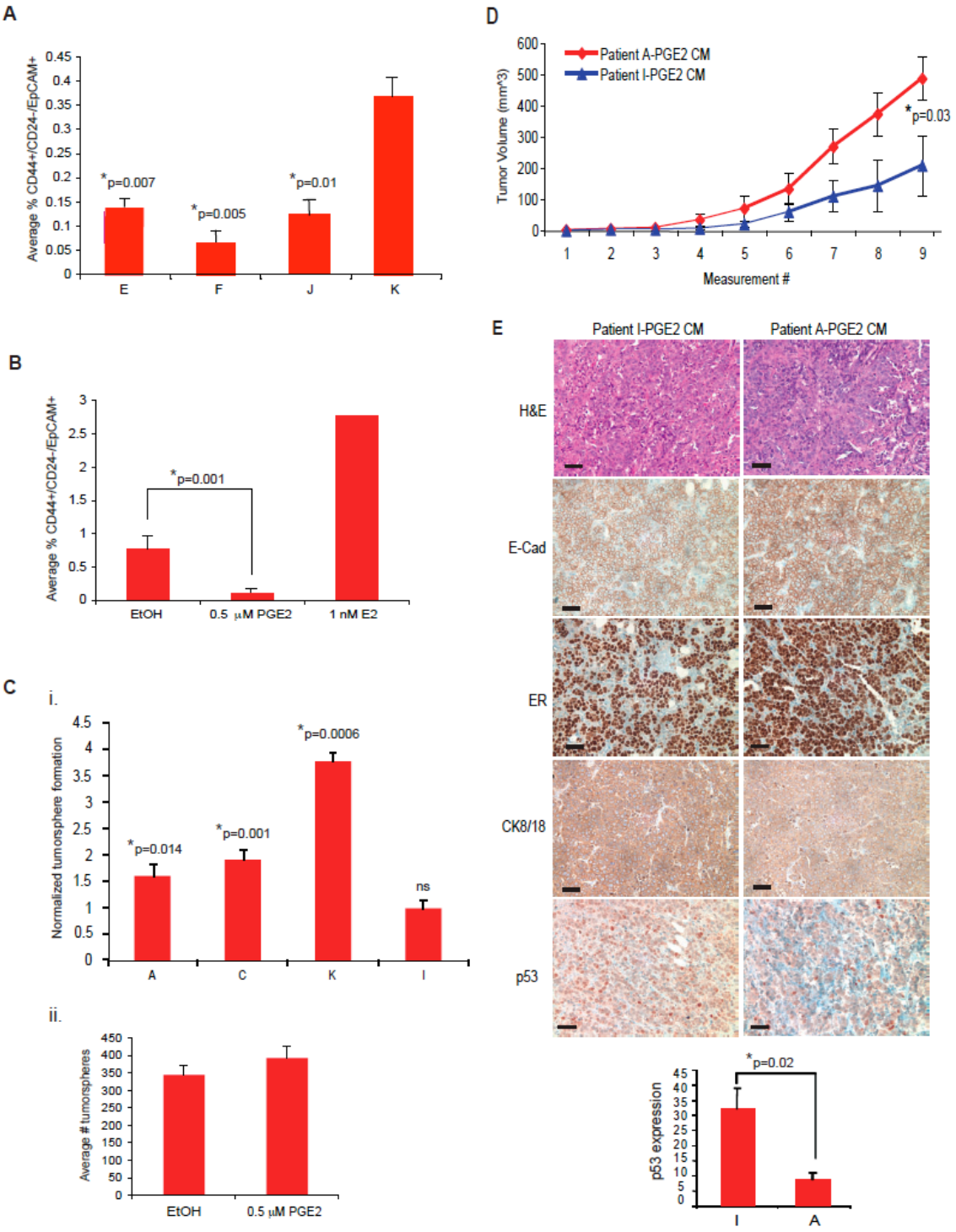
A
Average % CD44+/CD24-/EpCAM+
*p=0.007
*p=0.005
*p=0.01
E
F
J
K
B
Average % CD44+/CD24-/EpCAM+
*p=0.001
EtOH
0.5 μM PGE2
1 nM E2
C
i.
Normalized tumorsphere formation
*p=0.014
*p=0.001
*p=0.0006
ns
A
C
K
I
ii.
Average # tumorspheres
EtOH
0.5 μM PGE2
D
Patient A-PGE2 CM
Patient I-PGE2 CM
Tumor Volume (mm^3)
*p=0.03
Measurement #
E
Patient I-PGE2 CM
Patient A-PGE2 CM
H&E
E-Cad
ER
CK8/18
p53
*p=0.02
p53 expression
I
A

<u>Figure 2.3:</u> PGE2 enhances the tumor promoting properties of breast tissue-derived fibroblasts.

(A) CM from various patient derived fibroblasts (E, F, J, K) were used to culture MCF7s for 6 days. The average percentage of $CD44^+/CD24^-/EpCAM^+$ cells was then assayed by FACS. Statistics were performed using a single factor ANOVA (p=0.007) followed by a Student's two-tailed t test of means: E vs. K, p=0.007; F vs. K, p=0.005; J vs. K, p=0.01. Error bars, SEM. **(B)** MCF7 cells were cultured in either PRF-DMEM + 10% CD-FBS supplemented with 1 nM E2 (positive control), 0.5 μM PGE2, or vehicle for 6 days. The average percentage of $CD44^+/CD24^-/EpCAM^+$ cells was assayed by FACS. Data is plotted as average of 3 independent experiments. Statistics were performed using a Student's two tailed t test of means: EtOH vs. PGE2, p=0.001. Error bars, SEM. **(C)** Quantification of MCF7 tumorspheres formed in the presence of CM from PGE2- or EtOH-fibroblasts from patient samples A, C, K, and I. Quantification was performed using a Beckman Coulter Multisizer and plotted as a fold induction over vehicle. Statistics were performed using a single factor ANOVA ($p=3.25 \times 10^{-5}$) followed by a Student's two-tailed t test of means comparing EtOH vs PGE2 for each patient sample: A, p= 0.014; C, p= 0.001; K, p=0.0006; I, not significant). Error bars, SEM. **(D),** Tumor growth curves of 10^4 MCF7 cells primed *in vitro* with CM from PGE2-treated fibroblasts from patient sample A (A-PGE2 CM) or CM from PGE2-treated fibroblasts from patient sample I (I-PGE2 CM). Statistics were generated using a Student's two-tailed t-test of means; p=0.03. Error bars, SEM **(E)** Top, H&E stains and immunohistochemical analysis (E-cadherin, ER,

CK8/18, p53) of tumors (200X). Scale bar, 50 μm. Bottom, quantification of the percentage of p53 positive cells within a given field based on the tumor sections from **(D)** Statistics were performed using a Student's two-tailed t-test of means, p=0.02).

aggressive MCF7 cells compared to those fibroblasts that had medium or low secretion of PGE2 *in vitro* (E vs K, p=0.007; F vs K, p=0.005; J vs K, p=0.01). Moreover, the ability to expand $CD44^+/CD24^-/EpCAM^+$ cells was associated with the ability to support MCF7 tumor growth *in vivo* (Fig. 2.3A and Fig. 2.2A, respectively).

Recently, it has been reported that PGE2 is necessary for the expansion of bone marrow hematopoietic stem cells (North et al., 2007). Since fibroblasts exhibiting high levels of PGE2 secretion also exhibited the most robust increase in cancer stem-like cells and promoted the largest MCF7 tumor formation, we reasoned that paracrine production of PGE2 by fibroblasts might be sufficient to expand $CD44^+/CD24^-/EpCAM^+$ MCF7 stem-like cells. Therefore, we treated MCF7 cells with 0.5 μM PGE2, 1 nM 17-β-estradiol (E2, positive control), or EtOH (vehicle) for 6 days, and quantified the percentage of $CD44^+/CD24^-/EpCAM^+$ cells by FACS. We found, however, that PGE2 alone was not sufficient to expand aggressive MCF7 cells (Fig. 2.3B).

Given the striking association between the ability of fibroblasts to secrete PGE2 *in vitro* and the ability to expand $CD44^+/CD24^-/EpCAM^+$ cells and support tumor growth, we speculated that perhaps PGE2 signaling enhances the tumor promoting phenotypes of fibroblasts. To test this hypothesis, we chose to examine the CM from fibroblast patient samples who did not robustly enhance the growth of MCF7 breast cancer cells *in vivo* (patient samples A and I, Fig. 2.2A). First, we confirmed that these tissue-derived fibroblasts express prostanoid receptors EP1, EP2, EP3 and EP4, making them sensitive to PGE2

signaling (Supplemental Fig. 2.3A). Next, we exposed these tissue-derived fibroblasts to exogenous 0.5 μM PGE2 or EtOH (vehicle) for 72 hours before harvesting CM. We then exposed MCF7 cells to this CM for 6 days before quantifying the population of $CD44^+/CD24^-/EpCAM^+$ cells by FACS. Interestingly, exposure to PGE2 before CM collection significantly augmented the ability of tissue sample A to increase the percentage of $CD44^+/CD24^-/EpCAM^+$ cells (Supplemental Fig. 2.3B), suggesting that PGE2 enhanced fibroblast tumor promoting ability. However, exposure to PGE2 did not significantly enhance the ability of tissue sample I to increase expansion of $CD44^+/CD24^-/EpCAM^+$ cells (Supplemental Fig. 2.3B), despite prostanoid receptor expression (Supplemental Fig. 2.3A).

We also performed *in vitro* and *in vivo* functional assays of MCF7 tumorgenicity using CM from PGE2- or vehicle (EtOH) treated fibroblasts. Specifically, MCF7 cells were grown under non-adherent culture conditions to promote tumorsphere formation in the presence of CM from PGE2- or vehicle (EtOH) treated fibroblasts of varying tumor promoting capability and endogenous PGE2 secretion status. As expected, CM from PGE2 treated tissue derived fibroblasts (tissue samples A, C and K), formed significantly more tumorspheres than those treated with CM from vehicle treated fibroblasts (A, $p=0.014$; C, $p=0.001$; K, $p=0.0006$; Fig. 2.3C). However, CM from fibroblasts derived from tissue sample I did not significantly enhance MCF7 tumorsphere formation when primed with exogenous PGE2 (Fig. 2.3C), consistent with the inability to further enhance $CD44^+/CD24^-/EpCAM^+$ cell expansion (Supplemental Fig. 2.3B).

Importantly, 0.5 μM PGE2 was not sufficient to enhance MCF7 tumorsphere formation compared to vehicle control (Fig. 2.3C).

We also sought to demonstrate that fibroblasts primed with PGE2 promote the aggressiveness of MCF7 cells *in vivo*. To this end, we exposed MCF7 cells first *in vitro* to CM from PGE2-treated tissue sample A, or CM from PGE2-treated tissue sample I, for 6 days to enrich for aggressive $CD44^+/CD24^-/EpCAM^+$ cells. After 6 days, 10^4 cells from each cohort were inoculated into the inguinal mammary gland of NOD/SCID mice. MCF7 cells exposed *in vitro* to CM from PGE2-treated tissue sample A formed significantly larger tumors than those exposed *in vitro* to CM from PGE2-treated tissue sample I ($p=0.03$, Fig. 2.3D). Histological and immunohistochemical analysis of these tumors revealed that the tumors were all ERα- and E-cadherin-positive with a significant degree of central necrosis, (Fig. 2.3E). Interestingly, tumors derived from MCF7 cells exposed *in vitro* to CM from PGE2-treated tissue sample A exhibited reduced p53 and CK8/18 expression compared to those tumors formed from MCF7 cells exposed to CM from PGE2-treated tissue sample I (Fig. 2.3E, $p=0.02$). Together, these data suggest that PGE2 signaling in fibroblasts enhances their tumor promoting abilities, resulting in expansion of aggressive tumor cell populations and increased tumor growth.

2.3.d. PGE2 mediated IL-6 secretion by tumor-promoting fibroblasts.

Since PGE2 alone was not sufficient to confer expansion of aggressive cancer stem-like cells (Fig. 2.3A), we hypothesized factors produced from PGE2-

stimulated fibroblasts were essential for this expansion. To identify the secreted proteins mediating breast cancer stem-like expansion, we examined the conditioned media from PGE2-treated or vehicle-treated tissue derived fibroblasts from patient A, and quantitatively assayed for 164 secreted growth factors and cytokines using an antibody-based protein array. We observed that the secretion of IL-6 was increased at least 5 fold upon PGE2-treatment compared to vehicle-treated control (Supplemental Fig. 2.4A).

To more comprehensively assess whether PGE2 treated fibroblasts secrete IL-6, we performed both qualitative and quantitative assays. We first isolated CM from PGE2 or vehicle treated fibroblasts from 3 patient derived tissue samples (C, A, and G), concentrated the CM, and immunoblotted for IL-6 (Fig. 2.4A). Nearly all patient samples showed an increase in IL-6 secretion upon exposure to PGE2, supporting the cytokine array results. For a more quantitative assessment of IL-6 secretion, we performed a human specific IL-6 ELISA with CM prepared from various breast tissue derived fibroblasts treated with either 0.5 μM PGE2 or EtOH (vehicle) for 3 days. Although the fold induction of IL-6 secretion in response to PGE2 was heterogeneous among tissue derived fibroblasts, nearly all patient samples showed at least a 1.5 fold increase in IL-6 secretion upon treatment with PGE2 (Fig. 2.4B). However, the induced secretion of IL-6 by PGE2 (Fig. 2.4B), as well as the basal levels of IL-6 secretion in these tissue derived fibroblasts (Supplemental Fig. 2.4B) both failed to associate with the tumor promoting abilities of these fibroblasts *in vivo* (Fig. 2.2A), or their ability to secrete PGE2 *in vitro* (Fig. 2.2C). Collectively, these data suggest that unlike

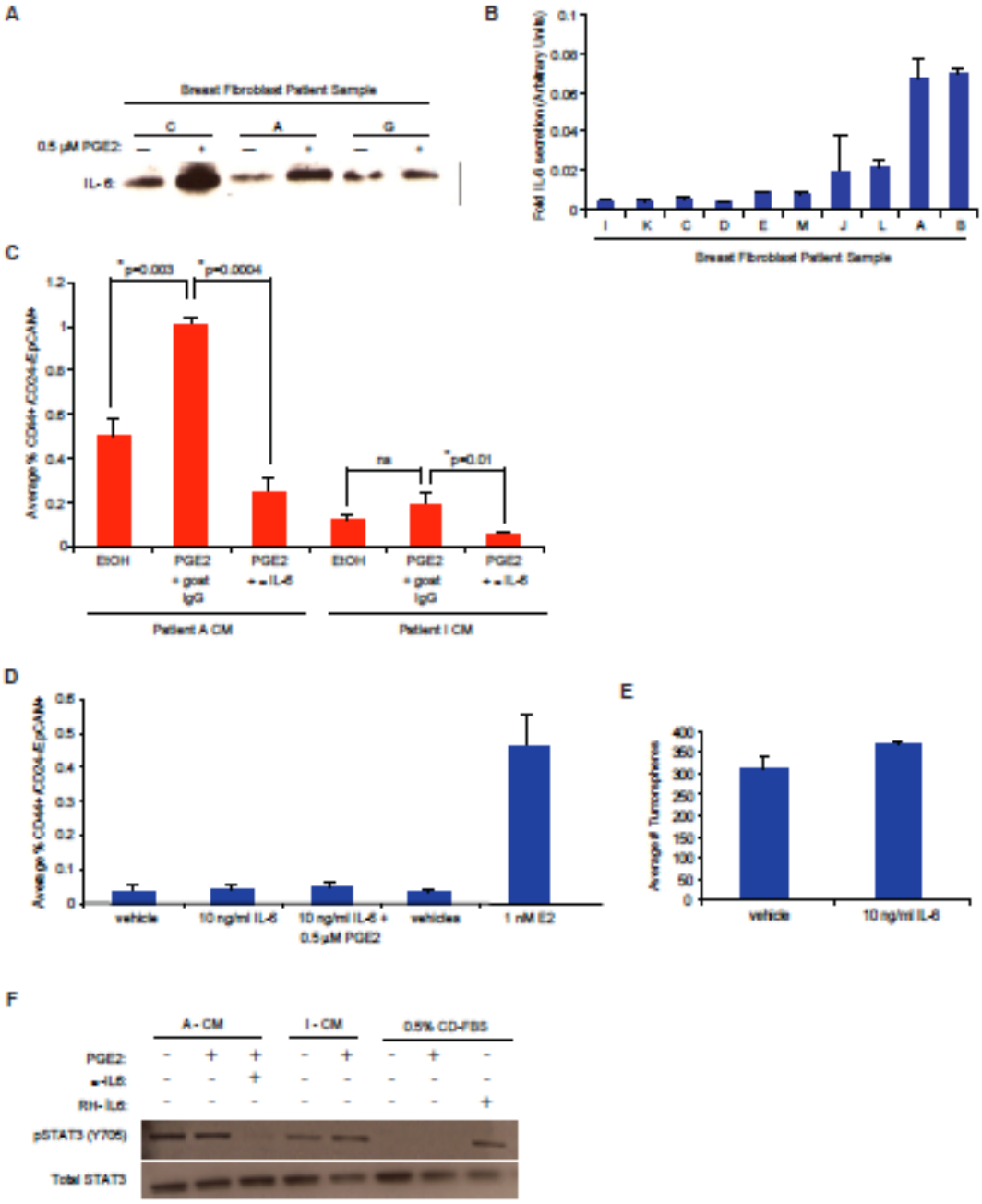
A
Breast Fibroblast Patient Sample
C
A
G
0.5 μM PGE2:
IL-6:
B
Fold IL6 secretion (Arbitrary Units)
I K C D E M J L A B
Breast Fibroblast Patient Sample
C
*p=0.003
*p=0.0004
ns
*p=0.01
Average % CD44+/CD24-/EpCAM+
EtOH
PGE2 + goat IgG
PGE2 + α-IL-6
Patient A CM
Patient I CM
D
Average % CD44+/CD24-/EpCAM+
vehicle
10 ng/ml IL-6
10 ng/ml IL-6 + 0.5 μM PGE2
vehicles
1 nM E2
E
Average # Tumorspheres
vehicle
10 ng/ml IL-6
F
A-CM
I-CM
0.5% CD-FBS
PGE2:
α-IL6:
RH-IL6:
pSTAT3 (Y705)
Total STAT3

Figure 2.4: Tissue-derived fibroblasts secrete IL-6, which is necessary, but not sufficient, for the expansion of $CD44^+/CD24^-/ESA^+$ cells.

(A) Immunoblot for IL-6 expression in CM from tissue derived fibroblasts (from patient samples C, A, G) exposed to either EtOH (vehicle) or 0.5 μM PGE2. **(B)** CM from various tissue derived fibroblasts treated with either 0.5 μM PGE2 or EtOH (vehicle) were assayed for the levels of IL-6 secretion using a human IL-6 ELISA. Concentration is normalized to the cell number post treatment and plotted as the geometric mean of the fold induction (in arbitrary units). Error bars, SEM. **(C)** Quantification of the average percentage of $CD44^+/CD24^-/EpCAM^+$ MCF7 cells after 6 day exposure to CM from PGE2 or EtOH treated fibroblasts from patient sample A (A-CM), or CM from PGE2 or EtOH treated fibroblasts from patient sample I (I-CM) in the presence of either goat IgG (control) or 1.5 μg/ml IL-6 neutralizing antibody. Statistics were performed using a Student's two-tailed t test of means: A-CM, EtOH vs. PGE2, p= 0.003; A-CM, PGE2 vs. α-IL6, p= 0.0004; I-CM, EtOH vs. PGE2, not significant. Error bars, SEM. **(D)** Quantification of the average percentage of $CD44^+/CD24^-/EpCAM^+$ MCF7 cells after 6 day exposure to either 0.1% BSA (vehicle) or 10 ng/ml recombinant human IL-6, alone or in combination with 0.5 μM PGE2 or EtOH (vehicle). Error bars, SEM. **(E)** Quantification of MCF7 tumorspheres formed in the presence of DMEM + 0.1% BSA (vehicle) or 10 ng/ml IL-6. Quantification was performed using a Multisizer-3 coulter counter. **(F)** Western blot of pSTAT3 and total STAT3 in lysates of MCF7 cells exposed for 30 min to CM from fibroblasts from patient A (A-CM) or fibroblasts from patient I (I-CM) treated with either EtOH, PGE2, or

PGE2 plus 1.5 μg/ml α-IL6. MCF7 cells exposed for 30 min to DMEM + EtOH, PGE2 or 10 ng/ml IL-6 are shown as negative and positive controls for pSTAT3, respectively.

high PGE2 secretion, high basal IL-6 secretion or PGE2 mediated induction of IL-6 secretion, are not necessarily hallmarks of tumor promoting fibroblasts.

2.3.e. IL-6 is necessary but not sufficient for tumor-promoting fibroblasts to expand stem-like cells.

It has been reported that IL-6 enhances aggressive, stem-like features in sphere-forming populations of human mammary epithelial cells (Sansone et al., 2007), and mediates a positive feedback loop that maintains oncogenic transformation (Iliopoulos et al., 2009). Thus, we suspected it might be an essential cytokine produced by fibroblasts that is required for expansion of $CD44^+/CD24^-/EpCAM^+$ cells. To test this, we exposed MCF7 cells to CM from PGE2- or vehicle (EtOH) treated fibroblasts from tissue sample A and tissue sample I for 6 days in the presence of an IL-6 neutralizing antibody (αIL-6) or goat IgG control. Quantifying the percentage of $CD44^+/CD24^-/EpCAM^+$ cells by FACS revealed that PGE2 significantly enhanced the ability of fibroblasts from tissue sample A to support expansion of $CD44^+/CD24^-/EpCAM^+$ cells ($p=0.003$, Fig. 2.4C) in an IL-6 dependent manner, as the expansion was attenuated in the presence of an IL-6 neutralizing antibody (αIL-6, $p=0.0004$). PGE2 did not enhance the ability of fibroblasts from tissue sample I to support $CD44^+/CD24^-/EpCAM^+$ cell expansion, despite some IL-6 present in the CM (Fig. 2.4C).

Given that IL-6 is necessary for fibroblast mediated expansion of $CD44^+/CD24^-/EpCAM^+$ cells, we asked if IL-6 was sufficient to confer this expansion. We treated MCF7 cells with 10 ng/mL recombinant human IL-6 or

0.1% BSA (vehicle), in either the presence or absence of 0.5 μM PGE2 or EtOH (vehicle). Interestingly, IL-6 alone, or in combination with 0.5 μM PGE2, was not sufficient to expand $CD44^+/CD24^-/EpCAM^+$ MCF7 cells, unlike 1 nM E2 (Fig. 2.4D). Also, IL-6 alone was not sufficient to confer increases in MCF7 tumorsphere formation (Fig. 2.4E). To confirm that MCF7 cells were capable of signaling through IL-6, we exposed MCF7 cells for 30 min to CM from PGE2 or EtOH treated fibroblasts of differing tumor-promoting capabilities, in the presence of an IL-6 neutralizing antibody or goat IgG control, and immunoblotted for the levels of phosphorylated STAT3 as an indicator of the IL-6 signaling pathway. pSTAT3 levels were higher in MCF7 cells exposed to CM from PGE2-treated fibroblasts from patient sample A as compared to CM from PGE2-treated fibroblasts from tissue sample I, and this was abrogated by addition of αIL-6. Moreover, 0.5 μM PGE2 was not sufficient to induce pSTAT3 expression, unlike the addition of 10 ng/mL recombinant human IL-6 (Fig. 2.4F). Collectively, these data indicate that IL-6 is enriched in CM from several patient tissue-derived fibroblasts, secreted by fibroblasts in response to PGE2, and is necessary, but not sufficient, for fibroblast-mediated expansion of $CD44^+/CD24^-/EpCAM^+$ MCF7 cells.

2.4 Discussion

Several studies have implicated fibroblasts as potent tumor promoting stromal cells through their ability to modulate the tumor microenvironment (Liao et al., 2009) and to promote the growth of cancer cells (Erez et al., 2010; Hwang

et al., 2008; Kojima et al., 2010; Olumi et al., 1999; Orimo et al., 2005). However, there also exists substantial evidence that fibroblasts from disease-free tissues have potent tumor suppressive properties (Proia and Kuperwasser, 2005). The characteristics of these fibroblasts that contribute to either a tumor promoting or tumor suppressive phenotype remain to be reconciled. In this study, we identified both fibroblast mediated PGE2 secretion and autocrine PGE2 signaling as a novel tumor promoting characteristic of these cells. Moreover, we identify a novel tumor promoting mechanism of these cells that is enhanced upon exposure to PGE2: the ability to secrete factors (such as IL-6) that are essential for the expansion of $CD44^+/CD24^-/EpCAM^+$ breast cancer cells.

There exist a number of citations to substantiate the notion that fibroblasts harvested from resected breast tumor specimens are αSMA+ and promote tumor growth *in vivo* (reviewed by (Orimo and Weinberg, 2006; Shimoda et al., 2010). These cells, commonly referred to as cancer associated fibroblasts (CAFs), lack specific markers to discriminate them from fibroblasts isolated from disease free tissues, because these normal fibroblast counterparts acquire the expression of αSMA when grown *in vitro*. Despite this, αSMA has become a widely used marker to discriminate these cells. We harvested both types of fibroblasts: fibroblasts from human breast tumors (CAFs), and fibroblasts from disease free reduction mammoplasty tissues; we confirmed that these cells differ drastically in αSMA expression *in vivo* (consistent with previous reports) but lacked significant differences in αSMA expression *in vitro*.

Despite similar αSMA expression *in vitro*, both sources of fibroblasts had differences in their tumor promoting abilities *in vivo*. Because tumor-promoting ability did not associate with robust αSMA expression, nor did it associate with tissue source, we sought for other characteristics of fibroblasts that may influence fibroblast tumor promoting abilities. Because fibroblasts isolated from dysplastic mouse skin support squamous cell carcinoma growth *in vivo* through pro-inflammatory cytokine secretion (Erez et al., 2010), we suspected that inflammatory mediators differ among the various patient derived fibroblasts, which ultimately influence their varying degrees of tumor promotion. Indeed, we found an association between tumor promoting ability *in vivo* and high PGE2 secretion *in vitro*. In addition, the ability to secrete PGE2 *in vitro* associates with the ability to expand $CD44^+/CD24^-/EpCAM^+$ breast cancer cells.

Interestingly, PGE2 alone was not sufficient to confer the expansion of these cells, despite MCF7 expression of the prostanoid receptors. PGE2 enhanced the inherent tumor promoting abilities of fibroblasts as shown by *in vitro* tumorsphere assays, and *in vivo* MCF7 limiting dilution experiments. Our data suggest that this is largely due to the increased secretion of IL-6 in response to PGE2, consistent with previous reports (Singh et al., 1999). The secretion of IL-6 by fibroblasts was necessary for expansion of $CD44^+/CD24^-/EpCAM^+$ cells. Because this particular cell population has been shown to contribute to tumorsphere formation and seed tumor growth at limiting dilution (Fillmore et al., 2010; Fillmore and Kuperwasser, 2008), we suspect that PGE2- mediated IL-6 secretion by fibroblasts was largely responsible for the increased MCF7

tumorsphere formation and tumor formation observed upon exposure to fibroblast CM.

Despite the requirement for IL-6 in mediating the tumor promoting abilities of fibroblasts, we found that IL-6 alone was not sufficient for expansion of $CD44^+/CD24^-/EpCAM^+$ cells in the MCF7 cell line. This is in contrast to previous reports using different breast cancer cell lines (Iliopoulos et al., 2009; Iliopoulos et al., 2011). IL-6 has been implicated in a positive feedback loop that perpetuates cellular transformation through NFκB (Iliopoulos et al., 2009), which may drive the secretion of the other necessary cytokines (in addition to IL-6) that are required for the induction and maintenance of this aggressive cell state. We failed to see activation of NFκB in response to CM from various tissue-derived fibroblasts (data not shown), suggesting that this feedback mechanism may not be activated in these cells, or only activated in various subpopulations (i.e. $CD44^+/CD24^-/EpCAM^+$ cells).

The basal level of IL-6 varied widely among patient derived breast fibroblasts, and also increased with passage number, consistent with previous reports using primary fibroblasts (Coppe et al., 2008). However, neither the basal secretion of IL-6 nor the induced secretion of IL-6 by PGE2 in fibroblasts correlated with fibroblast tumor promoting ability *in vivo* or their ability to expand $CD44^+/CD24^-/EpCAM^+$ cells *in vitro*. This is consistent with the notion that IL-6 is required, but is not sufficient for expansion of $CD44^+/CD24^-/EpCAM^+$ cells, nor is it sufficient for tumorsphere formation. In addition, although IGF-II was significantly induced by fibroblasts exposed to PGE2 more so than IL-6, we failed

to observe a requirement for this cytokine in expansion of $CD44^+/CD24^-/EpCAM^+$ cells (data not shown). In lieu of these data, we speculate that a certain stoichiometric balance of specific cytokines is required to promote the expansion of these cells. This stoichiometric balance may be obtained *in vivo* by secreted factors from tumor cells as well as inflammatory cells in the tumor microenvironment. It therefore follows that non-tumor promoting fibroblasts (i.e., those with very low PGE2 secretion; i.e. tissue sample I) perhaps lack the ability to activate certain pathways downstream of PGE2 that modulate the balance of cytokine secretion required for $CD44^+/CD24^-/EpCAM^+$ cell expansion and tumor promoting ability *in vivo*.

Since PGE2 enhanced fibroblast secretion of IL-6, it is plausible that PGE2 also induces secretion of other cytokines yet to be identified that together in concert with IL-6 orchestrate the process of $CD44^+/CD24^-/EpCAM^+$ cell expansion. For example, SDF1α is a growth factor secreted by myofibroblasts (Orimo et al., 2005) that promotes breast cancer cell growth (Marlow et al., 2008) as well as expansion of $CD44^+/CD24^-$ cells (Huang et al., 2010), and may be upregulated by PGE2 (Katoh et al., 2010). Also, IL-8 increases tumorsphere forming ability and the percentage of ALDEFLUOR-positive breast cancer cells, which enriches for cancer stem-like cell populations (Charafe-Jauffret et al., 2009). Further studies are needed to elucidate if these cytokines contribute to IL-6 mediated expansion of $CD44^+/CD24^-/EpCAM^+$ cells.

In summary, our results indicate that the pro-inflammatory, tumor-promoting phenotype of fibroblasts does not necessarily correlate with high

expression of αSMA, a frequently used marker of myofibroblasts and CAFs. Moreover, we were unable to identify differential expression of well-established markers of CAFs and tumor-promoting fibroblasts that correlated with their observed tumor promoting phenotypes. It is also notable that we failed to identify a correlation between fibroblasts isolated from invasive carcinomas (either ER+ or ER-) and a high PGE2 secreting, tumor promoting phenotype, as compared to those isolated from reduction mammoplasty tissues. Our results suggest that tumor promoting potency of fibroblasts may lie in their endogenous secretion of PGE2 and their ability to mediate autocrine PGE2 signaling, which activates the increased secretion of IL-6, more so than if they are derived from diseased tissues. The identification of specific markers for these tumor promoting fibroblasts would likely allow for the observation of more robust phenotypic discrepancies between various fibroblast tissue sources, and would possibly discriminate among patients that would likely benefit from tumor-associated stroma drug targeting strategies for use as adjuvant therapies in the treatment of human breast cancers.

2.5 Acknowledgements and publication status

This work would not be possible without kind contributions from Lisa M. Arendt, Ina Klebba, John W. Hinds, Vandana Iyer, Piyush B. Gupta, Stephen P. Naber, and Charlotte Kuperwasser. Thank you Grace Gill, Philip Hinds, Jonathan Garlick, Christine Fillmore, Patty Keller, and Jessica McCready for many

insightful discussions leading up to the publication of this manuscript. This work is in press by *PLoS One*.

A

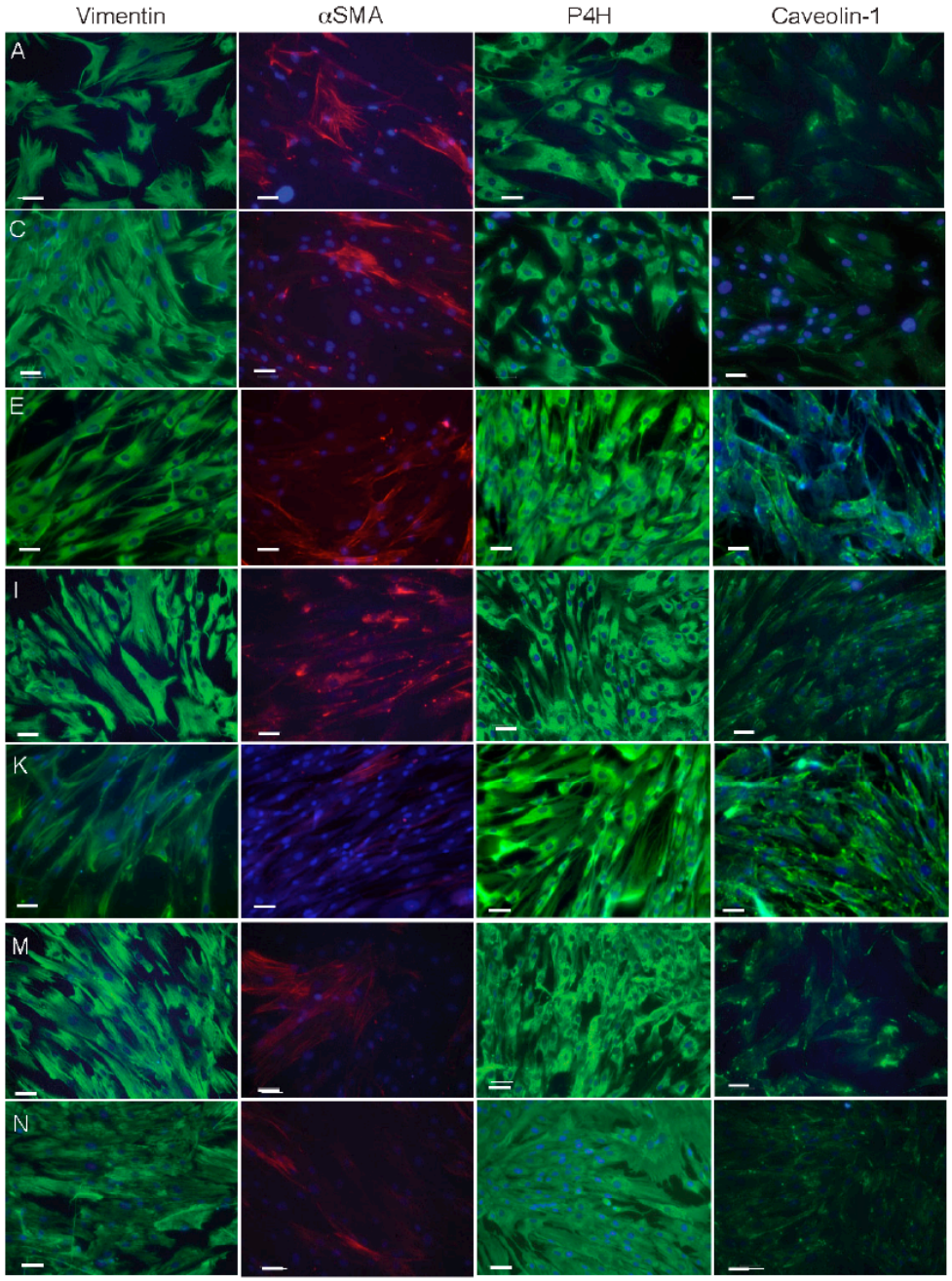
Vimentin
αSMA
P4H
Caveolin-1
A
C
E
I
K
M
N

B

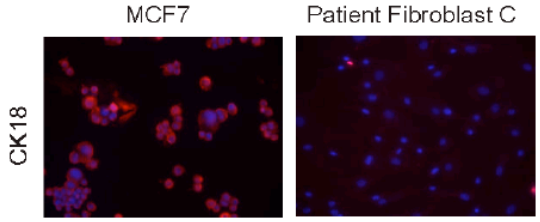
MCF7
Patient Fibroblast C
CK18

<u>Supplemental Figure 2.1:</u> Characterization of patient derived fibroblasts from human breast tumor tissues and reduction mammoplasty tissues. **(A)** IF results for the expression of mesenchymal markers vimentin and prolyl-4-hydroxylase (P4H), and myofibroblast/cancer associated fibroblast markers αSMA and Caveolin-1, in tissue-derived fibroblasts from patient samples A, C, E, I, M, N, and K. Nuclei are stained with DAPI. Scale bar, 50 μm. **(B)** IF results for the expression of the breast epithelial marker CK18 in tissue-derived fibroblasts from patient sample C, which showed high transcript levels of CK18 in Fig. 2-1A. MCF7 cells are a positive control.

A

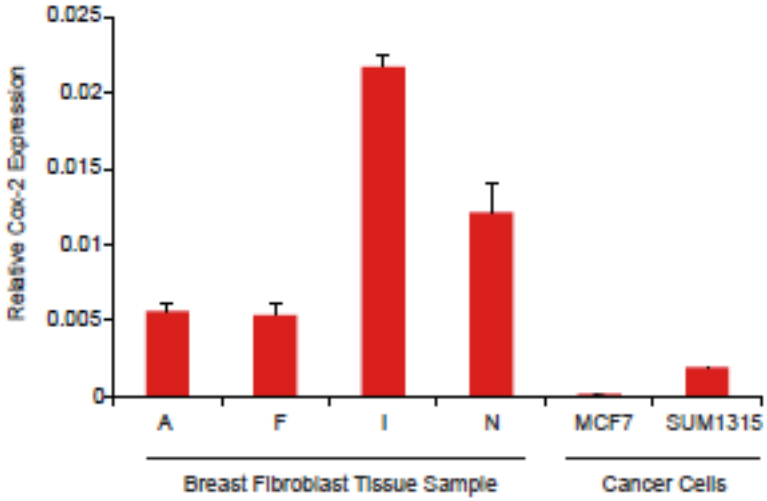
Relative Cox-2 Expression
0.025
0.02
0.015
0.01
0.005
0
A
F
I
N
MCF7
SUM1315
Breast Fibroblast Tissue Sample
Cancer Cells

B

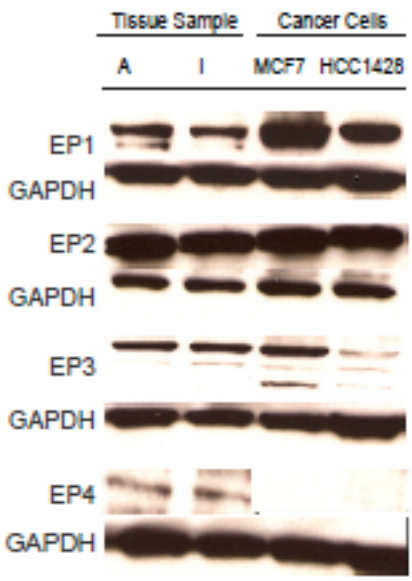
Tissue Sample
Cancer Cells
A
I
MCF7
HCC1428
EP1
GAPDH
EP2
GAPDH
EP3
GAPDH
EP4
GAPDH

<u>Supplemental Figure 2.2:</u> Tissue derived fibroblasts have variable expression of Cox-2 transcript.

(A) qPCR for the relative levels of Cox-2 transcript in tissue derived fibroblasts from patient samples A, N, I and F. MCF7 and SUM1315 breast cancer cells serve as negative and positive controls for Cox-2 expression, respectively. **(B)** Western blot for EP1, EP2, EP3 and EP4 expression in lysates extracted from tissue-derived fibroblasts (patients A and I), MCF7 and HCC1428 breast cancer cell lines.

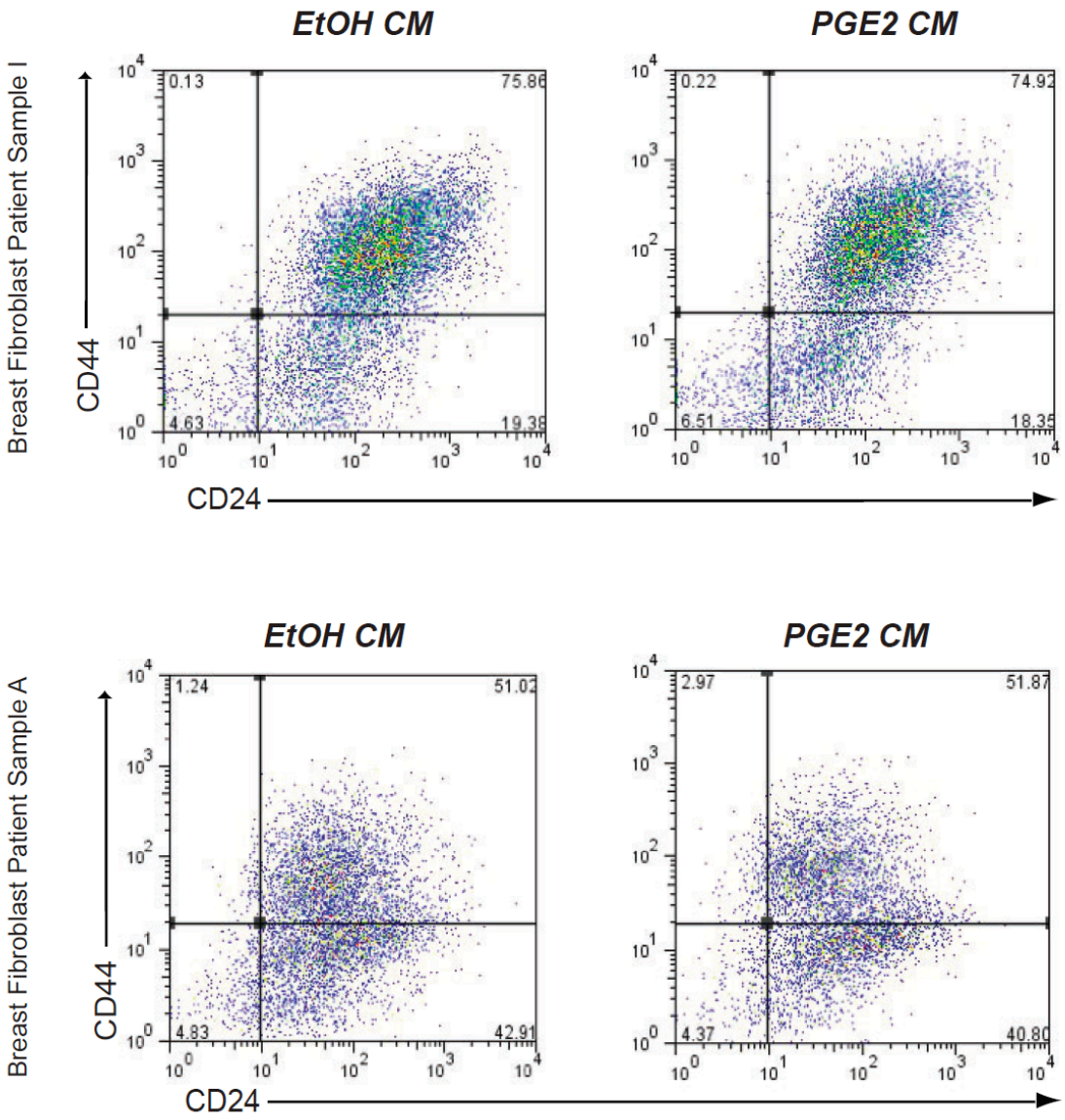
EtOH CM
PGE2 CM
Breast Fibroblast Patient Sample I
CD44
CD24
0.13
75.86
4.63
19.38
0.22
74.92
6.51
18.35
Breast Fibroblast Patient Sample A
1.24
51.02
4.83
42.91
2.97
51.87
4.37
40.80

<u>Supplemental Figure 2.3:</u> PGE2 enhances the ability of fibroblasts to expand $CD44^+/CD24^-/EpCAM^+$ cells.

FACS dot plots of MCF7 cells treated with CM from tissue derived fibroblasts (patient samples A and I) treated with EtOH (vehicle) or 0.5 μM PGE2. Cell populations are gated first for EpCAM+, then for CD44+ and CD24-.

A

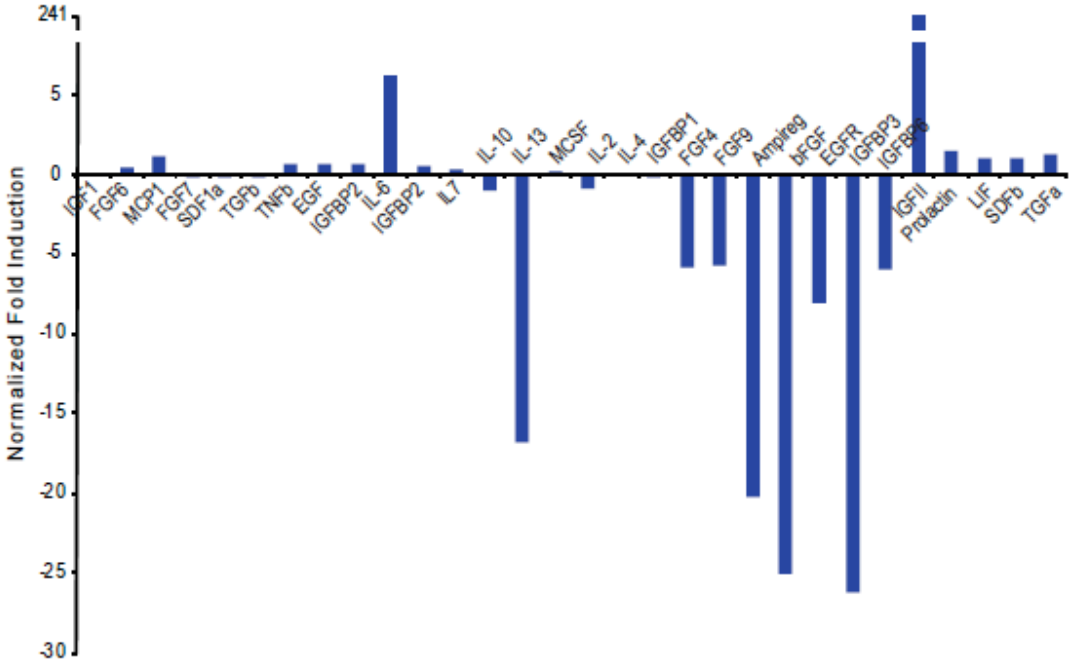
241
5
0
-5
-10
-15
-20
-25
-30
Normalized Fold Induction
IGF1
FGF6
MCP1
FGF7
SDF1a
TGFb
TNFb
EGF
IGFBP2
IL-6
IGFBP2
IL7
IL-10
IL-13
MCSF
IL-2
IL-4
IGFBP1
FGF4
FGF9
Ampireg
bFGF
EGFR
IGFBP3
IGFBP6
IGFII
Prolactin
LIF
SDFb
TGFa

B

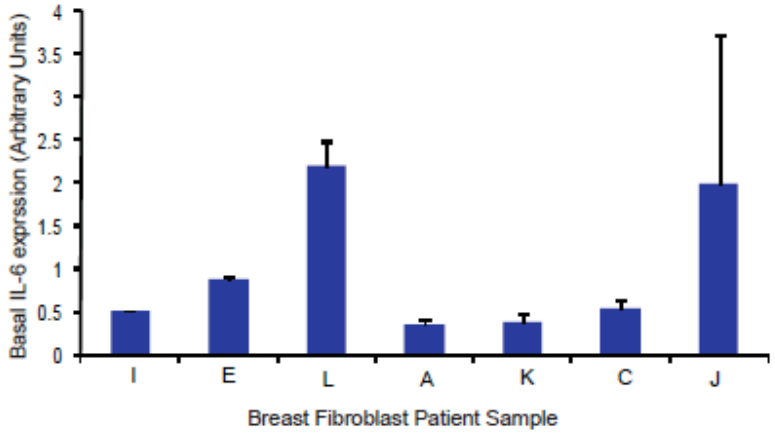
4
3.5
3
2.5
2
1.5
1
0.5
0
Basal IL-6 exprssion (Arbitrary Units)
I
E
L
A
K
C
J
Breast Fibroblast Patient Sample

<u>Supplemental Figure 2.4:</u> Basal levels of IL-6 in various patient derived fibroblasts.

(A) Cytokine array results of CM from PGE2 and EtOH (vehicle) treated fibroblasts (from patient sample A). Data is plotted as a normalized fold induction over vehicle. **(B)** Quantification of the average basal levels of IL-6 secretion by various patient-derived fibroblasts using a human IL-6 ELISA. IL-6 secretion was normalized to the total number of fibroblasts present at the time of CM harvest.

Supplemental Table 2.1: Primer sequences used for qRT-PCR.

Gene	Forward Primer	Reverse Primer
αSMA	5'CAGGGCTGTTTTCCCATCCT3'	5'GCCATGTTCTATCGGGTACTTC3'
FAP	5'AATGAGAGCACTCACACTGAAG3'	5'CCGATCAGGTGATAAGCCGTAAT3'
FSP	5'GATGAGCAACTTGGACAGCAA3'	5'CTGGGCTGCTTATCTGGGAAG3'
CK18	5'TGATGACACCAATATCACACGAC3'	5'TACCTCCACGGTCAACCCA3'
CK14	5'CATGAGTGTGGAAGCCGACAT3'	5'GCCTCTCAGGGCATTCATCTC3'
Cox2	5'TGAGCATCTACGGTTTGCTG3'	5'TGCTTGTCTGGAACAACTGC3'

CHAPTER III:

Differential TGFβ mediated microRNA processing in cancer associated fibroblasts

3.1. Abstract

While breast cancer associated fibroblasts (CAFs) have more robust tumor promoting properties *in vivo* as compared to fibroblasts from disease free breast tissues (RMFs), the molecular mechanisms governing CAF gene expression and phenotype remain largely understood. Reports indicate that genetic alterations in tumor associated stromal cells are extremely rare, although CAFs reportedly have differences in DNA methylation and microRNA (miR) expression compared to fibroblasts from disease-free tissues. These data suggest that CAFs likely utilize alternative mechanisms for regulating differences in gene expression that are required for their tumor promoting phenotype. We hypothesized that induction of certain miRs by growth factors such as TGFβ are specific to CAFs and are required to maintain CAF phenotype. In particular, miR21 is important for maintaining an activated phenotype in both myofibroblasts and fibroblasts from fibrotic tissues and is regulated by TGFβ in these cells. Here, we show that TGFβ induces miR21 expression by promoting the processing of its precursor, pre-miR21, in CAFs. The TGFβ mediated induction of miR21 is specific to CAFs because it is not induced in RMFs, despite similar TGFβ signaling sensitivity in these cell types and similar expressions of miR processing molecules. Pre-miR21 in CAFs associates with key proteins involved in RNA editing. In particular, p100 binds pre-miR21 in a TGFβ dependent manner

and is a known component of the RNA induced silencing complex (RISC). Understanding the differences in miR induction and regulation between CAFs and RMFs may elucidate whether CAFs are epigenetically reprogrammed resident tissue breast fibroblasts, and how miRs govern CAF phenotype.

3.2. Introduction

Within the last decade, it has become widely accepted that tumor cells frequently rely on signals from an activated microenvironment in order to proliferate and survive within a tissue. This activated tissue microenvironment involves the recruitment of various immune cells (macrophages, T cells, B cells, T regulatory cells), EPCs, myeloid cells, and the appearance of αSMA+ fibroblasts (referred to as "cancer associated fibroblasts," (CAFs)). Each of these cell types has been demonstrated to support the growth of tumor cells through use of xenograft mouse models (de Visser et al., 2005; DeNardo et al., 2009; Doedens et al., 2010; Iyer et al., 2011; Olumi et al., 1999; Orimo et al., 2005; Tan et al., 2011).

While systemic signals and tumor derived-chemotactic signals are likely responsible for the recruitment of these bone marrow derived cells, the mechanism describing how CAFs originate at the tumor site remains largely elusive. Evidence supported by the appearance of αSMA+ fibroblasts (myofibroblasts) during wound healing suggests that CAFs originate from BMDCs (possibly fibrocytes) that are recruited to the tumor site and are differentiated into αSMA+ positive fibroblasts (Bellini and Mattoli, 2007; Direkze et al., 2004; Kisseleva et al., 2006; Mori et al., 2005; Phillips et al., 2004; Schmidt

et al., 2003). This differentiation process may be fostered by interactions with other stromal cells within the microenvironment as well as the tumor cells. However, recent studies suggest that only approximately 20% of the CAFs within tumor associated stroma are bone marrow derived (Quante et al., 2011; Worthley et al., 2009), providing speculation for other cellular origins of these cells. Although lacking rigorous evidence at present, it has been hypothesized that an additional source of CAFs may arise from the epigenetic reprogramming of resident breast fibroblasts. Co-evolving with tumor cells over time may influence chromatin remodeling changes within these cells as a consequence of chronic exposure to tumor cell secreted factors and matrix changes that accompany the progression of breast tumors. Indeed, CAFs are found in close association with tumor cells in the tumor microenvironment (Orimo and Weinberg, 2006).

Recent epigenome profiling data may provide insight into the cellular origin of CAFs and their tumor promoting phenotype. CAFs isolated from human breast tumors have differences in DNA methylation compared to fibroblasts isolated from reduction mammoplasty tissues (Allinen et al., 2004), and CAFs isolated from human gastric carcinomas have globally reduced DNA methylation compared to normal gastric myofibroblasts (Jiang et al., 2008). While these methylation profiles are characteristic of CAFs, precisely how these epigenetic alterations contribute to CAF phenotype remains elusive at present.

The contribution of certain microRNAs (miRs) in influencing CAF phenotype is a new area of investigation within the research field of "microenvironmental influences in cancer progression." miRs are a class of short

noncoding regulatory RNAs that are involved in stem cell maintenance, developmental programming and cell fate specification, as well as various disease pathogeneses (Fazi and Nervi, 2008; Gangaraju and Lin, 2009; Leung and Sharp, 2006; Tiscornia and Izpisua Belmonte, 2010). Their altered expression has been implicated in several types of cancers, including breast cancer (Davis and Hata, 2010; Farazi et al., 2011; Iliopoulos et al., 2009; Iliopoulos et al., 2010a; Iliopoulos et al., 2010b; Iorio et al., 2005; Jazbutyte and Thum, 2010; Lu et al., 2008; Pan et al., 2011; Papagiannakopoulos and Kosik, 2008). They are transcribed by RNA polymerase II into long 5' capped and 3' polyadenylated transcripts of several hundred kilobases (referred to as primary microRNAs (pri-miRs)). Within the nucleus, they are then processed by the Drosha microprocessor complex, which yields a ~70 nucleotide precurser hairpin microRNA ("pre-miR") that is exported out of the nucleus by Exportin-5 and Ran-GTP. Once in the cytoplasm, the pre-miR is recognized by the endonuclease Dicer. Dicer, in complex with the double stranded RNA binding proteins TAR RNA binding protein (TRBP) and protein kinase R- activating protein (PACT), cleaves the pre-miR into a double stranded ~22 nucleotide complex, comprised of the mature miRNA guide strand and the miRNA passenger strand. The designation for the mature miRNA guide strand, which will load onto the RISC, is based on the thermodynamic properties of the miR-miR complex; the passenger strand is degraded.

The primary component of the RISC and the effectors of miR-mediated regulation of gene expression, are the Argonaute (Ago) proteins. There are 8

Ago proteins in the human genome, although Ago2 is the only one with RNA cleavage and likely plays a prominent role in miR target recognition. Ago2 associates with Dicer, TRBP, and PACT to form the RISC loading complex (RLC), which loads the miR-miR duplex from Dicer onto the RISC (Davis and Hata, 2009). Once the mature miR is loaded onto the RISC, it serves to recognize target mRNAs that have semi-complementarity within their 3' untranslated regions (UTRs). This recognition triggers translational downregulation and/or increased degradation of the target mRNA (Davis and Hata, 2009) (Fig 3.1). Despite semi-complimentary binding to target mRNAs, Watson-Crick base pairing of nucleotides 2-8 in the 5' portion of the mature miR (commonly referred to as the miR "seed sequence") is essential for target identification (Doench and Sharp, 2004). This seed sequence is an important component to common algorithms that predict miR targets, such as TargetScan and TargetBoost (Rajewsky and Socci, 2004; Rehmsmeier et al., 2004; Saetrom et al., 2005). However, these algorithms can be highly inaccurate, making miR target prediction particularly challenging because one miR can have several hundred target mRNAs, demonstrating their strong influence over gene expression (Breving and Esquela-Kerscher, 2009). The promiscuity associated with miR target recognition highlights the importance for several regulatory mechanisms along the miR biogenesis pathway. miRs are regulated primarily through three general mechanisms: at the level of pri-miR transcription, at the level of processing both by Drosha and by Dicer, and at the level of target

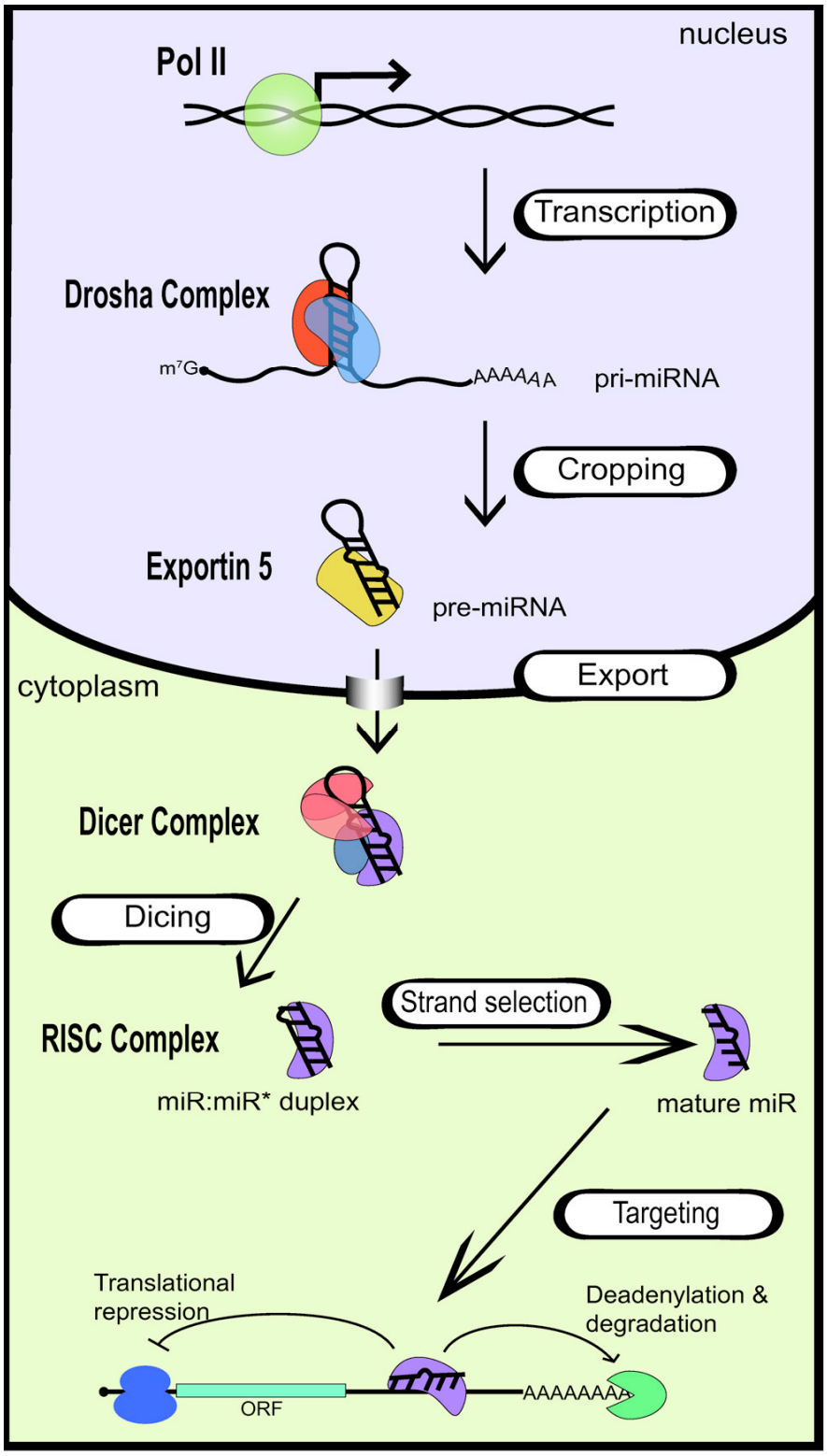
nucleus
Pol II
Transcription
Drosha Complex
m7G
AAAAAA
pri-miRNA
Cropping
Exportin 5
pre-miRNA
cytoplasm
Export
Dicer Complex
Dicing
RISC Complex
miR:miR* duplex
Strand selection
mature miR
Targeting
Translational repression
Deadenylation & degradation
ORF
AAAAAAA

<u>Figure 3.1:</u> Biogenesis of microRNAs and assembly into RISC.

RNA polymerase II generates 5' capped and 3' polyadenylated pri-miRs which are processed by Drosha in the nucleus to generate a 72-nucleotide hairpin pre-miR. After translocation to the cytoplasm, pre-miRs are processed by Dicer to form the mature miR/miR* duplex. Following further processing, miRs are assembled into the RISC. Only one strand of the duplex is stably associated with the RISC and will become the mature miR. This mature miR, in assembly with RISC, will repress gene expression by semi-complementary binding to the 3' UTR of target mRNAs, thereby impeding their translation and/or promoting their degradation. From Davis & Hata, *Cell Commun Signal*, 2009.

recognition (Breving and Esquela-Kerscher, 2009; Davis and Hata, 2009; Hata and Davis, 2009).

Recent studies have shown that miR31 is significantly downregulated in CAFs isolated from endometrial cancer compared to fibroblasts from disease-free endometrium, resulting in high levels of the miR31 target gene “special AT-rich sequence binding protein 2” (SATB2). Modulation of the levels of miR31 or its target SATB2 influences the CAFs ability to promote tumor cell invasion and migration (Aprelikova et al., 2010). Similarly, miR15a and miR16 are downregulated in prostate CAFs, resulting in upregulation of FGF-2 signaling which enhances cancer cell survival, proliferation and migration (Musumeci et al., 2011). The contribution of specific miRs to the etiology of CAFs in breast cancer remains largely unknown.

Interestingly, certain miRs have been identified as important mediators in tissue fibrosis, a process that requires fibroblast activation. Both CAFs and fibrotic fibroblasts are two types of activated fibroblasts that proliferate similarly and deposit significant amounts of ECM (Desmouliere et al., 2005; Desmouliere et al., 2004; Krenning et al., 2010), lending speculation to the possibility that these different fibroblast populations share common miRs that govern their gene expression and thus, phenotype. In particular, miR21 is induced by TGFβ in both fibrotic fibroblasts and myofibroblasts (Davis et al., 2008; Liu et al., 2010; Thum et al., 2008; Yao et al., 2011). The ability of TGFβ to mediate fibroblast activation has been well established (Ronnov-Jessen and Petersen, 1993; Ronnov-Jessen et al., 1995; Vaughan et al., 2000; Yao et al., 2011), although the precise

mechanism through which it does so is an active area of research. Interestingly, the duration of the TGFβ stimulus may be an important determinant in whether the fibroblast activation is transient (as in wound healing) or permanent (as in tissue fibrosis) (Bechtel et al., 2010), and fibroblast activation may be mediated by miR21 (Liu et al., 2010; Thum et al., 2008; Yao et al., 2011).

Specifically, miR21 is upregulated in the lungs of mice in an idiopathic pulmonary fibrosis (IPF) mouse model and in the lungs of human IPF patients, predominately localized to lung myofibroblasts. Attenuation of miR-21 expression in these cells using miR21 antisense oligos significantly reduces the disease progression in IPF mice, even after initiation of pulmonary injury, suggesting possible targeting of miR21 expression could be clinically relevant in human IPF (Liu et al., 2010). Also, miR21 is upregulated in cardiac fibroblasts during myocardial disease. The upregulation of miR21 in these cells causes a downregulation in the miR21 target gene Sprouty1, which results in augmented ERK-MAPK signaling in these cells. Similar to the IPF mouse model, a miR21 specific, chemically modified antisense oligo (called an antagomiR) reversed Sprouty1 expression and diminished MAPK activation in cardiac fibroblasts, ultimately restoring cardiac function in a mouse model of myocardial infarction (Thum et al., 2008). Collectively, these data suggest that miR21 signaling in fibroblasts contributes to disease. Surprisingly, however, it was recently discovered that miR21 is actually not required for development of stress-dependent cardiac disease. miR21 knockout mice are phenotypically normal and respond to a variety of cardiac stresses similarly to WT mice (Patrick et al.,

2010). Thus, while miR21 may play a role in fibrosis, in the absence of miR21, other miRs likely compensate for its loss.

Interestingly, miR21 not only promotes the activated fibroblast/myofibroblast phenotype, but also promotes the activated, contractile phenotype of vascular smooth muscle cells (VSMCs). Smooth muscle cells harbor two different states of differentiation depending on the presence of growth factors (BMP, TGFβ, PDGF), matrix composition, and hypoxia (Mack, 2011; Runo and Loyd, 2003). Vascular injury initiates and perpetuates the de-differentiation of VSMCs from their contractile phenotype into a more synthetic, proliferative phenotype, which plays a central role in neointimal hyperplasia during the progression of vascular diseases such as idiopathic pulmonary hypertension (IPH), atherosclerosis, and restenosis (Orlandi et al., 2006; Runo and Loyd, 2003). Because the TGFβ super family of proteins promotes the differentiation of VSMCs to their contractile, quiescent phenotype, BMP receptor type II (BMPRII) mutations that inhibit BMP signaling inadvertently lock VSMCs into their synthetic, proliferative state of differentiation, causing the pathogenesis of IPH (Chan et al., 2011; Lagna et al., 2007).

Similar to the mechanism described in fibrotic fibroblasts and myofibroblasts, the VSMC contractile gene expression program is mediated by TGFβ and BMP induction of miR21 through a non-canonical TGFβ/BMP signaling pathway. Specifically, TGFβ and BMP ligands promote the processing of pri-miR21 into pre-miR21, thereby promoting the upregulation of mature miR21 (Fig. 3.2) and inhibition of PDCD4, a negative regulator of differentiated

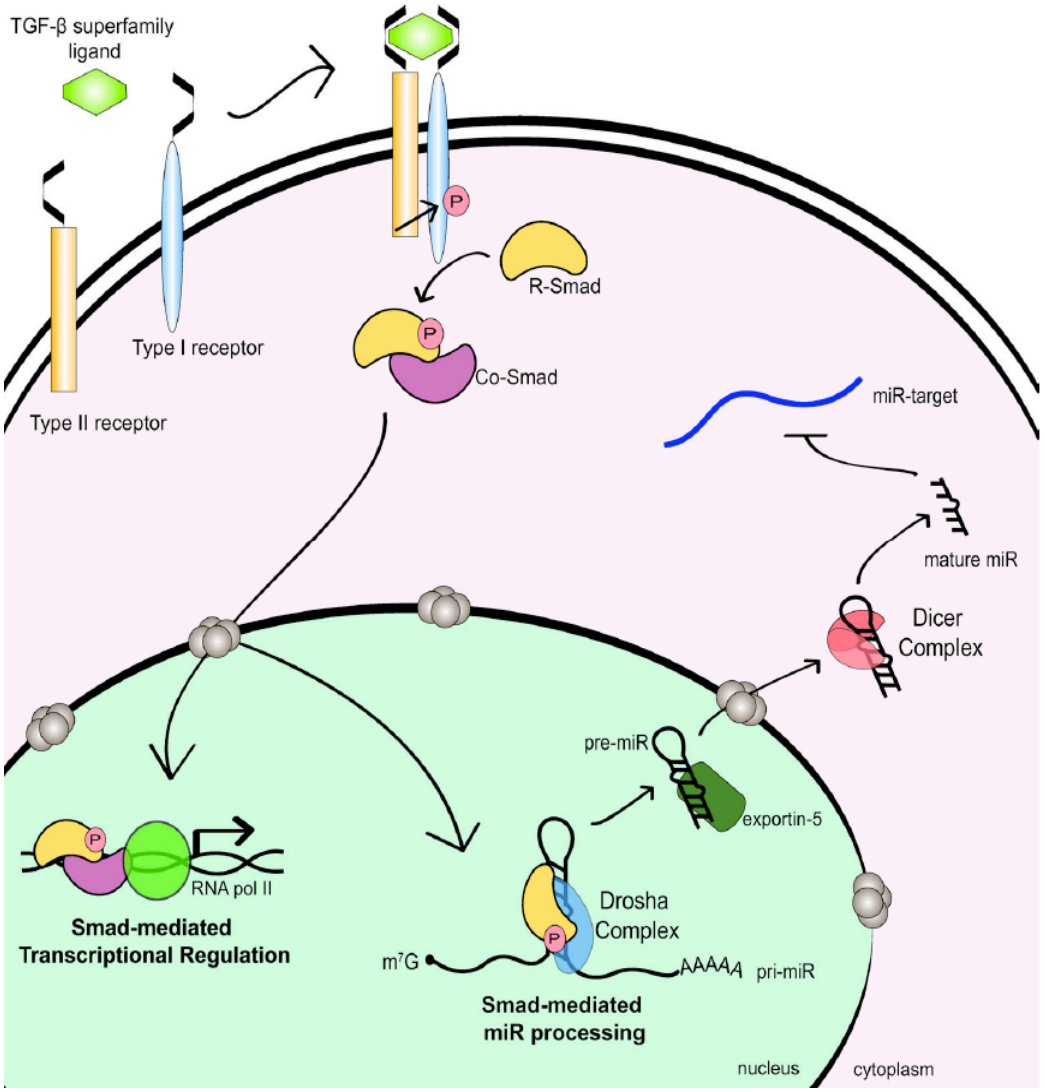

Figure 3.2: TGFβ and Smad mediated microRNA processing.

TGFβ1 and BMP4 signaling stimulate the processing of pri-miR21 to pre-miR21 by promoting Drosha's interaction with R-Smad proteins. This is a non-canonical role for R-Smads in the regulation of gene expression. From Davis & Hata, *Cell Comm Signal*, 2009.

VSMC gene expression. Interestingly, the processing of miR21 by TGFβ and BMP occurs without any transcriptional activation of the pri-miR21 gene, despite both of these ligands inducing the Smad family of transcription factors. While canonical TGFβ superfamily signaling involves Smad phosphorylation and activation, causing their binding to Smad-response elements in various target gene promoters, Smads can also function to facilitate Drosha-mediated miR processing (Davis et al., 2008; Davis et al., 2011). This mechanism may be involved in VSMC phenotypic switching during disease pathogenesis, as high expression of miR21 has been found in the vascular wall of balloon-injured rat carotid arteries (Ji et al., 2007).

The relationship between miR21 and TGFβ exists in other cell types aside from fibroblasts and VSMCs. Interestingly, overexpression of miR21 in human breast tumors significantly correlates with dual overexpression of TGFβ and poor patient outcome (Qian et al., 2008). In breast cancer cells harboring constitutive activation of TGFβ signaling, miR21 expression is elevated, and exogenous TGFβ induces pre-miR21 expression while pri-miR21 levels are unchanged (Davis et al., 2008). These data suggest that mechanisms regulating TGFβ induced miR21 expression may be similar in different cell types. miR21 is known to be overexpressed in several different types of solid tumors, including breast tumors (Volinia et al., 2006), although it is unclear if the mechanism of overexpression is regulated by TGFβ in each tumor type.

We hypothesized that miR21, responsible for governing myofibroblast and smooth muscle cell gene expression programs, might also be responsible for

governing CAF phenotype, as both of these processes are regulated by TGFβ. Here, we demonstrate that CAFs and RMFs respond to TGFβ differently; in response to ligand stimulation, CAFs induce the processing of miR21 while RMFs do not. These findings demonstrate a reproducible, unifying characteristic of CAFs from all breast tumors examined, and identify an *in vitro* characteristic of CAFs that is distinct from RMFs.

3.3. Results

3.3.a. Both miR21 and miR199a, but not miR25, are differentially processed in CAFs and RMFs in a TGFβ dependent manner.

First, we confirmed that miR21 expression in primary human breast tumors was not solely confined to breast tumor cells. Using fluorescence in situ hybridization (FISH) with a probe specific for the mature form of miR21, we detected specific signal in the tumor associated stroma, in a region dense with cells of fibroblast morphology, suggesting miR21 may be expressed by CAFs (Supplemental Fig. 3.1). Corroborating previous reports (Iorio et al., 2005), miR21 was not expressed in disease-free human breast tissue (data not shown).

We next sought to determine if miR21 was upregulated in CAFs and RMFs in response to TGFβ, such as that reported for fibrotic fibroblasts, myofibroblasts and VSMCs (Davis et al., 2008; Liu et al., 2010; Thum et al., 2008; Yao et al., 2011). We treated several patient derived CAFs and RMFs with 100 pM TGFβ1 or vehicle control, under serum starvation conditions, for 24 hours before harvesting total RNA. Using qRT-PCR, we assayed for the fold

induction (over vehicle) of pri-miR21, pre-miR21, mature miR21, in response to TGFβ1 treatment. Interestingly, there was a significant induction of mature miR21 in CAFs, but not RMFs, in response to TGFβ treatment, with no significant induction of pri-miR21 or pre-miR21 ($p=0.006$, Fig. 3.3A,B). Because of the lack of de novo miR21 transcription (as determined by the pri-miR levels), and the similar levels of pre-miR21, these data suggested that mature miR21 processing was induced by TGFβ, but only in CAFs and not in RMFs.

To rule out the possibility that the induction of mature miR21 in CAFs but not RMFs was due to cell type specific differences in the response to TGFβ signaling, we assayed for the fold induction of the TGFβ target gene PAI1 in CAFs and RMFs treated with TGFβ in 24 hour time period. There was no significant difference between CAFs and RMFs ability to induce PAI1 expression, suggesting that both cell types have equal capacity to respond to canonical TGFβ signaling (Fig. 3.3A).

To rule out the possibility that the induction of mature miR21 levels in TGFβ treated CAFs was due to higher basal transcript levels of pri- or pre-miR21 in these cells compared to RMFs, were performed qRT-PCR for the basal levels of pri-, pre- or mature miR21 in several patient derived CAFs and RMFs. We failed to find a statistically significant difference in the basal levels of all three forms of miR21 between these two different cell types ($p>0.05$, Supplemental Fig. 3.2A,B). Collectively, these data suggested that the TGFβ mediated pre-to mature miR21 processing was likely due to a non-canonical response to TGFβ specifically in CAFs.

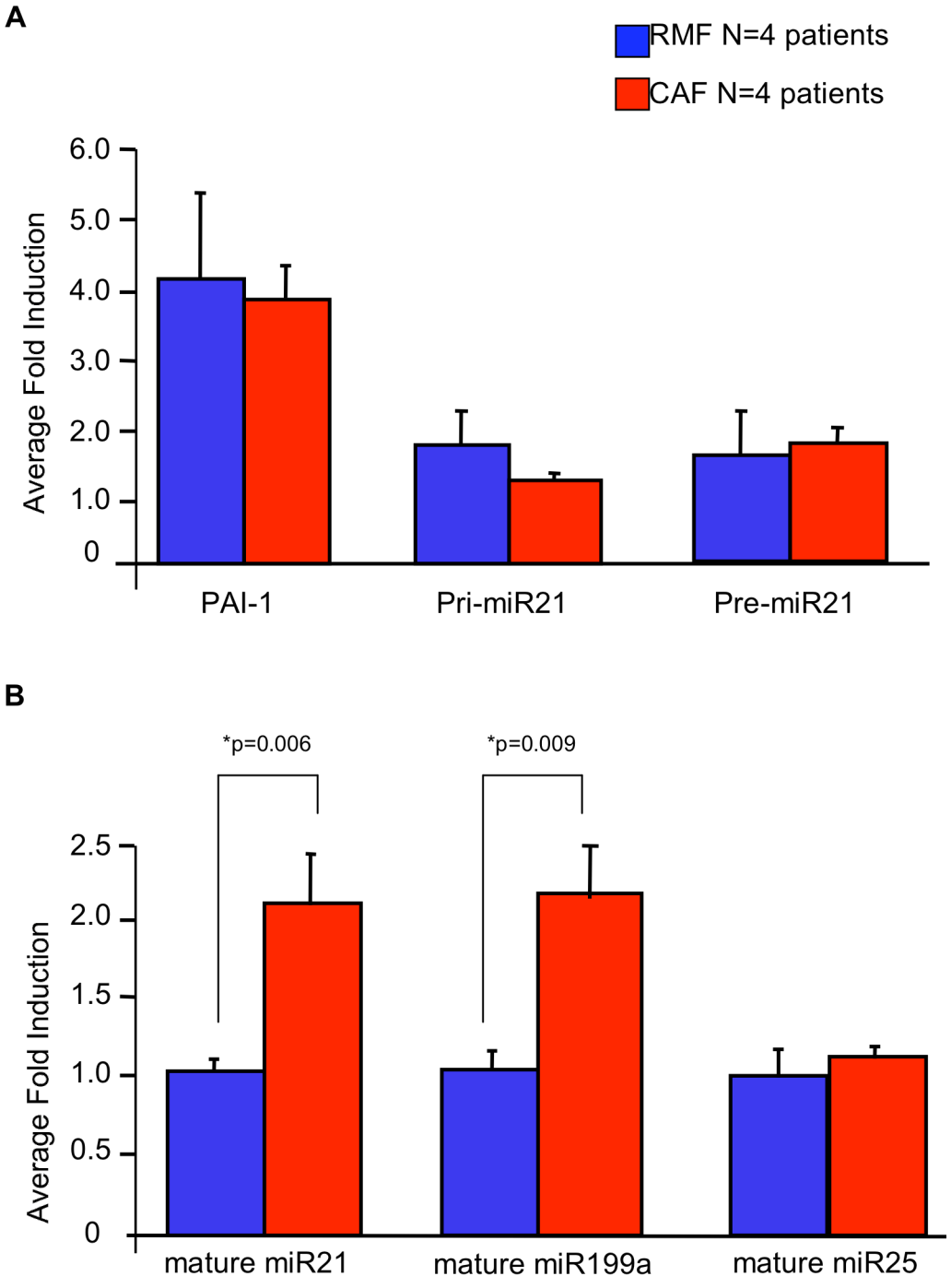
A
RMF N=4 patients
CAF N=4 patients
Average Fold Induction
6.0
5.0
4.0
3.0
2.0
1.0
0
PAI-1
Pri-miR21
Pre-miR21
B
*p=0.006
*p=0.009
Average Fold Induction
2.5
2.0
1.5
1.0
0.5
0
mature miR21
mature miR199a
mature miR25

<u>Figure 3.3:</u> TGFβ promotes the processing of mature miR21 and miR199a in CAFs but not in RMFs.

(A) qRT-PCR results for the average fold induction (over vehicle) of PAI-1 (a TGFβ target gene), pri-miR21, and pre-miR21 in 4 patient derived RMFs and 4 patient derived CAFs treated with 100 pM TGFβ1 for 24 hours. PAI-1 is normalized to GAPDH whereas pri-miR21 and pre-miR21 are normalized to U6. Error bars, SEM. **(B)** qRT-PCR results for the average fold induction of mature miR21, mature miR199a, and mature miR25 in the same 4 patient derived RMFs and 4 patient derived CAFs as in (A) treated with 100 pM TGFβ1 for 24 hours. All are normalized to U6. Statistics were performed using a Student's two-tailed t test of means: mature miR21, p=0.006; mature miR199a, p=0.009. Error bars, SEM. Data collected in collaboration with Brandi Davis, Hata Laboratory.

To rule out the possibility that both cell types were indeed inducing mature miR21 in response to TGFβ, but RMFs were degrading the mature miR within the 24 hr time period, we performed a preliminary time course analysis with one representative RMF and two representative CAFs. Each cell type was treated with 100 pM TGFβ or vehicle control, and after 0, 2, 6, and 12 hrs, total RNA was harvested for qRT-PCR analysis for the fold induction (over vehicle) of pri-, pre- and mature miR21. While these data are difficult to interpret due to the lack of representative CAFs and RMFs for statistical significance, mature miR21 was ~1.5 fold induced at 12 hrs in TGFβ treated CAFs, but not in TGFβ treated RMFs (Supplemental Fig. 3.3A-C).

Intriguingly, mature miR199a responded in the same fashion as mature miR21 in response to TGFβ. Mature miR199a was significantly induced upon TGFβ treatment in CAFs only, with no significant induction of pri- or pre-miR199a levels ($p=0.009$, Fig. 3.3B and data not shown).

The specificity of TGFβ mediated miR processing of miR21 and miR199a (among others) has been described in pulmonary arterial smooth muscle cells (PASMCs), as the stem region of pri-miR transcript contains a consensus sequence recognized by Smad proteins (Davis et al., 2011). Intriguingly, mature miR25 and mature miR100, whose pri-miRs lack the Smad consensus sequence and do not respond to TGFβ mediated miR processing in PASMCs, were not induced by TGFβ in CAFs (Fig 3.3B and data not shown). While these data suggested similar levels of miR processing regulation between CAFs and that described for PASMCs, there was a striking difference in these two mechanisms:

while TGFβ promotes the processing of pri-miRs to pre-miRs by inducing Smad interactions with Drosha in PASMCs (Davis et al., 2008), TGFβ appeared to promote the processing of pre-miR21 and pre-miR199a, but not pre-miR25 or pre-miR100, to their mature forms in CAFs, but not in RMFs.

3.3.b. Possible explanation for the specificity of TGFβ mediated miR21 and miR199a processing

Because TGFβ appeared to be inducing the pre-miR processing of only a subset of miRs, we sought to determine the sequence similarities between pre-miR21 and pre-miR199a in comparison to pre-miR25 and pre-miR100. Interestingly, the consensus motif "UCUCA" was identified within the 3' end of the terminal loop of both pre-miR21 and pre-miR199a, but not in pre-miR25 or pre-miR100 (Fig. 3.4). Upon further examination of all the other pre-miRs within the human genome, we found 9 additional pre-miRs with the UCUCA motif within the 3' end of the terminal loop, and 6 additional pre-miRs with the UCUCA motif within the 5' end of the terminal loop (Supplemental Fig. 3.4). We speculate that pre-miRs with a conserved UCUCA motif in the 3' end of the terminal loop may have similar secondary structure to pre-miR21 and pre-miR199a, and these pre-miRs should be tested for possible responses to TGFβ signaling.

Pre-miR21

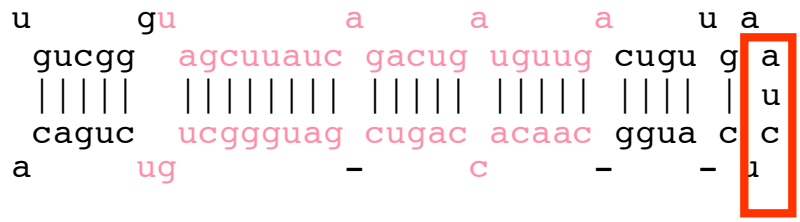

Pre-miR199a

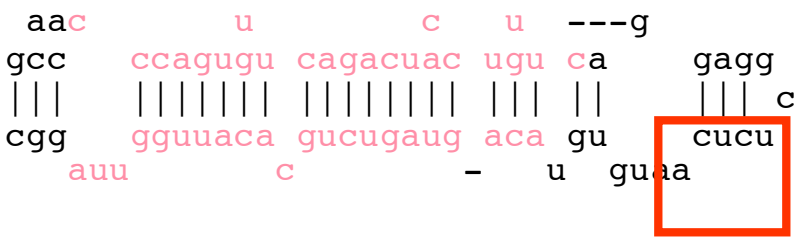

Pre-miR25

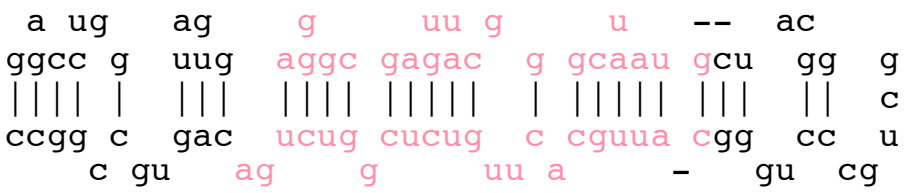

Pre-miR100

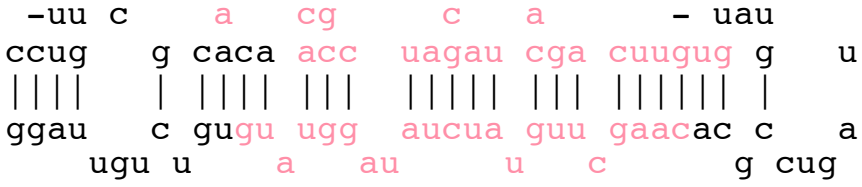

<u>Figure 3.4:</u> Possible explanation for the specificity of TGFβ mediated miR21 and miR199a processing.

Comparison of the hairpin structures and sequences of the TGFβ responsive pre-miRs: pre-miR21 and pre-miR199a, to that of the TGFβ insensitive pre-miRs: pre-miR25 and pre-miR100. Notice that pre-miR25 and pre-miR100 lack the common UCUCA motif within the hairpin terminal loop region. Data from miRBase, an online microRNA database.

3.3.c. Differential miR processing in CAFs and RMFs is not attributed to differences in the expression of key miR processing molecules

In attempt to reconcile the differences in processing of certain pre-miRs between CAFs and RMFs in response to TGFβ, we assayed for the relative levels of major miR processing molecules in these two cell types treated with either 100 pM TGFβ or vehicle control using qRT-PCR. Surprisingly, there was no significant difference in expression of Dicer, Drosha, or p68 (a subunit of Drosha important for Smad and Drosha mediated miR processing, (Davis et al., 2008)) in several different patient derived CAFs and RMFs, with or without TGFβ treatment ($p>0.05$, Fig. 3.5A-C). This was also true for the expression of Ago2, a protein essential for Dicer mediated pre- to mature miR processing (Diederichs and Haber, 2007) (Supplemental Fig. 3.5).

3.3.d. Suggestive miR21 targets

We investigated the levels of putative miR21 target genes in TGFβ treated CAFs by generating a list of miR21 targets based on TargetScan and PubMed. TargetScan listed nearly 100 possible target mRNAs for miR21. To narrow down this list, we considered genes whose transcription is induced by TGFβ signaling, genes with 5' ends harboring high sequence complimentary to the seed region of miR21, and genes that might be inherently downregulated in CAFs. Thus, we remained with a list of only a handful of genes, many of which have already been shown to be miR21 targets in other forms of activated fibroblasts (Table 3.1). At first pass, we examined the protein levels of "tissue inhibitor of

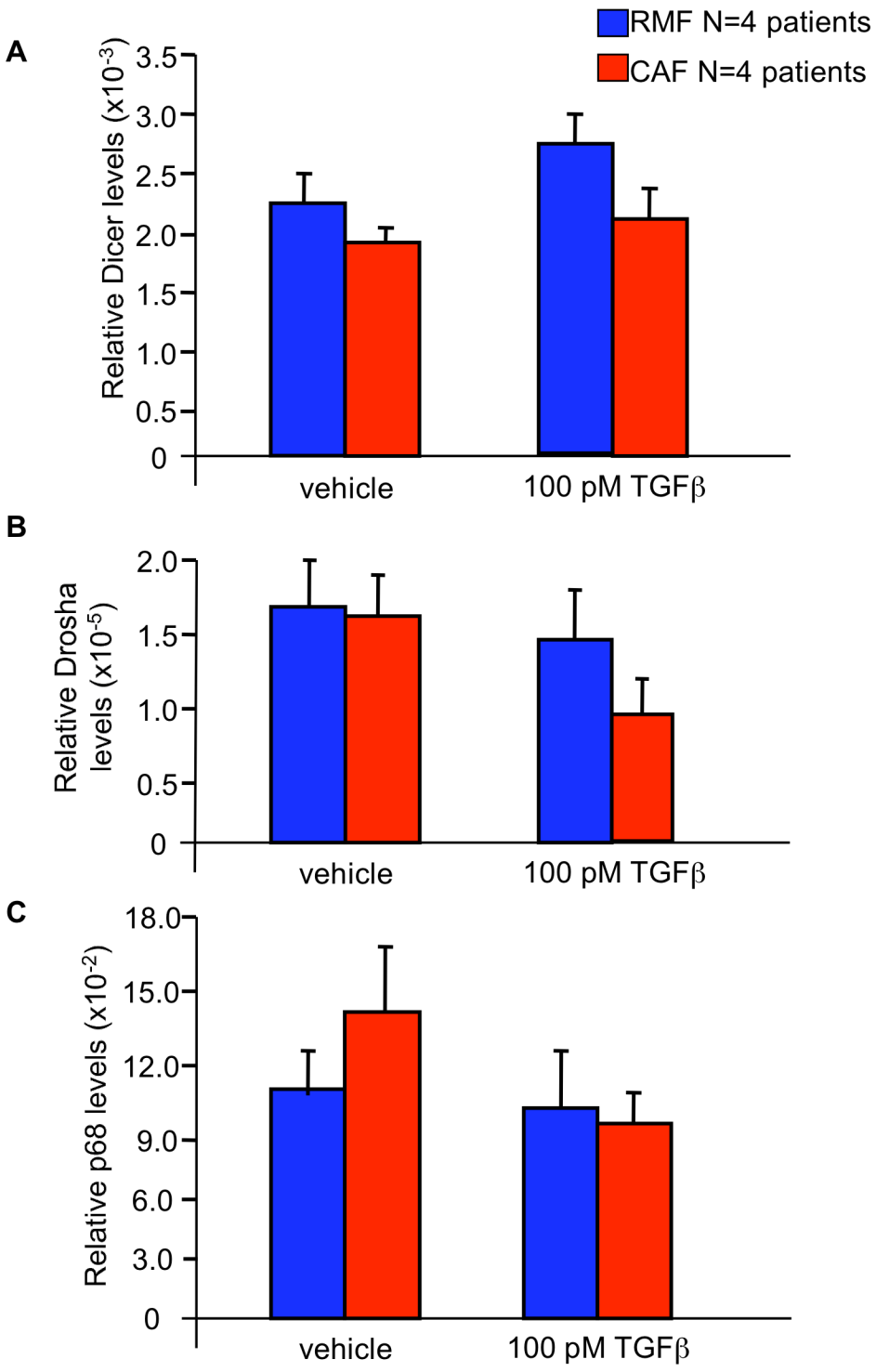
A
RMF N=4 patients
CAF N=4 patients
Relative Dicer levels (x10-3)
3.5
3.0
2.5
2.0
1.5
1.0
0.5
0
vehicle
100 pM TGFβ
B
Relative Drosha levels (x10-5)
2.0
1.5
1.0
0.5
0
vehicle
100 pM TGFβ
C
Relative p68 levels (x10-2)
18.0
15.0
12.0
9.0
6.0
3.0
0
vehicle
100 pM TGFβ

Figure 3.5: Differential miR processing in CAFs and RMFs is not attributed to differences in the expression of key miR processing molecules.

(A) qRT-PCR for the average relative expression of Dicer in 3 patient derived RMFs and 3 patient derived CAFs, treated with either vehicle control or 100 pM TGFβ1 for 24 hours. Levels are normalized to GAPDH. Error bars, SEM. **(B)** qRT-PCR for the average relative expression of Drosha in the same 3 patient derived RMFs and 3 patient derived CAFs as in (A), treated with either vehicle control or 100 pM TGFβ1 for 24 hours. Levels are normalized to GAPDH. Error bars, SEM. **(C)** qRT-PCR for the average relative expression of the Drosha subunit p68 in the same 3 patient derived RMFs and 3 patient derived CAFs as in (A), treated with either vehicle control or 100 pM TGFβ1 for 24 hours. Levels are normalized to GAPDH. Error bars, SEM.

Table 3.1: miR21 target genes in other cell types.

Gene	Name	Cell Type	Reference
PDCD4	Programmed cell death gene 4	PASMs; cholangiocarcinoma cells; RAW264.7 macrophages; myofibroblasts	(Davis et al., 2008; Selaru et al., 2009; Sheedy et al., 2010; Yao et al., 2011)
Spry1	Sprouty1	Cardiac fibroblasts	(Thum et al., 2008)
PTEN	Phosphatase and tensin homolog	Breast cancer cells; non-small cell lung cancer cells	(Iliopoulos et al., 2010a; Zhang et al., 2010)
TIMP3	Tissue inhibitor of metalloproteinases-3	Cholangiocarcinoma cells; breast cancer cells; glioma cells	(Gabriely et al., 2008; Selaru et al., 2009; Song et al., 2010)
SMARCD1	SWI/SNF related, matrix associated, actin dependent regulator of chromatin, subfamily d, member-1	ND	TargetScan Algorithm

ND: not determined

metalloproteinases 3" (TIMP3), an inhibitor of several MMPs, an anti-angiogenic factor, and an established TGFβ target gene in fibroblasts (Gabriely et al., 2008; Garcia-Alvarez et al., 2006; Song et al., 2010). Western blotting revealed that two patient derived RMFs responded to TGFβ by inducing TIMP3 protein, as expected, while two patient derived CAFs failed to show an induction of TIMP3 protein in response to the growth factor (Fig. 3.6A). The failure of CAFs to induce the TGFβ target gene TIMP3 in response to ligand stimulation could possibly be due to the concomitant induction of mature miR21, although this needs to be examined through direct modulation of miR21 levels in these cells.

At second pass, we continued our search for other possible TGFβ induced miR21 targets in CAFs using qRT-PCR. We treated three patient derived RMFs and three patient derived CAFs with 400 pM TGFβ for 24 hours, harvested total RNA, and assayed for the fold induction (over vehicle) of several putative miR21 target genes. To address the specificity of possible TGFβ mediated induction of each of these genes, we included one RMF and CAF patient sample that was treated both with ligand and 10 μM SB431542, an ALK5 inhibitor which blocks the TGFβ type II receptor and abrogates TGFβ superfamily signaling. Interestingly, we found that the levels of Sprouty1 were significantly downregulated in TGFβ treated CAFs compared to TGFβ treated RMFs, and this downregulation was relieved upon inhibition of TGFβ signaling ($p=0.03$, Fig. 3.6B). The levels of TIMP3 message were also slightly lower in TGFβ treated CAFs compared to RMFs, although this failed to reach statistical significance ($p>0.05$). Collectively, these data suggest that Sprouty1 may be a TGFβ induced

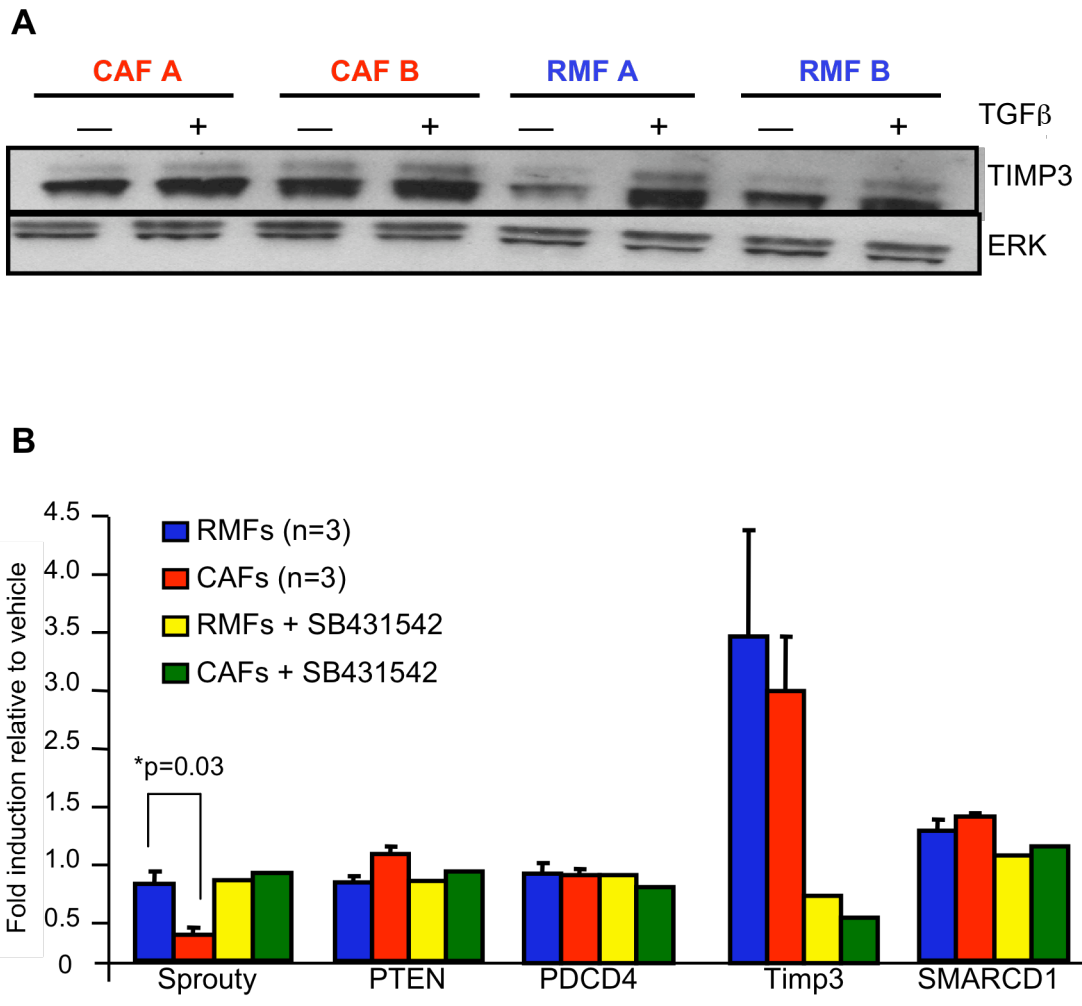
A
CAF A
CAF B
RMF A
RMF B
— + — + — + — +
TGFβ
TIMP3
ERK
B
Fold induction relative to vehicle
4.5
4.0
3.5
3.0
2.5
1.5
1.0
0.5
0
RMFs (n=3)
CAFs (n=3)
RMFs + SB431542
CAFs + SB431542
*p=0.03
Sprouty
PTEN
PDCD4
Timp3
SMARCD1

Figure 3.6: Indirect assessment of possible miR21 target genes in TGFβ treated CAFs and RMFs.

(A) Western blot for the levels of Timp3 protein in vehicle or TGFβ1 treated CAFs and RMFs from 2 different patient samples each (A and B). Total Erk protein is used as a loading control. Data from Anna Maione, rotation student. **(B)** qRT-PCR for the fold induction (over vehicle) of various putative miR21 target genes in 3 different patient derived CAFs and 3 different patient derived RMFs treated with vehicle controls or 400 pM TGFβ1 with or without 10 μM SB431542 (ALK5 inhibitor). All genes are normalized to GAPDH. Statistics were performed using a Student's two-tailed t test of means: Endogenous Sprouty1 levels in RMFs vs. CAFs, p=0.03. Error bars, SEM. Data from Vandana Iyer, Kuperwasser Laboratory.

miR21 target gene in CAFs, although further experiments utilizing antisense miR21 oligos are required to determine if/how TGFβ and miR21 regulate Sprouty1 levels in these cells.

3.3.e. Pre-miR21 associates with three key proteins involved in RNA editing

Given that miRs can have several hundred target mRNAs, they harbor tremendous influence over cellular gene expression and require many regulatory networks to modulate their affects. There are three major levels of miR regulation: at the level of pri-miR transcription, at the level of pri- and pre-miR processing, and at the level of mature miR target recognition. Various regulatory molecules that either promote or suppress miR function control each of these steps in miR biogenesis (Davis and Hata, 2009). We sought to determine which regulatory molecules might be interacting with pre-miR21 to promote the processing to mature miR21 in a TGFβ responsive manner. To do this, we used a previously described pre-miR pull down assay (Heo et al., 2009). In this assay, both pre-miR21 and pre-miR100 (as a control for specificity) with 5' end extensions were *in vitro* transcribed using PCR products as direct templates. A 3' biotinylated adaptor DNA, with complimentarity to the 5' end extension of the *in vitro* transcription product, was incubated with streptavidin conjugated agarose beads and then incubated with the *in vitro* transcribed pre-miRs (Fig. 3.7A). This mixture was then incubated with cell extract prepared from a representative patient derived CAF, treated with either 100 pM TGFβ or vehicle. After incubation, any proteins associated with pre-miR21 or pre-miR100 were

A

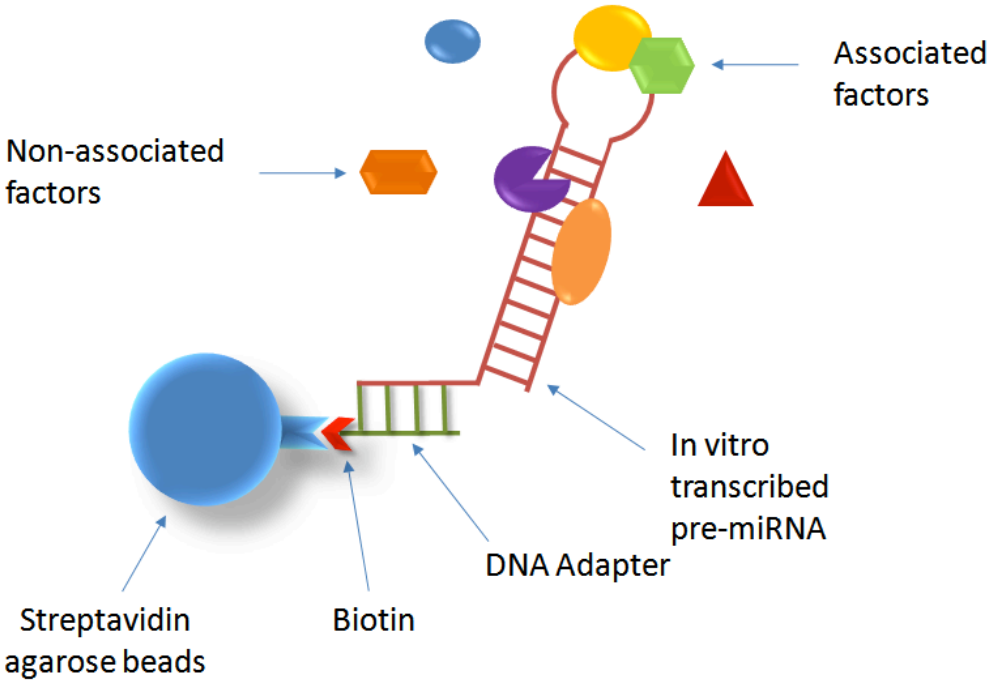
Associated factors
Non-associated factors
In vitro transcribed pre-miRNA
DNA Adapter
Streptavidin agarose beads
Biotin

B

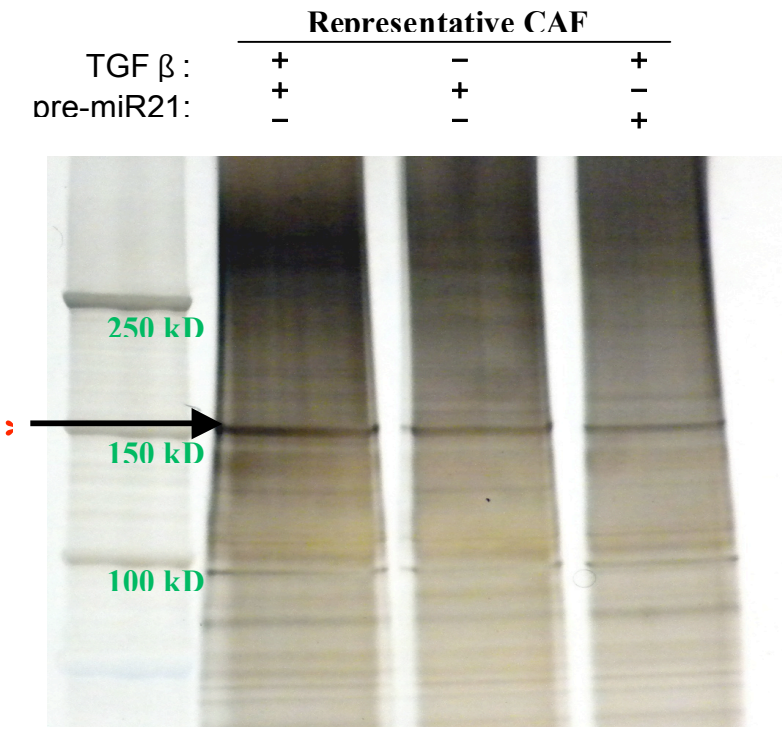
Representative CAF
TGF β :
pre-miR21:
+ − +
+ + −
− − +
250 kD
150 kD
100 kD

<u>Figure 3.7:</u> Preliminary pre-miR21 pull down assay reveals associated proteins have involvement in the RNA editing process.

(A) Schematic of pull down technique published by Heo *et al., Cell,* 2009. *In vitro* transcription creates a pre-miR with a 5' extension, specifically designed for complementarity to the 3' extension of a biotinylated oligonucleotide (oligo). Incubation of the 5' extended-pre-miR with the 3' extended-biotinylated oligo bound to streptavidin coated beads promotes interaction. Incubation of this mixture in cell extracts from a representative vehicle or TGFβ1 treated CAF will allow any molecules that normally associate with the pre-miR to bind and be pulled down in complex with streptavidin coated beads. **(B)** Silver stained gel from the pull down technique described in (A) using a 5' modified pre-miR21, incubated with cell extracts from a representative patient derived CAF treated with either vehicle or TGFβ1, and resolved by SDS-PAGE. A 5' modified pre-miR100 is used as a negative control in the pull down for specificity. Certain bands within this gel were cut for Mass Spec analysis. Data from Xiang Liu, Kuperwasser Laboratory. **(C)** Mass Spec results of proteins associated with 5' modified pre-miR21 (but not 5' modified pre-miR100) from a representative patient derived CAF, treated with either vehicle or TGFβ1. Only 1 protein was associated with pre-miR21 in a TGFβ1 specific manner (Tudor-SN/p100). Data from Xiang Liu, Kuperwasser Laboratory.

separated by SDS-PAGE. We removed a band at 150 kilodaltons (kDa) from the gel and sent it for liquid chromatography tandem mass spectrometry (mass spec) analysis (Fig. 3.7B).

The band removed for mass spec at 150 kDa resolved three proteins of interest: vigilin, RNA helicase A (RHA), and p100 (also known as Tudor SN and SND1, hereafter referred to as p100 for simplicity; Table 3.2). Interestingly, all three proteins were involved in A → I RNA editing, a process by which specific or random adenosines within protein coding sequences or untranslated regions are hydrolyticly deaminated into inosines (Nishikura, 2010). Moreover, it has recently been discovered that miRs are often edited in this manner, which can affect their processing by Dicer, their stability, and their mRNA target recognition (Habig et al., 2007; Kawahara et al., 2007a; Kawahara et al., 2007b; Nishikura, 2006, 2010; Scadden, 2005).

Based on the mass spec results, p100 was the only protein associated with pre-miR21, but not pre-miR100, in a TGFβ dependent manner. Interestingly, p100 (reportedly 100 kDa) was pulled down at a molecular weight of 150 kDa, which suggested it was heavily post-translationally modified. To confirm that p100 was indeed expressed in both CAFs and RMFs and to determine if it was responsive to TGFβ, we performed western blot analysis with two patient derived RMFs and one patient derived CAF, each treated with 400 pM TGFβ or vehicle for 24 hrs. To our surprise, we detected only one band, with clean resolution, at precisely 100 kDa; we failed to identify any other band at 150 kDa as we saw in the pre-miR pull down gel (Fig. 3.8A).

Table 3.2: Proteins isolated from pre-miR21 pull down and subsequent mass spec analysis.

Protein	MW (kDa)	Subcellular localization	Description	Reference
Vigilin (HDL binding protein)	110	Nucleus; cytoplasm	Binds to A→I edited RNA; facilitates formation of heterochromatin; found in complex with ADAR and RHA; all may participate in chromatin silencing	(Fernandez et al., 2005; Wang et al., 2005)
RNA Helicase A (DEAH box protein 9; NDHII)	141	Nucleus, nucleolus, cytoplasm	Enzymatically unwinds RNA-RNA duplexes and RNA-DNA hybrids in a 3' to 5' direction but the RNA must have unpaired 3' overhangs; Interacts with RISC and facilitates RISC loading	(Reenan et al., 2000; Robb and Rana, 2007; Seeburg, 2000)
p100 (Tudor-SN; SND1)	100	Nucleus; cytoplasm	Component of RISC; promotes cleavage and degradation of edited pre-miRs	(Caudy et al., 2003; Li et al., 2008; Scadden, 2005)

Name bolded in black is more commonly used and referred to in text.

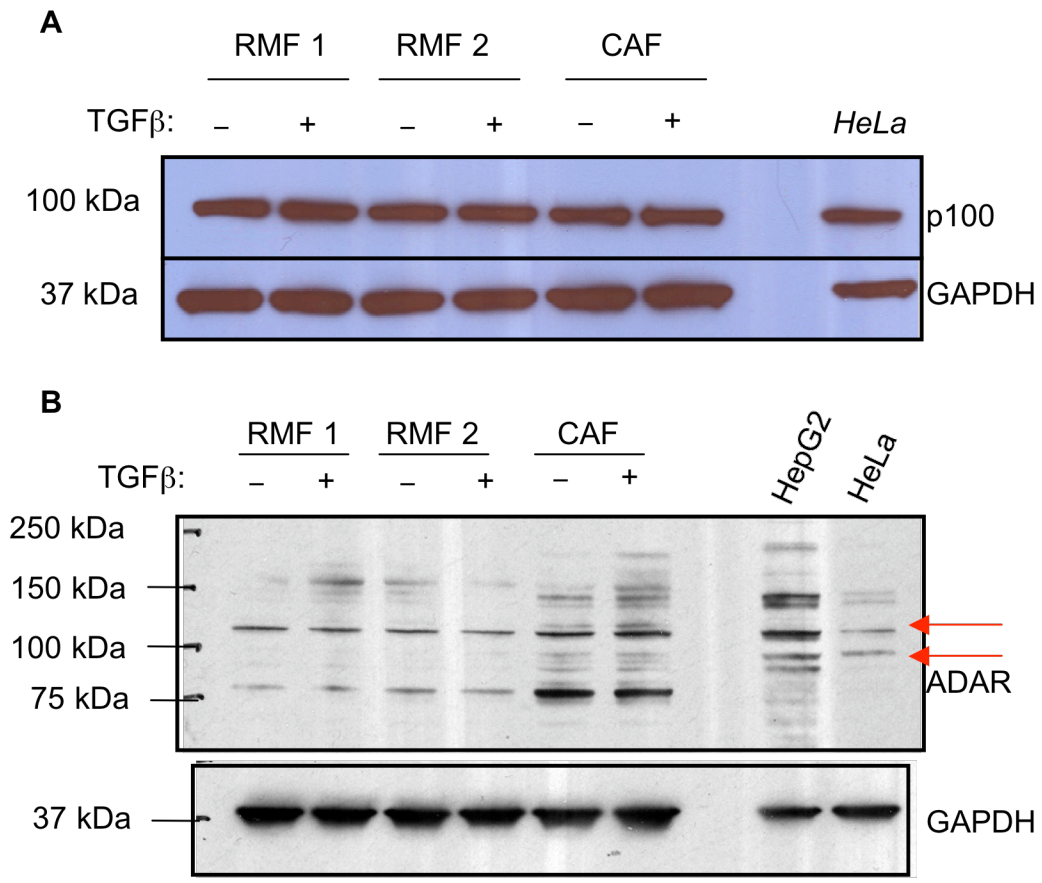

Figure 3.8: p100 and ADAR expression in vehicle and TGFβ treated CAFs and RMFs. Western blot for p100 **(A)** and ADAR **(B)** expression in whole cell lysates from vehicle or TGFβ treated RMFs (from patient 1 or patient 2), or one representative CAF. HepG2 and HeLa cell lysates are used as positive controls. Red arrows indicate bands corresponding to the size of ADAR1. Data from Vandana Iyer, Kuperwasser Laboratory.

p100 was one of three proteins involved in RNA editing that associates with pe-miR21 based on the pull down assay. Since our preliminary data suggested that CAFs and RMFs have similar levels of p100 protein, we sought to identify other proteins involved in miR and RNA editing that may have differential expression in TGFβ treated CAFs and RMFs. Because ADARs are ubiquitously expressed enzymes capable of deaminating any double stranded RNA (Nishikura, 2010), and ADAR1 reportedly associates with the proteins identified in our pull down assay (Fernandez et al., 2005; Scadden, 2005; Wang et al., 2005), we examined the expression of ADAR1 in two TGFβ or vehicle treated RMFs, and one TGFβ or vehicle treated CAF. Interestingly, our preliminary data suggest that CAFs may have higher levels of ADAR1 protein than do RMFs, although these data need to be expanded to multiple patient samples (Fig. 3.8B).

3.3.f. Transient knockdown of miR21 may affect the CAFs ability to support MCF7 tumorsphere formation

We sought to determine a biological consequence for TGFβ mediated miR21 induction in CAFs, hypothesizing that miR21 was important for CAF tumor promoting ability. To test this, we harvested CM from TGFβ or vehicle treated CAFs or RMFs after transfecting each with an antisense miR21 oligo or scramble oligo control. We then used this CM to grow MCF7 breast cancer cells under tumorsphere forming conditions (described in Sec 2.3), an *in vitro* assay for tumorgenicity (Fig. 3.9). We specifically chose a representative CAF that had previously shown to augment MCF7 tumorsphere forming ability in this assay,

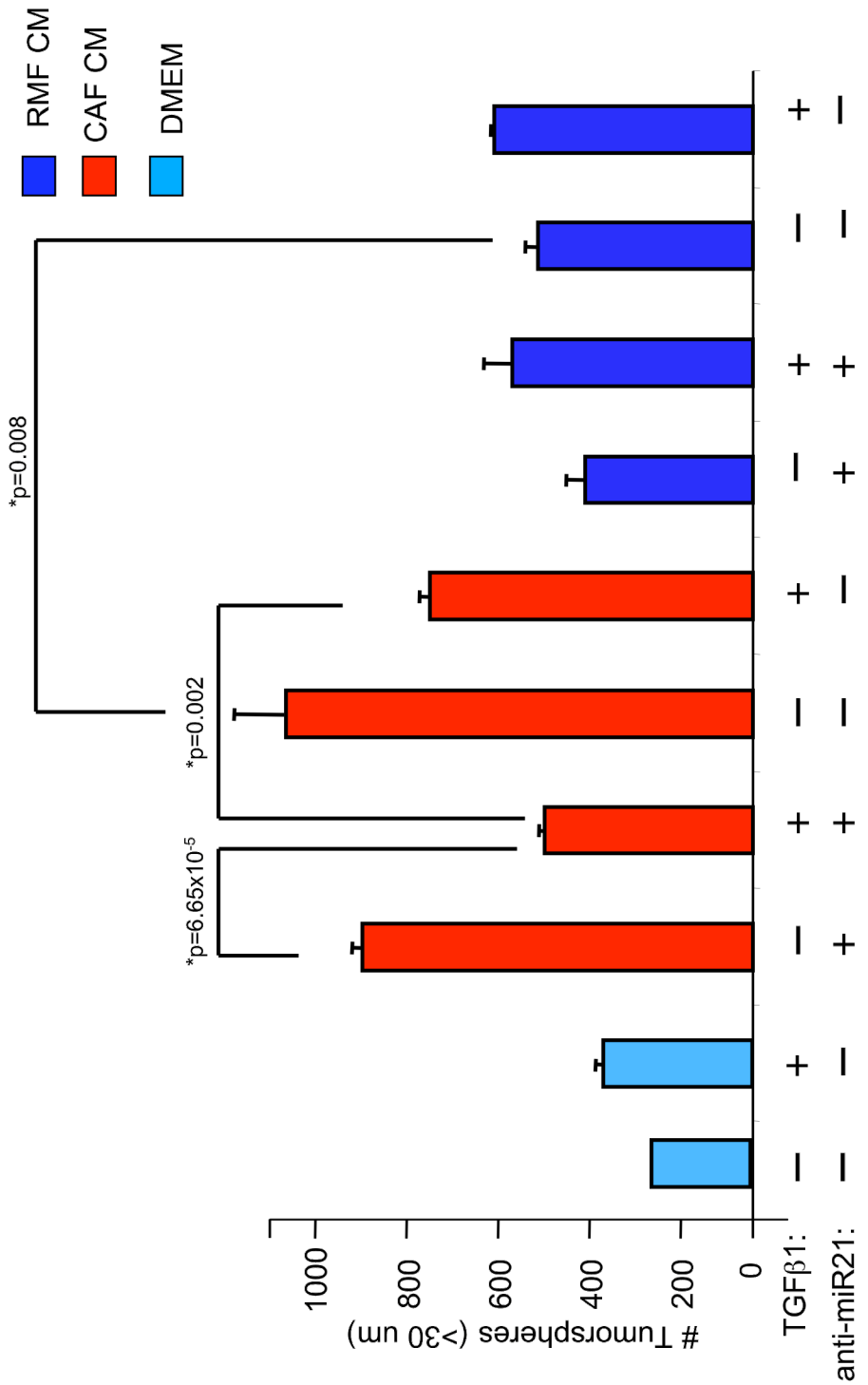
RMF CM
CAF CM
DMEM
*p=0.008
*p=0.002
*p=6.65x10-5
Tumorspheres (>30 um)
0
200
400
600
800
1000
TGFβ1:
anti-miR21:
-
+
-
+
-
+
-
+
-
+
-
+

Figure 3.9: Transient knockdown of miR21 may affect the CAFs ability to support MCF7 tumorsphere formation.

(A) Quantification of MCF7 tumorspheres formed in the presence of CM from miR21 knockdown or mock knockdown CAFs or RMFs, in the presence of 400 pM TGFβ1 or vehicle. Normal growth medium (PRF-DMEM) in the presence of 400 pM TGFβ1 or vehicle is shown as control. miR21 knockdown efficacy was confirmed using qRT-PCR for mature miR21 transcript by Brandi Davis (data not shown). Statistics were performed using a Student's two-tailed t test of means comparing: miR21 knockdown CAF CM in the presence of TGFβ1 to mock knockdown CAF CM in the presence of TGFβ1 ($p=0.002$); miR21 knockdown CAF CM in the presence of TGFβ1 or vehicle ($p=6.65 \times 10^{-5}$); comparing mock knockdown CAF CM to mock knockdown RMF CM both in the presence of vehicle as a baseline comparison of CAF vs. RMF CM ($p=0.008$). Error bars, SEM. Data from Crystal Bryan, rotation student.

and a representative RMF that failed to do so (Rudnick *et al.,* 2011), so we could directly assess the role of miR21 in the CAFs ability to secrete factors that enhance MCF7 tumorsphere formation. As a control, we treated MCF7s, grown in their normal growth media (DMEM), with 400 pM TGFβ throughout the duration of the assay to rule out any effects that the residual growth factor might have in the CAF and RMF CM. In addition, we confirmed that CM from scramble transfected, vehicle treated CAFs promoted significantly more MCF7 tumorspheres than did CM from scramble transfected, vehicle treated RMFs ($p=0.008$, Fig. 3.9). Interestingly, CM from antisense-miR21 transfected, TGFβ treated CAFs promoted significantly less MCF7 tumorspheres than CM from scramble transfected, TGFβ treated CAFs ($p=0.002$, Fig. 3.9). The addition of TGFβ to the miR21-knockdown CAFs before CM harvest appeared to have significant MCF7 tumorsphere suppressing properties ($p=6.65 \times 10^{-5}$, Fig. 3.9), and interestingly, this was not true for RMFs. Collectively, these preliminary data suggest that TGFβ mediated miR21 may govern the tumor promoting properties of CAFs, and should be followed up with *in vivo*.

3.4 Discussion

To our knowledge, this is the first mechanism described for TGFβ mediated processing of pre to mature miRs, and the first description of differential miR processing between CAFs and RMFs. Our data suggest that CAFs, but not RMFs, respond to TGFβ signaling by promoting the processing of pre-miR21 and pre-miR199a to their mature forms, without inducing transcription

of the pri-miRs nor inducing the processing of the pri-miR into the pre-miR form. These data lend speculation to the possibility that CAFs and RMFs have a reservoir of pre-miRs that are only processed to their mature forms in response to various signaling pathways, such as TGFβ. Our data are consistent with previous work demonstrating that TGFβ induces miR21 expression in other types of activated fibroblasts (Liu et al., 2010; Thum et al., 2008; Yao et al., 2011), although the mechanism of mature miR21 induction may differ in these cell types.

In addition, the response to various signaling pathways likely induces processing of only specific pre-miRs within this cytoplasmic reservoir. The specificity for certain pre-miRs over others is likely due to similar secondary structure and consensus binding sites within them, recognized by certain molecules induced upon ligand stimulation; such a mechanism has been described in smooth muscle cells (Davis et al., 2011). Both pre-miR21 and pre-miR199a have a similar consensus sequence within the 3' end of the terminal loop (UCUCA motif), in addition to several other pre-miRs we have not yet characterized. We suspect that, given the similar secondary structure of these pre-miRs and the common terminal loop motif, that they would also be responsive to TGFβ induced pre-miR processing in CAFs but not RMFs.

The inability of RMFs to induce pre-miR21 and pre-miR199a to their mature forms cannot be explained by differences in sensitivity to TGFβ signaling in comparison to CAFs, nor can it be explained by a reduction in the essential miR processing machinery such as Dicer, Drosha, p68 and Ago-2. While we only

looked at the levels of mRNA for Dicer, Drosha and p68, western blot analysis for their protein expression and possibly differences in post-translational modifications should be examined in greater detail. For example, Ago-2 protein stability is regulated by hydroxylation at proline 700 by prolyl-4-hydroxylase (P4H); depletion of both the alpha and beta subunits of P4H results in reduced stability of Ago2 and impaired RNA interference (Qi et al., 2008). Interestingly, P4H has been implicated as a marker of activated fibroblasts (myofibroblasts and CAFs) (Krenning et al., 2010; Orimo et al., 2005). This finding could suggest that CAFs have higher Ago-2 activity and more efficient processing of various miRs; further examination by knocking down P4H in CAFs and attempting to induce pre-miR21 processing in response to TGFβ will provide better insight into the link between P4H and Ago-2.

Another possibility for the differences between pre-miR processing in CAFs and RMFs could be due to differences in expression of certain adaptor molecules, induced in response to TGFβ, that bind a common region with these pre-miRs (possibly the UCUCA motif within the terminal loop) and mediate specific pre-miR processing. Based on the pre-miR21 pull down result, these adaptor molecules may play a role in RNA editing. Specifically, we identified vigilin, RHA and p100 in this pull down assay, although only p100 was pulled down in a TGFβ dependent manner. Interestingly, p100 is a component of the RISC and may modulate miR processing through RNA editing (Caudy et al., 2003; Li et al., 2008). Moreover, RHA interacts with RISC as well (Robb and Rana, 2007). These molecules may be facilitating RISC loading and Dicer activity

to modulate pre-miR cleavage to the mature form; these processes may be independent of RNA editing activity, or contingent upon A → I alterations.

Interestingly, because p100 was pulled down at a higher molecular weight than reported (150 kDa versus reported 100 kDa), we hypothesize that TGFβ mediates some form of posttranslational modification to this protein that facilitate interactions with RHA, vigilin, and pre-miR21 in a TGFβ dependent manner. Unfortunately, western blot analysis of vehicle or TGFβ treated CAFs and RMFs failed to demonstrate differences in p100 expression, additional bands suggestive of posttranslational modifications, or differences in the predicted molecular weight. A p100 immunoprecipitation assay, followed by western blotting for various posttranslational modifying proteins (such as phosphorylation, ubiquitination, sumoylation, etc) would perhaps corroborate the molecular weight discrepancy of the p100 western blot versus the pre-miR pull down assay results. Furthermore, possible differences in expression of vigilin and RHA between vehicle and TGFβ treated CAFs and RMFs should also be verified by western blot analysis.

While further analysis of p100 signaling in the context of pre-miR RNA editing sounds promising, it should be noted that since p100 possesses RNA cleavage activity and is reported to degrade A → I edited pre-miRs (Scadden, 2005; Yang et al., 2006), these reports would conflict with our results demonstrating mature miR21 induction in response to TGFβ in CAFs. Repeating the pre-miR21 pull down assay with vehicle and TGFβ treated RMFs might resolve this contradiction. It is plausible that p100 posttranslational modifications

occur only in TGFβ treated CAFs and not RMFs, due to differences in non-canonical TGFβ signaling pathways. Perhaps these posttranslational modifications of p100 prevent its endonuclease activity, thereby preventing pre-miR21 degradation and allowing mature miR21 biogenesis.

Because RNA editing is mediated by ADARs (Nishikura, 2010; Yang et al., 2006), we examined the levels of ADAR1 in two representative RMFs and one representative CAF, treated with either TGFβ or vehicle. While our results are preliminary and with only one patient sample, it is possible that CAFs have higher levels of ADAR1 expression than do RMFs. The consequence of higher ADAR expression levels may result in a higher percentage of pre-miRs that undergo A → I editing. While it is unlikely that this editing is promiscuous, the regulation of RNA editing in CAFs is completely unknown. One may speculate that perhaps specific RNA edited pre-miRs allow for alternative mRNA targets, due to the inability to bind the 3' UTRs of some mRNAs. This may explain why we failed to generate any preliminary data to suggest that PDCD4 and PTEN were miR21 target genes in CAFs.

In summary, we have identified a molecular difference in TGFβ mediated miR21 and miR199a processing in CAFs and RMFs. The consequence of this difference in miR processing remains unknown, although our preliminary data suggest it may contribute to CAF phenotype. We suspect that TGFβ promotes the pre- to mature miR processing step of several other miRs in addition to miR21 and miR199a; collectively, these miRs may modulate CAF gene expression. The role of RNA editing in TGFβ mediated pre-miR processing in

CAFs warrants further investigation. Understanding how TGFβ mediated miR processing and miR editing contribute to CAF phenotype may allow these cells to be targeted as an adjuvant therapy in treating human breast cancers, given the widespread use and delivery of miR sponges (Cohen, 2009) and modified antisense miR oligos (Patrick et al., 2010; Thum et al., 2008) for biological inhibition of miRs *in vivo*.

3.5 Acknowledgements and publication status

Thank you Charlotte for allowing me to explore this idea and learn a new, fascinating area of biology in the process. This side project would not be possible without significant contribution from Brandi Davis and Akiko Hata. Thank you Brandi for teaching me the basics of microRNAs. In addition, I have received generous help from Xiang Liu, Vandana Iyer, Anna Maione, Crystal Bryan, and Daisy Nakamura. This work is currently entirely unpublished.

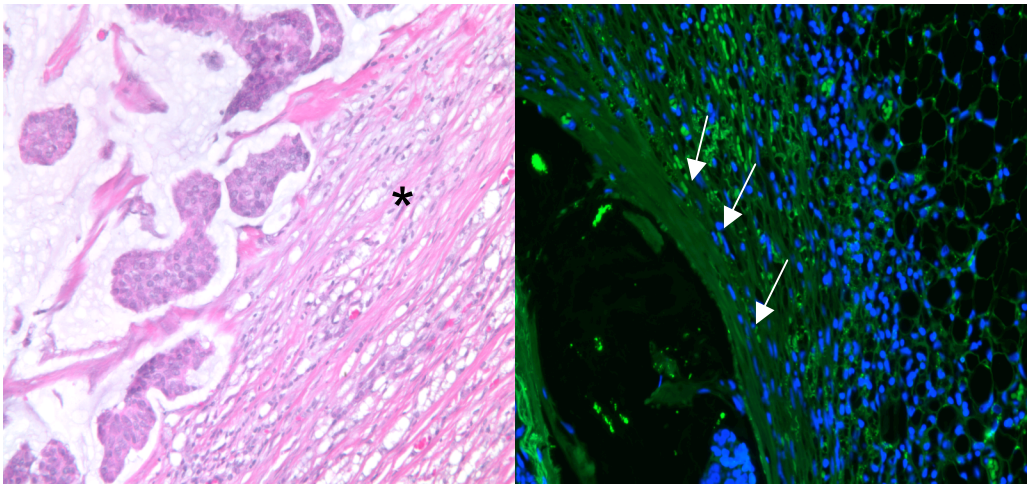

<u>Supplemental Figure 3.1:</u> Fluorescence in situ hybridization (FISH) of mature miR21 transcript in breast tumor stroma.

Left, H&E stain of a breast tumor section showing patches of tumor cells adjacent to the stroma (*). Right, FISH for mature miR21 expression, showing signal within the tumor stroma (arrows). Nuclei (stained with dapi) are elongated and have a typical fibroblast morphology. Note that dapi signal and FISH signal do not overlay, suggesting that the mature transcript is indeed cytoplasmic (as expected).

A

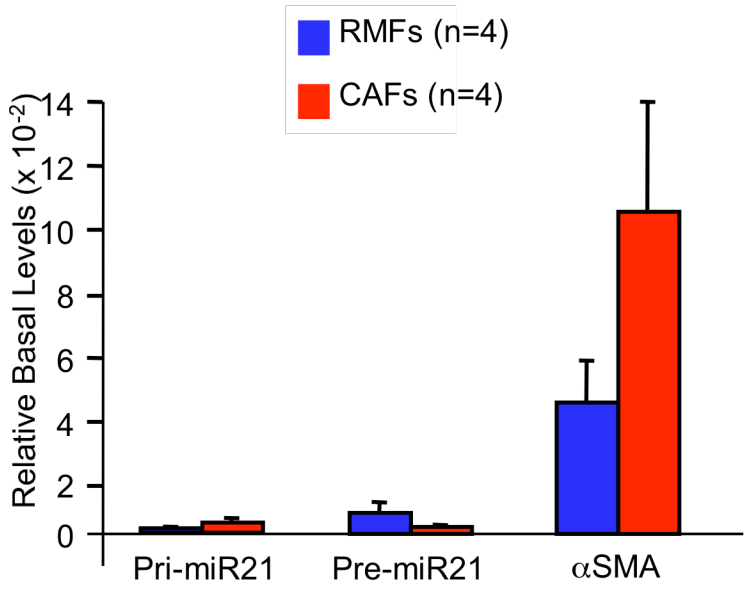
RMFs (n=4)
CAFs (n=4)
Relative Basal Levels (x 10-2)
14
12
10
8
6
4
2
0
Pri-miR21
Pre-miR21
αSMA

B

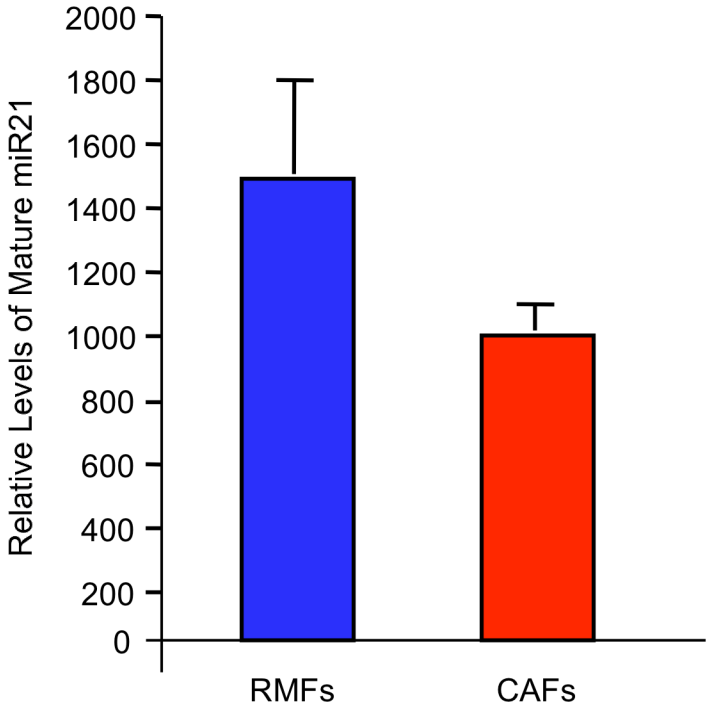
Relative Levels of Mature miR21
2000
1800
1600
1400
1200
1000
800
600
400
200
0
RMFs
CAFs

<u>Supplemental Figure 3.2:</u> Basal levels of pri, pre, and mature miR21 and miR199a in vehicle and TGFβ treated CAFs and RMFs.

(A) qRT-PCR for the relative basal levels of pri-miR21, pre-miR21, and αSMA in 4 different patient derived (vehicle treated) RMFs and CAFs. No significant differences reported. Error bars, SEM. **(B)** qRT-PCR for the relative basal levels of mature miR21 in the same 4 different patient derived (vehicle treated) RMFs and CAFs as in (A). No significant differences reported. Error bars, SEM. Data collected in colloboration with Brandi Davis, Hata Laboratory.

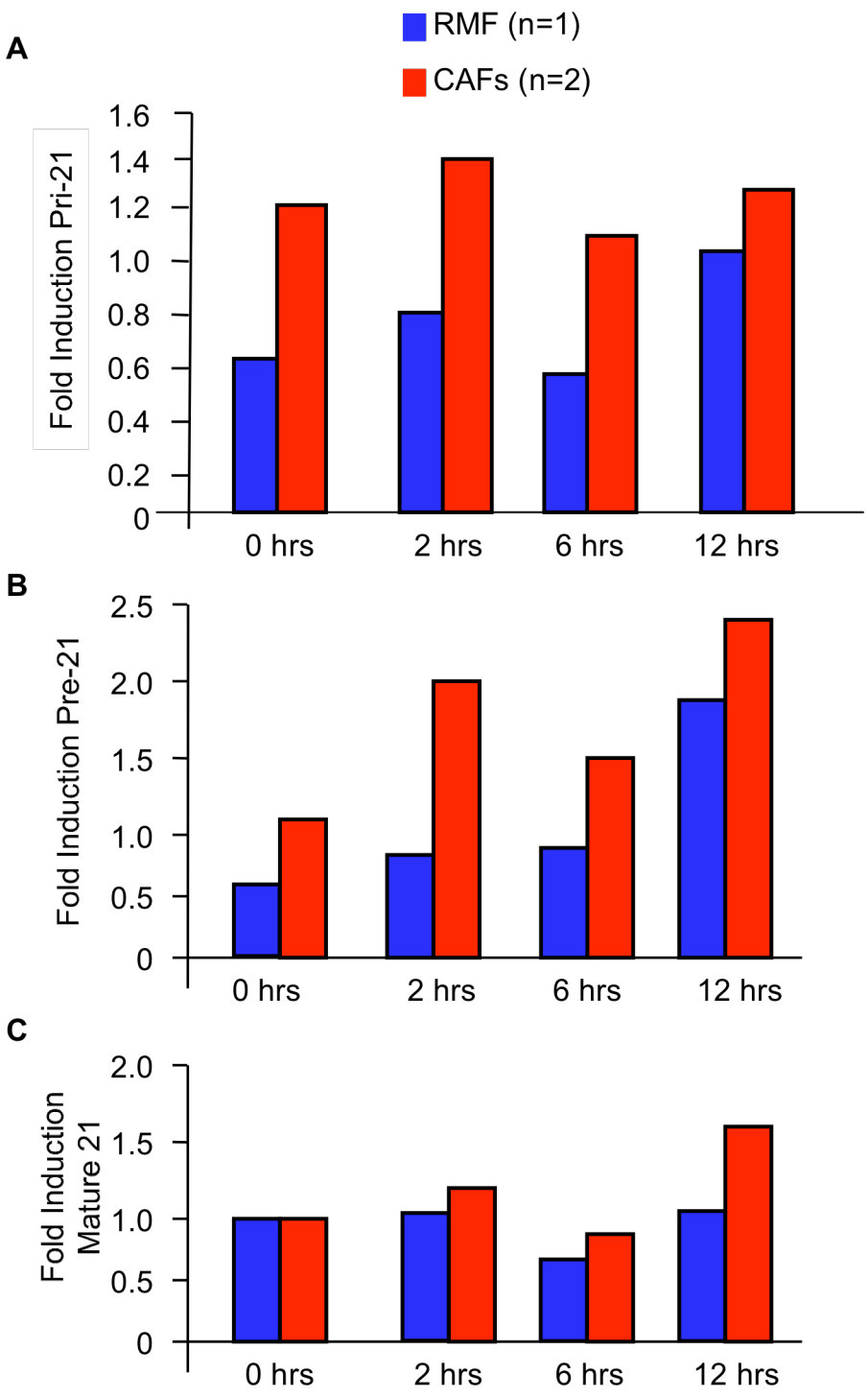
A
RMF (n=1)
CAFs (n=2)
Fold Induction Pri-21
1.6
1.4
1.2
1.0
0.8
0.6
0.4
0.2
0
0 hrs
2 hrs
6 hrs
12 hrs
B
Fold Induction Pre-21
2.5
2.0
1.5
1.0
0.5
0
0 hrs
2 hrs
6 hrs
12 hrs
C
Fold Induction Mature 21
2.0
1.5
1.0
0.5
0
0 hrs
2 hrs
6 hrs
12 hrs

<u>Supplemental Figure 3.3:</u> Time course analysis for the fold induction (over vehicle) of pri, pre, and mature miR21 levels in TGFβ treated CAFs and RMFs.

(A) qRT-PCR results for the fold induction (over vehicle) of pri-miR21 at 0, 2, 6 and 12 hrs post TGFβ1 treatment in one patient derived RMF and two patient derived CAFs (averaged). **(B)** qRT-PCR results for the fold induction (over vehicle) of pre-miR21 at 0, 2, 6 and 12 hrs post TGFβ1 treatment in one patient derived RMF and two patient derived CAFs (averaged). **(C)** qRT-PCR results for the fold induction (over vehicle) of mature miR21 at 0, 2, 6 and 12 hrs post TGFβ1 treatment in one patient derived RMF and two patient derived CAFs (averaged).

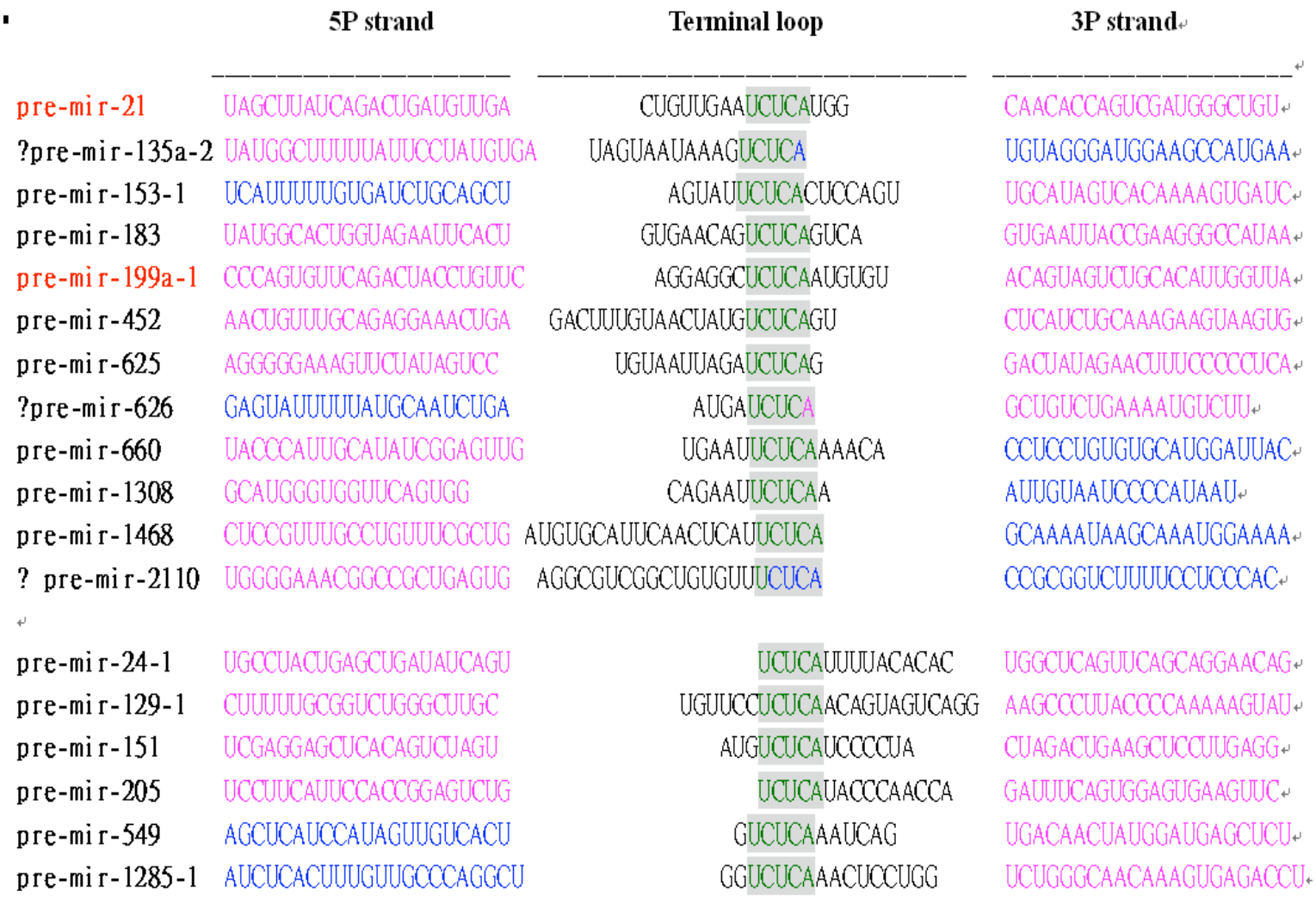
5P strand
Terminal loop
3P strand
pre-mir-21 UAGCUUAUCAGACUGAUGUUGA CUGUUGAAUCUCAUGG CAACACCAGUCGAUGGGCUGU
?pre-mir-135a-2 UAUGGCUUUUUAUUCCUAUGUGA UAGUAAUAAAGUCUCA UGUAGGGAUGGAAGCCAUGAA
pre-mir-153-1 UCAUUUUUGUGAUCUGCAGCU AGUAUUCUCACUCCAGU UGCAUAGUCACAAAAGUGAUC
pre-mir-183 UAUGGCACUGGUAGAAUUCACU GUGAACAGUCUCAGUCA GUGAAUUACCGAAGGGCCAUAA
pre-mir-199a-1 CCCAGUGUUCAGACUACCUGUUC AGGAGGCUCUCAAUGUGU ACAGUAGUCUGCACAUUGGUUA
pre-mir-452 AACUGUUUGCAGAGGAAACUGA GACUUUGUAACUAUGUCUCAGU CUCAUCUGCAAAGAAGUAAGUG
pre-mir-625 AGGGGGAAAGUUCUAUAGUCC UGUAAUUAGAUCUCAG GACUAUAGAACUUUCCCCCUCA
?pre-mir-626 GAGUAUUUUUAUGCAAUCUGA AUGAUCUCA GCUGUCUGAAAAUGUCUU
pre-mir-660 UACCCAUUGCAUAUCGGAGUUG UGAAUUCUCAAAACA CCUCCUGUGUGCAUGGAUUAC
pre-mir-1308 GCAUGGGUGGUUCAGUGG CAGAAUUCUCAA AUUGUAAUCCCCAUAAU
pre-mir-1468 CUCCGUUUGCCUGUUUCGCUG AUGUGCAUUCAACUCAUUCUCA GCAAAAUAAGCAAAUGGAAAA
? pre-mir-2110 UGGGGAAACGGCCGCUGAGUG AGGCGUCGGCUGUGUUUCUCA CCGCGGUCUUUUCCUCCCAC
pre-mir-24-1 UGCCUACUGAGCUGAUAUCAGU UCUCAUUUUACACAC UGGCUCAGUUCAGCAGGAACAG
pre-mir-129-1 CUUUUUGCGGUCUGGGCUUGC UGUUCCUCUCAACAGUAGUCAGG AAGCCCUUACCCCAAAAAGUAU
pre-mir-151 UCGAGGAGCUCACAGUCUAGU AUGUCUCAUCCCCUA CUAGACUGAAGCUCCUUGAGG
pre-mir-205 UCCUUCAUUCCACCGGAGUCUG UCUCAUACCCAACCA GAUUUCAGUGGAGUGAAGUUC
pre-mir-549 AGCUCAUCCAUAGUUGUCACU GUCUCAAAUCAG UGACAACUAUGGAUGAGCUCU
pre-mir-1285-1 AUCUCACUUUGUUGCCCAGGCU GGUCUCAAACUCCUGG UCUGGGCAACAAAGUGAGACCU

<u>Supplemental Figure 3.4:</u> Additional pre-miRs containing the UCUCA consensus motif in the hairpin terminal loop that might also respond to TGFβ by inducing pre-miR processing.

Sequence alignment of several pre-miRs within the human genome that harbor a similar sequence motif (UCUCA) within the pre-miR terminal loop region. Pre-miRs with the UCUCA motif at the 3' end of the terminal loop may have very similar secondary structures to pre-miR21 and pre-miR199a, and may respond to TGFβ1 in a similar fashion as these two miRs do in CAFs. Data from Xiang Liu, Kuperwasser Laboratory.

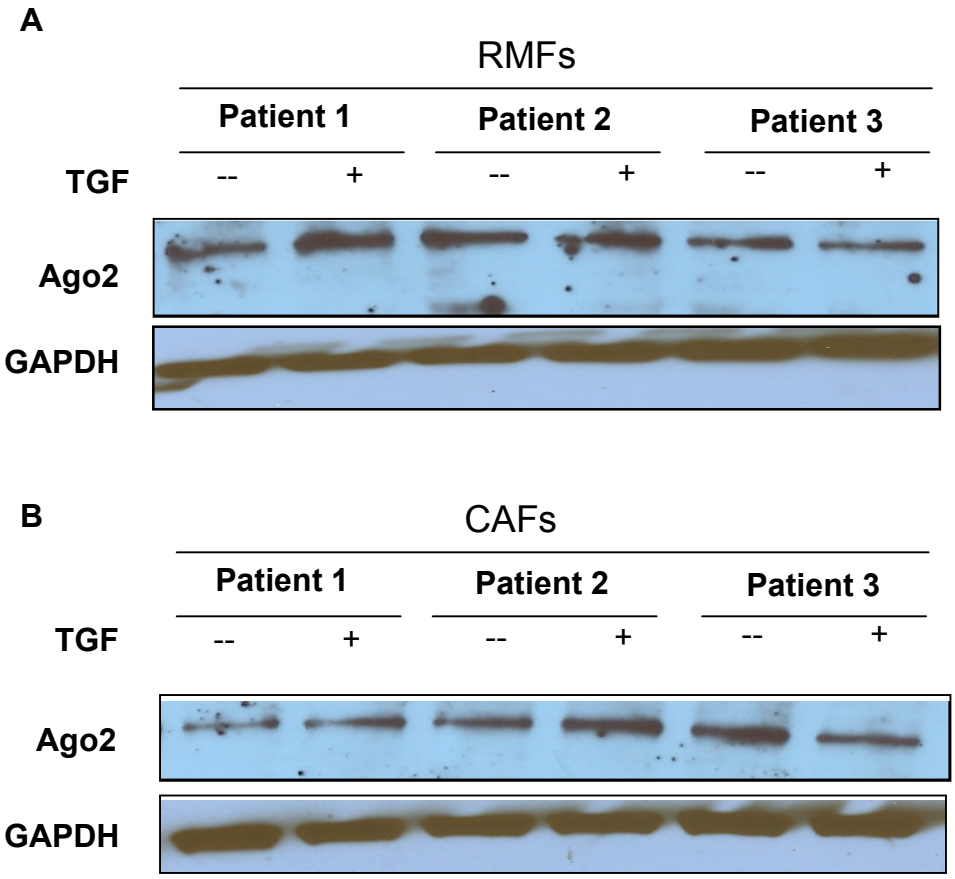

<u>Supplemental Figure 3.5:</u> Argonaute-2 expression in vehicle and TGFβ treated CAFs and RMFs.

Western blot for Argonaute-2 (Ago2) expression in whole cell lysates from vehicle or TGFβ treated RMFs **(A)** or CAFs **(B)**, each isolated from 3 different patient samples.

Supplementary Table 3.1: Primer sequences used for qRT-PCR.

Gene	Forward Primer	Reverse Primer
Pri-miR-21	5′-TTTTGTTTTGCTTGGGAGGA-3′	5′-AGCAGACAGTCAGGCAGGAT-3′
Pre-miR-21	5′-TGTCGGGTAGCTTATCAGAC-3′	5′-TGTCAGACAGCCCATCGACT-3′
Mature miR21	ND; proprietary (Applied Biosystems)	ND; proprietary (Applied Biosystems)
U6	ND; proprietary (Applied Biosystems)	ND; proprietary (Applied Biosystems)
αSMA	5′-CCAGCTATGTGTGAAGAAGAGG-3′	5′-GTGATCTCCTTCTGCATTCGGT-3′
GAPDH	5′-ACCACAGTCCATGCCATCAC-3′	5′-TCCACCACCCTGTTGCTGTA-3′
Drosha	(awaiting information from Hata Lab)	(awaiting information from Hata Lab)
p68	5′-TATGATGTGGAGGAGGTGGATGTGA-3′	5′-TATGATGTGGAGGAGGTGGATGTGA-3′
Dicer	(awaiting information from Hata Lab)	(awaiting information from Hata Lab)
Sprouty1	5’-CCTGTTTGGCCTGTAACCG-3’	5’-CCTTCGTCGTCATTGGAGCA-3’
PTEN	5’-TGGATTCGACTTAGACTTGACCT-3’	5’-TTTGGCGGTGTCATAATGTCTT-3’
PDCD4	5’-TAAGTGACTCTCTCTTTTCCGGT-3’	5’-TTTTTCCTTAGTCGCCTTTTTGC-3’
TIMP3	5’-CAACTCCGACATCGTGATCCG-3’	5’-GAAGCCTCGGTACATCTTCATC-3’
SMARCD1	5’-GCTCCATGCCTTGCTTATGC-3’	5’-CATGAACTCCCGCTGAGTCTT-3’

<u>Supplemental Table 3.2:</u> Primer sequences used for *in vitro* transcription of pre-miR21 and pre-miR100 with 5' extensions and T7 promoters.

Gene	Primer
Pre-miR21-5p (F)	5'-GAATTAATACGACTCACTATAGGGAGAATAGATAGTTAGCTTATCAGACTGATGTT-3'
Pre-miR21-3p (R)	5'-ACAGCCCATCGACTGGTGTT-3′
Pre-miR100-5p (F)	5'-GAATTAATACGACTCACTATAGGGAGAATAGATAGTAACCCGTAGATCCGAACTTG-3'
Pre-miR100-3p (R)	5′-CATACCTATAGATACAAGCT-3′
Biotinylated Oligo	5′-ACTATCTATTCTCCC-biotin-3'

CHAPTER IV:

Discussion and Future Directions

4.1 Heterogeneity among fibroblasts

CAFs isolated from various solid tumors have tumor promoting properties *in vivo* (Erez et al., 2010; Hwang et al., 2008; Liao et al., 2009; Olumi et al., 1999; Orimo and Weinberg, 2006), while fibroblasts isolated from disease-free tissues can harbor either tumor promoting or tumor suppressive properties (Dotto et al., 1988; Elenbaas et al., 2001; Elenbaas and Weinberg, 2001; Kuperwasser et al., 2004). Aside from αSMA, markers used to discriminate tumor promoting fibroblasts from non-tumor promoting fibroblasts remain entirely unknown. Moreover, αSMA may not fully discriminate between these functional differences in fibroblasts grown *in vitro* (Rudnick *et al.,* 2011), despite this being a well established marker of activated fibroblasts in the literature (Desmouliere et al., 2004; Sousa et al., 2007; Sugimoto et al., 2006). In this work, I have identified a functional attribute of tumor promoting fibroblasts: the ability to secrete PGE2 and respond to PGE2 signaling. These data corroborate previous work demonstrating that fibroblasts isolated from arthritic synovium express Cox-2 and support breast tumor growth in a xenograft mouse model (Hu et al., 2008).

Our results suggest that PGE2 secretion and signaling may be more indicative of fibroblast tumor promoting ability than αSMA expression. However, we cannot exclude the possibility that given the inability to sort for pure populations of fibroblasts (due to lack of specific markers for these cells), the culture conditions used may obscure robust differences in αSMA expression

between various patient derived fibroblast populations. Additionally, several cell types within the breast tumor microenvironment in addition to fibroblasts express αSMA, and may be inadvertently propagated in our fibroblast cultures, confounding our results. In the future, FACS sorting of fibroblasts using strategies published by other laboratories (Erez et al., 2010) may further enrich for fibroblasts and control for these issues.

There are several other variables that possibly play an important role in fibroblast tumor promoting ability that we cannot investigate due to patient privacy and Institutional Review Board (IRB) law. First, fibroblasts from different breast developmental stages may have higher or lower levels of Cox-2 expression and PGE2 secretion. For example, because the involuting mammary gland is a highly pro-inflammatory microenvironment with extensive matrix remodeling and immune cell recruitment (McDaniel et al., 2006), fibroblasts isolated from involuting glands may have higher basal levels of PGE2 secretion and may be more tumor promoting than those isolated from a nulliparous gland. Similarly, stromal cells isolated from the glands of lactating mice significantly enhance mammary tumor growth compared to stromal cells isolated from any other stage of mammary gland development in a xenograft mouse model of breast cancer (McCready et al., 2011). It would be interesting to measure the levels of PGE2 secretion from these stromal cells to see if stromal cell tumor promoting ability correlates with PGE2 secretion as it does with human fibroblasts.

Secondly, the parity status of the woman from which the breast fibroblasts were isolated may be another uncontrollable factor in their inherent tumor promoting abilities. It is known that one lifetime pregnancy reduces overall breast cancer risk, however breast cancer risk increases within 5 yrs following pregnancy (Schedin, 2006). The reason for this elevated risk within 5 yrs is largely unknown, although some investigators speculate this is due to the rapid rise in hormones during pregnancy (Schedin, 2006). However, changes within the breast stroma after robust expansion of the breast epithelium, the hormonal changes and other systemic factors released during and after pregnancy may invoke changes in fibroblast gene expression, which may increase their tumor promoting potential.

A novel and exciting area of future research would involve the investigation of fibroblast heterogeneity and tumor promoting ability in a larger sample size of human breast tumors encompassing different tumor subtypes. It seems possible that basal-like breast tumors, associated with poor clinical outcome and limited adjuvant treatment options, might contain fibroblasts with higher PGE2 and IL-6 secretion compared to fibroblasts from luminal-type tumors, contributing to the increased aggressiveness of these tumors overall. Moreover, *BRCA1* mutation carriers may have differences in fibroblast gene expression that contribute to the elevated risk of tumor development in these women. Not only would these data further elucidate fibroblast heterogeneity, but they may also provide a framework for specialized treatments in treating different breast tumor subtypes.

In summary, the data presented here suggest that tumor promoting fibroblasts can be distinguished based on their secretion of PGE2 and autocrine PGE2 signaling. These data could have clinical applications for breast cancer patients whose desmoplastic stroma is strongly immunoreactive for Cox-2 expression. These patients may benefit greatly from an adjuvant therapy targeting both the tumor cells as well as the adjacent tumor promoting fibroblasts. Although the use of Cox-2 inhibitors as anti-cancer agents and remedies for inflammatory based diseases reportedly have had deleterious side effects in patients (Meric et al., 2006; Ulrich et al., 2006), new generations of non-steroidal anti-inflammatory drugs (NSAIDs) may have promising results in the treatment of breast cancer.

4.2 Fibroblast mediated expansion of BCSCs

Since the discovery of BCSCs (Al-Hajj et al., 2003), tumor promoting molecular mechanisms that specifically invoke this cell population have important implications for future breast cancer drug design. While fibroblasts have been implicated in promoting breast tumor growth, the mechanisms by which fibroblasts expand this population of aggressive cells has remained largely unknown. In this work, I have elucidated a novel mechanism by which fibroblasts respond to PGE2 signaling by increasing secretion of IL-6, which is required, but not sufficient, for expansion of BCSCs. Recently, the IL-6/JAK-2/Stat-3 pathway was shown to be preferentially upregulated in BCSCs compared to more differentiated cell types within the tumor bulk (Marotta et al., 2011), validating IL-

6 signaling as a potential therapeutic option for eradication of this highly tumorigenic cell population.

I speculate that certain cytokines work in concert with IL-6 to mediate expansion of BCSCs. Future studies should focus on identifying these cooperating cytokines and the signaling pathways in fibroblasts that promote their secretion. Interestingly, recent work has shown that *PTEN* loss in stromal fibroblasts significantly accelerates Erbb2 driven mammary tumor growth (Trimboli et al., 2009). These data provide speculation for the role of the PI3K/Akt pathway in governing the tumor promoting abilities of fibroblasts; the possibility that these pathways are activated downstream of PGE2 signaling warrants further investigation.

4.3 CAFs are wired differently than RMFs

CAFs resected from human breast tumor tissues retain their tumor promoting phenotype when they are explanted *in vitro* and devoid of tumor cell secreted factors (Erez et al., 2010; Olumi et al., 1999; Orimo and Weinberg, 2006). These data suggest that CAFs permanently retain a memory of co-evolving with tumor cells possibly over several decades, inferring they may have permanently remodeled chromatin and epigenetic marks. At present, there lacks strong, convincing data to support the notion that CAFs are genetically modified (Campbell et al., 2009; Kojima et al., 2010), suggesting their phenotype is entirely dependent upon these epigenetic modifications. In this work, I have demonstrated that CAFs are distinguished from RMFs based on their ability to

induce the processing of mature miR21 and mature miR199a from their precursors in a TGFβ dependent manner. To my knowledge, these data are the first characteristic of CAFs, aside from their tumor promoting abilities *in vivo*, which distinguishes them from RMFs. Given that both cell types respond to TGFβ signaling with equal capabilities, have similar levels of miR processing molecules, and similar basal levels of these miRs, we speculate that epigenetic differences in the response to non-canonical TGFβ signaling govern this discrepancy in miR processing.

While it has been known for decades that TGFβ induces fibroblast activation and myofibroblast phenotype in breast tissue fibroblasts (Ronnov-Jessen and Petersen, 1993; Ronnov-Jessen et al., 1990; Sousa et al., 2007; Vaughan et al., 2000), the precise molecular mechanisms through which TGFβ mediates these effects has remained largely elusive. Moreover, until recently, there lacked any direct evidence for TGFβ in mediating the conversion of breast tissue fibroblasts into tumor promoting CAFs. However, recent data suggest that the TGFβ and SDF1α signaling pathways work in an autocrine cooperative fashion to promote and sustain CAF phenotype in immortalized RMFs (Kojima et al., 2010). While limited evidence suggests canonical Smad 2/3 signaling mediates this process (Kojima et al., 2010), future work should investigate if non-canonical TGFβ mediated miR processing also contributes to this CAF conversion. It seems likely that co-evolving with tumor cells over decades results in significantly elevated levels of TGFβ and SDF1α in the tumor microenvironment, which perpetuate these signaling pathways. Because chronic,

but not transient, TGFβ stimulation in fibrotic fibroblasts induces changes in DNA methylation (Bechtel et al., 2010), this may occur in CAFs as well. The activating or repressing chromatin marks of certain gene promoters in CAFs may cause the upregulation of proteins involved in miR biogenesis, which may explain why CAFs, but not RMFs, can induce the processing of mature miR21 and miR199a (and likely others not yet investigated) from their precursor forms. These proteins likely respond to TGFβ signaling, since the processing differences observed were entirely dependent on this cytokine.

It is unclear if the Smad proteins are involved in this pre-miR to mature miR processing step, as they are in TGFβ induced Drosha mediated processing (Davis et al., 2008). We failed to pull down any Smad proteins in our pre-miR pull down assay. However, we identified three proteins that interact with pre-miR21, but not pre-miR100, and are involved in the process of A→I RNA editing. While we lack definitive evidence that pre-miR21 is indeed edited by ADAR, these findings would conflict with the fact that the edited form gives rise to a mature miR product that is stable for at least 24 hrs, given that dsRNAs edited by ADAR are less efficient substrates for Dicer (Scadden and Smith, 2001). It is possible that ADAR mediated editing of pre-miR21 does not reduce its stability and half-life, but only serves to modify mRNA target recognition by creating a steric hindrance with the 3' UTR of target genes. The consequence of changes in miR target recognition may be largely responsible for governing CAF phenotype. Perhaps it is the alterations of certain miR target genes that dictate differences in gene expression between CAFs and RMFs. A direct, extensive analysis of the

miR21 target genes in CAFs and RMFs is essential to investigating the possibility that CAFs are indeed resident tissue breast fibroblasts with epigenetically distinct miR profiles and target genes.

4.4 Conclusion

In conclusion, I have identified a novel characteristic of tumor promoting breast fibroblasts that distinguishes them from non-tumor promoting breast fibroblasts: PGE2 secretion and signaling. My results indicate that these characteristics better predict the inherent tumor promoting ability of fibroblasts more so than the origin of the tissue from which these fibroblasts were derived (i.e. reduction mammoplasty or breast tumor) or the extent of αSMA expression.

In addition, I have identified a novel characteristic of CAFs that distinguishes them from RMFs: the ability to promote the processing of pre-miR21 to mature miR21 and miR199a in a TGFβ dependent manner. These results corroborate previous reports of epigenetic distinctions between CAFs and RMFs. While the consequence of this miR21 and miR199a induction in CAFs remains unknown, preliminary evidence suggests it may play a part in mediating CAF phenotype, possibly through the process of RNA editing. Moreover, it is likely that several additional miRs are processed in response to TGFβ signaling and play a role in CAF phenotype as well.

Collectively, these data provide a promising framework for the development of adjuvant breast cancer therapies targeting tumor associated stroma.

CHAPTER V:

Materials and Methods

5.1 Materials and Methods for Chapter II

Isolation of primary fibroblasts from human breast tumors and reduction mammoplasty tissues.

All human breast tissue procurement for these experiments was obtained in compliance with the laws and institutional guidelines, as approved by the institutional IRB committee from Tufts University School of Medicine. Primary breast tumor tissues were obtained from discarded material at Tufts Medical Center and non-cancerous breast tissue was obtained from patients undergoing elective reduction mammoplasty at Tufts Medical Center. Breast tissues were minced and enzymatically digested overnight with a mixture of collagenase and hyaluronidase as previously described (Keller et al., 2010; Proia and Kuperwasser, 2006). Large clusters of undigested tissue were allowed to settle and the supernatant enriched for stromal cells was collected, washed and plated in serum containing medium to enrich for mammary fibroblasts. Cells were grown in DMEM supplemented with 10% calf serum (CS) and antibiotic/antimycotic (AB/AM, Invitrogen, Carlsbad, CA) for multiple passages until senescent as described previously (Proia and Kuperwasser, 2006). Senescent fibroblasts were not included in subsequent experiments.

Cell cultures, conditioned media collection, and cell treatments.

Fibroblasts were grown as described above. MCF7 breast cancer cells were grown in DMEM + 10% CS + 1% AB/AM. All cultures were maintained at 37 °C and 5% CO_2. To generate conditioned media, fibroblasts were seeded at 1.5 x 10^6 cells/plate in phenol red free DMEM (PRF-DMEM, Invitrogen), supplemented with either 0.5% or 2% charcoal/dextran stripped FBS (Invitrogen) and 1% AB/AM, treated with ethanol or 0.5 μM PGE2 (Sigma-Aldrich, St. Louis, MO), or left untreated, for 72 hrs. CM was then harvested, filtered through a 0.22 μm filter (Millipore, Danvers, MA), aliquoted and stored at -80 °C. For MCF7 treatments, cells were grown in PRF-DMEM supplemented with 5% charcoal/dextran stripped FBS, 1% AB/AM, and treated with ethanol, 0.5 μM PGE2, or 1 nM 17-β-Estradiol (Sigma Aldrich). For MCF7 treatments involving fibroblast CM, CM was collected as previously described, supplemented with 5% charcoal/dextran stripped FBS, and administered to MCF7 cells for 6 days. α-IL6 and recombinant human IL-6 (R&D Systems, Minneapolis, MN) were used at 1.5 μg/mL and 10 ng/mL, respectively.

Preparation of cells for mouse mammary fat pad inoculation.

All animal procedures were performed in accordance with an approved protocol by Tufts University Institutional Animal Care and Use Committee. A colony of NOD/SCID mice was maintained under sterile housing conditions and received food and water *ad libum*. Nulliparous female mice between 8 to 14 weeks age were utilized in all experiments. For co-mixing experiments, 1.5 x 10^6 human breast fibroblasts were mixed with 500,000 MCF7 breast cancer cells,

resuspended in a 3:1 (vol/vol) ratio of media to Matrigel (BD Biosciences, San Jose, CA) mixture, and inoculated into the 4th inguinal mammary gland. Tumor formation was assessed by palpitation weekly. For MCF7 limiting dilution experiments, 500,000 MCF7 cells were cultured in conditioned media (CM) from PGE2-treated fibroblasts for 6 days, after which 10,000 cells were resuspended in a 3:1 (vol/vol) ratio of media to Matrigel mixture, and inoculated into the 4th inguinal mammary gland. Tumor formation was assessed by palpitation weekly.

Immunofluorescence.

Fibroblasts were seeded at 5,000 cells/well of 8 well-chamber slides (Becton Dickinson, Franklin Lakes, NJ) in DMEM + 10% CS + 1% AB/AM (Invitrogen) for 96 hours before fixed in methanol. Cells were then permeabilized with 0.1% Triton X-100 (Sigma) in PBS, washed and blocked in 1% BSA in PBS at ambient temperature. Cells were incubated with the following antibodies overnight at 4 °C: mouse α-alpha SMA (1:200, Vector Labs, Burlingame, CA), mouse α-Vimentin (1:200, Vector Labs), mouse α-prolyl-4-hydroxylase (1:300, Millipore), and mouse α-caveolin-1 (1:150, Novus Biologicals, Littleton, CO). Fluorescence signal was detected using goat α-mouse secondary antibodies (1:500, conjugated with Alexa488 and Alexa588, Invitrogen). Nuclei were stained with 4', 6-diamidino-2-phenylindole (DAPI) and images were captured with the Spot imaging software system (Diagnostic Instruments, Inc., Sterling Heights, MI). Quantification was performed using Image-J software.

qRT-PCR.

RNA was isolated and purified using an RNeasy kit (Qiagen, Valencia, CA) for cultured cells. RNA was reverse transcribed to cDNA using an iScript cDNA synthesis kit (Biorad). Quantitative real time RT-PCR analysis was performed using SyBR Green and an iCycler thermocycler (Biorad). Primer sequences used for quantitative real-time PCR are listed in Supplementary Table 1.

FACS.

Nonconfluent cultures of MCF7 cells were trypsinized into single cell suspension, counted, and resuspended in FACS buffer (PBS + 3% CS). 100,000 cells were stained with the following antibodies for 15 minutes at ambient temperature: α-human CD24-PE (BD Biosciences), α-human CD44-APC (BD Biosciences), α-human ESA-FITC (Stem Cell Technologies, Vancouver, BC, Canada), and isotype controls for each antibody (Mouse IgG_{2a}-PE, Mouse IgG_{2b}-APC, Mouse IgG_1-FITC, BD Biosciences). Unbound antibody was washed away with FACS buffer, and cells were analyzed no longer than 1 hr post staining on a BD FACS Calibur.

Tumorsphere assays.

Fibroblasts were treated with either ethanol or 0.5 μM PGE2, and conditioned media was prepared as described above. Upon use, CM was supplemented with 5% charcoal/dextran-stripped FBS. MCF7s were dissociated

to a single cell suspension, plated at 20,000 cells/ml, and grown on ultra-low adherence 6-well plates (Corning Life Sciences, Lowell, MA) in the presence of supplemented CM for 6 days. For recombinant human IL-6 studies or exogenous PGE2 studies, MCF7s were plated as described above in the presence of PRF-DMEM supplemented with 5% charcoal/dextran-stripped FBS and the following treatments: 0.1% BSA in PBS or 10 ng/mL recombinant human IL-6 (R&D Systems), or ethanol or 0.5 μM PGE2 (Sigma Aldrich). Tumorspheres were quantified using a Multisizer-3 coulter counter (Beckman-Coulter, Brea, CA).

PGE2 enzyme immunoassay.

Fibroblast conditioned media was prepared as described above and subjected to a Prostaglandin E2 monoclonal EIA kit according to the manufacturer's instructions (Cayman Chemical, Ann Arbor, MI). Concentration (pg/ml) was determined by generating a standard curve with known concentrations of PGE2. Absorbance was read at 405 nm using a 96 well plate μQuant spectrophotometer (Biotek, Winooski, VT) and the KC Junior software program (Biotek).

Cytokine array.

Fibroblasts were treated with either ethanol or 0.5 μM PGE2, and CM was prepared as described above. Human cytokine arrays (2000 series, RayBiotech, Norcross, GA) were exposed to CM isolated from ethanol or 0.5 μM PGE2-treated fibroblasts and processed according to the manufacturer's instructions.

Exposed films were quantified for chemiluminescence intensity using a Xenogen phosphoimager.

IL-6 ELISA.

Fibroblast CM was prepared as described above and subjected to a human specific IL-6 ELISA according to the manufacturer's instructions (eBiosciences, San Diego, CA). Concentration (pg/ml) was determined by generating a standard curve with known concentrations of recombinant human IL-6. Absorbance was read at 450 nm using a 96 well plate μQuant spectrophotometer (Biotek, Winooski, VT) and the KC Junior software program (Biotek). Concentrations were normalized to total numbers of fibroblasts after 72 hour exposure to either ethanol or 0.5 μM PGE2 and reported as arbitrary units.

Western blotting.

MCF7 cells were seeded at 250,000 cells/well and exposed to CM or treatments as described above. After 6 days, cells were pelleted and lysed in RIPA buffer to prepare cell lysates. Fibroblast CM was prepared as previously described and concentrated using Amicon Ultra Centrifugal Filters (Millipore). Protein concentration from both lysates and CM was determined using a Lowry Assay according to manufacturer's instructions (Biorad, Hercules, CA). 30 or 50 μg of protein was resolved on a 4-12% polyacrylamide gel, transferred to a nitrocellulose membrane (Biorad), and immunoblotted using the following antibodies: mouse α-GAPDH (1:5000, Millipore), mouse α-phosphorylated-

STAT3 (Y705, 1:1000, Cell Signaling Technologies, Danvers, MA), rabbit α-total-STAT3 (1:2000, Cell Signaling Technologies), mouse α-Cox-2 (Cayman Chemical), mouse α-Cox-1 (Cayman Chemical), or rabbit α-IL6 (1:10,000, Abcam, Cambridge, MA). Signal was detected using HRP-conjugated goat α-mouse (1:14,000) or goat α-rabbit (1:12,000) secondary antibodies (Cell Signaling) and West Dura Extended Chemiluminescence Substrate (Fisher).

Immunohistochemistry.

Tumor tissues from MCF7 xenografts were fixed in 10% neutral buffered formalin and paraffin embedded with standard procedures. Tumor sections were deparaffinized, re-hydrated through graded ethanols and subjected to heat-induced antigen retrieval. Staining was performed by the Department of Pathology Core Facility at Tufts Medical Center.

5.2 Materials and Methods for Chapter III

Isolation of primary fibroblasts from human breast tumors and reduction mammoplasty tissues.

All human breast tissue procurement for these experiments was obtained in compliance with the laws and institutional guidelines, as approved by the institutional IRB committee from Tufts University School of Medicine. Fibroblasts were isolated as described in Section 5.1.

TGFβ treatment.

Fibroblasts were grown as described above. All cultures were maintained at 37 °C and 5% CO_2. CAFs and RMFs were seeded at 100,000 cells per well of 6 well plates (Becton Dickinson) in normal growth medium (DMEM + 10% CS + AB/AM). At 70% confluence, cells were changed to starvation medium (DMEM + 0.2% CS + AB/AM). For wells receiving the ALK5 inhibitor SB431542 (Sigma), the inhibitor was reconstituted at 10 mM in DMSO and stored -80 °C. Upon use, SB431542 was added to cells one hour prior to treatment with TGFβ at a final concentration of 10 μM. For wells receiving TGFβ treatment, human recombinant TGFβ1 (R&D Systems) was reconstituted in 4 mM HCl + 0.1% BSA to a final concentration of 2 μg/mL, aliquotted and stored at -80 °C until use. Upon use, TGFβ was diluted 1:1000 in DMEM + 0.2% CS + AB/AM and added to cells for a final concentration of 100 pM (or 400 pM for some assays described in text). Cells were harvested after 24 hrs of TGFβ treatment. Cells were washed twice in sterile PBS and 300 μL TRIzol (Invitrogen) was added to each well. After a 5 minute incubation at RT in TRIzol to lyse cells, plates were wrapped in parafilm and stored at -80 °C until continuation with RNA isolation and qRT-PCR.

TaqMan microRNA assay.

For quantitative analysis of the levels of mature miRs, the TaqMan MicroRNA assay kit (Applied Biosystems, Carlsbad, CA), specific for mature miR21, mature miR199a, mature miR25 and mature miR100, was used according to the manufacturer's instructions. As recommended by the

manufacturer, total RNA was harvested using the TRIzol method (as described by Invitrogen). RNA concentration was determined using a Nanodrop.

qRT-PCR for all other investigated transcripts.

For the pri-miRs and pre-miRs examined, RNA was isolated using the TRIzol method (as described by Invitrogen). cDNA was synthesized from 1 μg of purified RNA by SuperScript II First-Strand cDNA synthesis system (Invitrogen) according to the manufacturer's instructions. qRT-PCR was performed with a real-time PCR machine (iQ5, Biorad). These experiments were performed by Brandi Davis in the Hata Laboratory. For all other investigated transcripts (aside from mature miRs), RNA was isolated and purified using an RNeasy kit (Qiagen, Valencia, CA) for cultured cells. RNA was reverse transcribed to cDNA using an iScript cDNA synthesis kit (Biorad). qRT-PCR analysis was performed using SyBR Green and an iCycler thermocycler (Biorad). These experiments were performed by members of the Kuperwasser Laboratory. All non-proprietary primer sequences used for qRT-PCR are listed in Supplementary Table 3.1.

Western blotting.

CAFs and RMFs were cultured on 10-cm plates (Becton Dickinson) in normal growth medium (DMEM + 10% CS + AB/AM). At 70% confluence, cells were switched to starvation medium (DMEM + 0.2% CS + AB/AM) and treated with 400 pM TGFβ or vehicle for 24 hours. After 24 hours, cells were pelleted and lysed in RIPA buffer to prepare cell lysates. Protein concentration was

determined using a Lowry Assay according to manufacturer's instructions (Biorad, Hercules, CA). 30 or 50 μg of protein was resolved on a 4-12% polyacrylamide gel, transferred to a nitrocellulose membrane (Biorad), and immunoblotted using the following antibodies: rabbit α-Ago2 (1:1000, Cell Signaling Technologies), rabbit α-SND1 (also known as p100/Tudor SN, 1:300, Abcam), mouse α-ADAR1 (1:1000, Abcam), mouse α-TIMP3 (5 μg/mL, Abcam), mouse α-GAPDH (1:5000, Millipore), rabbit α-total ERK (1:1000, Cell Signaling Technologies). Signal was detected using HRP-conjugated goat α-mouse (1:14,000) or goat α-rabbit (1:12,000) secondary antibodies (Cell Signaling) and West Dura Extended Chemiluminescence Substrate (Fisher).

Preparation of CAF cell extract and in vitro *transcription of pre-miR template for pull down assay.*

A representative CAF patient sample was significantly expanded on 15-cm plates for sufficient starting material of cell extract. At 90% confluence, plates were washed twice with PBS and switched to starvation medium (DMEM + 0.2% CS + AB/AM). Half of the plates were treated with 400 pM TGFβ, and half were treated with vehicle control or 24 hours before harvesting cells. Upon harvest, cells were washed twice with PBS and removed from the plate using a cell lifter. 10 μl of cell suspension was removed for a future miR TaqMan assay to ensure miR21 induction in response to TGFβ. The remaining cell suspension was pelleted and frozen -80 °C until time of assay. At time of pre-miR pull down assay, cell pellets were thawed on ice and lysed in 4X the volume of Buffer I (20

mM Tris-HCl pH 7.5, 100 mM KCl, 2 mM EDTA, dH_2O) containing protease inhibitor on ice for 30 min. Pellets were dounced with a glass dounce tissue grinder for at least 30 times on ice and transferred to epindorf tubes. Cell debris was removed by centrifuging at 13,000 rpm for 10 min at 4 °C and repeated, if necessary, until the supernatant was clean. Protein concentration was determined using a Lowry Assay according to manufacturer's instructions (Biorad).

Pre-miR21 and pre-miR100 with 5' extensions were produced by *in vitro* transcription. PCR was performed to prepare the template DNA (with 5' extensions and T7 promoter) for *in vitro* transcription. pTOPO-pre-miR21 plasmid or pTOPO-pre-miR100 plasmids were used as PCR templates diluted at 1:50. A 100 μl PCR was performed using a HotStarTaq plu Master Mix Kit (Qiagen) with the following PCR conditions: 94 °C 30s, 55 °C 30s, 72 °C 30s, repeated 35 cycles. Primer sequences are listed in Supplementary Table 3.2. PCR product was harvested using 2.5X the volume of ethanol at -20 °C for 30 min, centrifuged at 13,000 rpm for 10 min and resuspended in 30 μl dH_20. PCR quality was verified by running the 1 μl of product on a 7M Urea PAGE gel and staining with ethidium bromide. *In vitro* transcription was performed in 20 μl reaction containing 2 μl 10X buffer, 4 μl 2.5 mM rNTP (Promega, Madison, WI), 0.5 μl RNase inhibitor (Ambion, Austin, TX), 1 μg DNA, 1 μl T4 RNA polymerase (Invitrogen) and water overnight at 37 °C. DNA template was erased using 1 μl DNase I (Roche Diagnostics, Indianapolis, IN) for every 20 μl reaction and incubate at 37 °C for 15 min, followed by phenol/chloroform purification and

ethanol precipitation. The RNA pellets yielded from the reaction were dissolved in 20 μl RNA Loading Buffer II (Invitrogen), denatured at 100 °C for 5 min, separated on a 7M Urea PAGE gel and stained with ethidium bromide for 5 min. After staining, the gel was washed with gel running buffer and the proper size RNAs were cut under ultraviolet light. 500 μl elution buffer were added to cut gel pieces and homogenized, rotated at room temperature for at least 2 hours, and eluted with mini-prep columns (Qiagen) centrifuging at 13,000 rpm for 5 min. RNA was precipitated using 2.5X the volume of ethanol.

Pre-miR pull down assay.

500-600 pmoles of 3' biotinylated adapter oligo were incubated with 8 μL streptavidin conjugated agarose beads per 1 mg of cell extract (Thermo-Fisher Scientific, Rockford, IL) in Buffer I (contents listed above) at 4 °C for 1 hr. Beads were then washed twice with Buffer D (20 mM Tris HCl pH 7.5, 300 mM KCl, 0.2 mM EDTA, dH_2O) and incubated with 100 pmoles of the *in vitro* transcribed pre-miR in Buffer D with 100 U/mL RNase inhibitor (Ambion) for 4.5 hrs at room temperature. Beads were then washed twice with Buffer I. Cell extracts were then incubated for 1 hr at 4 °C with adaptor DNA immobilized agarose beads for pre-clearing. The pre-cleared cell extract (3-4 mg) was incubated with pre-miRs immobilized onto the streptavidin coated beads (25 μL) and rotated constantly for 12 hrs at 4 °C. After washing 5-6 times with Buffer I, beads were collected in one tube and the associated proteins were denatured by boiling with 1.5X SDS sample buffer and resolved using 4-12% Bis-Tris gradient gels (Biorad). The gel

was silver stained with Invitrogen SilverQuest Silver Staining Kit (Invitrogen) following manufacturer's instructions. The in-gel digested proteins were then cut and analyzed by mass spec analysis.

Tumorsphere assay with CM from miR21 knockdown CAFs and RMFs.

CAFs and RMFs were seeded at 275,000 cells per 10-cm plate in normal growth medium (DMEM + 10% CS + AB/AM). The next day, cells were washed twice with PBS and switched to phenol red-free, serum starvation medium without antibiotics (PRF-DMEM + 0.5 % charcoal/dextran stripped FBS + 2 mM L-glutamine). 300 pmoles anti-miR21 inhibitor (Applied Biosystems) or scramble control inhibitor (Applied Biosystems) were transfected into cells using a 1:1 ratio of inhibitor to RNAi Max Lipofectamine (Invitrogen) diluted in Optimem media (Invitrogen), for a final concentration of 40 nM transfected construct. The complete transfection mixture was added dropwise to cells over the surface area of the dish and left at 37 °C, 5% CO_2 for 18 hours. Cells were then treated with 400 pM TGFβ or vehicle control for 24 hours. After 24 hours, CM was harvested, filtered through a 0.22 μm filter and stored -80 °C until ready for tumorsphere assays; cells were washed in PBS, lysed in TRIzol for RNA extraction as described above. qRT-PCR for mature miR21 levels was performed to confirm the efficacy of the knockdown (described above).

To perform tumorsphere assays, CM was thawed and supplemented with 5% charcoal/dextran stripped FBS and 2 mM L-glutamine. A single cell suspension of MCF7 breast cancer cells were seeded at 30,000 cells/well of

ultra-low attachment 6 well plates (Corning) in CM collected and supplemented as previously described. In addition, MCF7s in specified wells were cultured in PRF-DMEM + 5% charcoal/dextran stripped FBS + 400 pM TGFβ or vehicle, to control for the effect of any residual TGFβ carried over in the CM treated wells. Cells were supplemented with fresh supplemented CM on day 3, and quantified using a Multisizer-3 coulter counter (Beckman-Coulter), using a 30 μm cutoff for minimum tumorsphere size.

CHAPTER VI:

References

Ademuyiwa, F.O., Edge, S.B., Erwin, D.O., Orom, H., Ambrosone, C.B., and Underwood, W., 3rd (2011). Breast cancer racial disparities: unanswered questions. Cancer Res *71*, 640-644.

Al-Hajj, M., Wicha, M.S., Benito-Hernandez, A., Morrison, S.J., and Clarke, M.F. (2003). Prospective identification of tumorigenic breast cancer cells. Proc Natl Acad Sci U S A *100*, 3983-3988.

Allinen, M., Beroukhim, R., Cai, L., Brennan, C., Lahti-Domenici, J., Huang, H., Porter, D., Hu, M., Chin, L., Richardson, A.*, et al.* (2004). Molecular characterization of the tumor microenvironment in breast cancer. Cancer Cell *6*, 17-32.

Anderson, E., and Clarke, R.B. (2004). Steroid receptors and cell cycle in normal mammary epithelium. J Mammary Gland Biol Neoplasia *9*, 3-13.

Aprelikova, O., Yu, X., Palla, J., Wei, B.R., John, S., Yi, M., Stephens, R., Simpson, R.M., Risinger, J.I., Jazaeri, A.*, et al.* (2010). The role of miR-31 and its target gene SATB2 in cancer-associated fibroblasts. Cell Cycle *9*, 4387-4398.

Arendt, L.M., Rudnick, J.A., Keller, P.J., and Kuperwasser, C. (2010). Stroma in breast development and disease. Semin Cell Dev Biol *21*, 11-18.

Asselin-Labat, M.L., Shackleton, M., Stingl, J., Vaillant, F., Forrest, N.C., Eaves, C.J., Visvader, J.E., and Lindeman, G.J. (2006). Steroid hormone receptor status of mouse mammary stem cells. J Natl Cancer Inst *98*, 1011-1014.

Asselin-Labat, M.L., Vaillant, F., Sheridan, J.M., Pal, B., Wu, D., Simpson, E.R., Yasuda, H., Smyth, G.K., Martin, T.J., Lindeman, G.J.*, et al.* (2010). Control of mammary stem cell function by steroid hormone signalling. Nature *465*, 798-802.

Baglole, C.J., Ray, D.M., Bernstein, S.H., Feldon, S.E., Smith, T.J., Sime, P.J., and Phipps, R.P. (2006). More than structural cells, fibroblasts create and orchestrate the tumor microenvironment. Immunol Invest *35*, 297-325.

Barcellos-Hoff, M.H., and Ravani, S.A. (2000). Irradiated mammary gland stroma promotes the expression of tumorigenic potential by unirradiated epithelial cells. Cancer Res *60*, 1254-1260.

Barth, P.J., Ebrahimsade, S., Ramaswamy, A., and Moll, R. (2002). CD34+ fibrocytes in invasive ductal carcinoma, ductal carcinoma in situ, and benign breast lesions. Virchows Arch *440*, 298-303.

Bauer, M., Su, G., Casper, C., He, R., Rehrauer, W., and Friedl, A. (2010). Heterogeneity of gene expression in stromal fibroblasts of human breast carcinomas and normal breast. Oncogene *29*, 1732-1740.

Bechtel, W., McGoohan, S., Zeisberg, E.M., Muller, G.A., Kalbacher, H., Salant, D.J., Muller, C.A., Kalluri, R., and Zeisberg, M. (2010). Methylation determines fibroblast activation and fibrogenesis in the kidney. Nat Med *16*, 544-550.

Bellini, A., and Mattoli, S. (2007). The role of the fibrocyte, a bone marrow-derived mesenchymal progenitor, in reactive and reparative fibroses. Lab Invest *87*, 858-870.

Bissell, M.J., and Labarge, M.A. (2005). Context, tissue plasticity, and cancer: are tumor stem cells also regulated by the microenvironment? Cancer Cell *7*, 17-23.

Bissell, M.J., and Radisky, D. (2001). Putting tumours in context. Nat Rev Cancer *1*, 46-54.

Bissell, M.J., Radisky, D.C., Rizki, A., Weaver, V.M., and Petersen, O.W. (2002). The organizing principle: microenvironmental influences in the normal and malignant breast. Differentiation *70*, 537-546.

Bonnet, D. (2005). Cancer stem cells: lessons from leukaemia. Cell Prolif *38*, 357-361.

Bonnet, D., and Dick, J.E. (1997). Human acute myeloid leukemia is organized as a hierarchy that originates from a primitive hematopoietic cell. Nat Med *3*, 730-737.

Booth, B.W., Boulanger, C.A., Anderson, L.H., and Smith, G.H. (2011). The normal mammary microenvironment suppresses the tumorigenic phenotype of mouse mammary tumor virus-neu-transformed mammary tumor cells. Oncogene *30*, 679-689.

Booth, B.W., Mack, D.L., Androutsellis-Theotokis, A., McKay, R.D., Boulanger, C.A., and Smith, G.H. (2008). The mammary microenvironment alters the differentiation repertoire of neural stem cells. Proc Natl Acad Sci U S A *105*, 14891-14896.

Boulanger, C.A., Mack, D.L., Booth, B.W., and Smith, G.H. (2007). Interaction with the mammary microenvironment redirects spermatogenic cell fate in vivo. Proc Natl Acad Sci U S A *104*, 3871-3876.

Boulanger, C.A., and Smith, G.H. (2009). Reprogramming cell fates in the mammary microenvironment. Cell Cycle *8*, 1127-1132.

Boulanger, C.A., Wagner, K.U., and Smith, G.H. (2005). Parity-induced mouse mammary epithelial cells are pluripotent, self-renewing and sensitive to TGF-beta1 expression. Oncogene *24*, 552-560.

Breving, K., and Esquela-Kerscher, A. (2009). The complexities of microRNA regulation: mirandering around the rules. Int J Biochem Cell Biol *42*, 1316-1329.

Brisken, C., and Duss, S. (2007). Stem cells and the stem cell niche in the breast: an integrated hormonal and developmental perspective. Stem Cell Rev *3*, 147-156.

Brisken, C., Park, S., Vass, T., Lydon, J.P., O'Malley, B.W., and Weinberg, R.A. (1998). A paracrine role for the epithelial progesterone receptor in mammary gland development. Proc Natl Acad Sci U S A *95*, 5076-5081.

Bunt, S.K., Yang, L., Sinha, P., Clements, V.K., Leips, J., and Ostrand-Rosenberg, S. (2007). Reduced inflammation in the tumor microenvironment delays the accumulation of myeloid-derived suppressor cells and limits tumor progression. Cancer Res *67*, 10019-10026.

Campbell, I., Polyak, K., and Haviv, I. (2009). Clonal mutations in the cancer-associated fibroblasts: the case against genetic coevolution. Cancer Res *69*, 6765-6768; discussion 6769.

Casey, T., Bond, J., Tighe, S., Hunter, T., Lintault, L., Patel, O., Eneman, J., Crocker, A., White, J., Tessitore, J.*, et al.* (2009). Molecular signatures suggest a major role for stromal cells in development of invasive breast cancer. Breast Cancer Res Treat *114*, 47-62.

Caudy, A.A., Ketting, R.F., Hammond, S.M., Denli, A.M., Bathoorn, A.M., Tops, B.B., Silva, J.M., Myers, M.M., Hannon, G.J., and Plasterk, R.H. (2003). A micrococcal nuclease homologue in RNAi effector complexes. Nature *425*, 411-414.

Chan, M.C., Weisman, A.S., Kang, H., Nguyen, P.H., Hickman, T., Mecker, S.V., Hill, N.S., Lagna, G., and Hata, A. (2011). The amiloride derivative phenamil attenuates pulmonary vascular remodeling by activating NFAT and the bone morphogenetic protein signaling pathway. Mol Cell Biol *31*, 517-530.

Chang, S.H., Ai, Y., Breyer, R.M., Lane, T.F., and Hla, T. (2005). The prostaglandin E2 receptor EP2 is required for cyclooxygenase 2-mediated mammary hyperplasia. Cancer Res *65*, 4496-4499.

Charafe-Jauffret, E., Ginestier, C., Iovino, F., Wicinski, J., Cervera, N., Finetti, P., Hur, M.H., Diebel, M.E., Monville, F., Dutcher, J.*, et al.* (2009). Breast cancer cell lines contain functional cancer stem cells with metastatic capacity and a distinct molecular signature. Cancer Res *69*, 1302-1313.

Clarke, R.B. (2006). Ovarian steroids and the human breast: regulation of stem cells and cell proliferation. Maturitas *54*, 327-334.

Cohen, S.M. (2009). Use of microRNA sponges to explore tissue-specific microRNA functions in vivo. Nat Methods *6*, 873-874.

Coppe, J.P., Patil, C.K., Rodier, F., Sun, Y., Munoz, D.P., Goldstein, J., Nelson, P.S., Desprez, P.Y., and Campisi, J. (2008). Senescence-associated secretory phenotypes reveal cell-nonautonomous functions of oncogenic RAS and the p53 tumor suppressor. PLoS Biol *6*, 2853-2868.

Creighton, C.J., Li, X., Landis, M., Dixon, J.M., Neumeister, V.M., Sjolund, A., Rimm, D.L., Wong, H., Rodriguez, A., Herschkowitz, J.I.*, et al.* (2009). Residual breast cancers after conventional therapy display mesenchymal as well as tumor-initiating features. Proc Natl Acad Sci U S A *106*, 13820-13825.

Daniel, C.W., De Ome, K.B., Young, J.T., Blair, P.B., and Faulkin, L.J., Jr. (1968). The in vivo life span of normal and preneoplastic mouse mammary glands: a serial transplantation study. Proc Natl Acad Sci U S A *61*, 53-60.

Davis, B.N., and Hata, A. (2009). Regulation of MicroRNA Biogenesis: A miRiad of mechanisms. Cell Commun Signal *7*, 18.

Davis, B.N., and Hata, A. (2010). microRNA in Cancer---The involvement of aberrant microRNA biogenesis regulatory pathways. Genes Cancer *1*, 1100-1114.

Davis, B.N., Hilyard, A.C., Lagna, G., and Hata, A. (2008). SMAD proteins control DROSHA-mediated microRNA maturation. Nature *454*, 56-61.

Davis, B.N., Hilyard, A.C., Nguyen, P.H., Lagna, G., and Hata, A. (2011). Smad proteins bind a conserved RNA sequence to promote microRNA maturation by Drosha. Mol Cell *39*, 373-384.

de Visser, K.E., Korets, L.V., and Coussens, L.M. (2005). De novo carcinogenesis promoted by chronic inflammation is B lymphocyte dependent. Cancer Cell *7*, 411-423.

Degen, M., Brellier, F., Kain, R., Ruiz, C., Terracciano, L., Orend, G., and Chiquet-Ehrismann, R. (2007). Tenascin-W is a novel marker for activated tumor stroma in low-grade human breast cancer and influences cell behavior. Cancer Res *67*, 9169-9179.

DeNardo, D.G., Barreto, J.B., Andreu, P., Vasquez, L., Tawfik, D., Kolhatkar, N., and Coussens, L.M. (2009). CD4(+) T cells regulate pulmonary metastasis of mammary carcinomas by enhancing protumor properties of macrophages. Cancer Cell *16*, 91-102.

Deome, K.B., Faulkin, L.J., Jr., Bern, H.A., and Blair, P.B. (1959). Development of mammary tumors from hyperplastic alveolar nodules transplanted into gland-free mammary fat pads of female C3H mice. Cancer Res *19*, 515-520.

Desmouliere, A., Chaponnier, C., and Gabbiani, G. (2005). Tissue repair, contraction, and the myofibroblast. Wound Repair Regen *13*, 7-12.

Desmouliere, A., Guyot, C., and Gabbiani, G. (2004). The stroma reaction myofibroblast: a key player in the control of tumor cell behavior. Int J Dev Biol *48*, 509-517.

Desmouliere, A., Rubbia-Brandt, L., Abdiu, A., Walz, T., Macieira-Coelho, A., and Gabbiani, G. (1992). Alpha-smooth muscle actin is expressed in a subpopulation of cultured and cloned fibroblasts and is modulated by gamma-interferon. Exp Cell Res *201*, 64-73.

Diederichs, S., and Haber, D.A. (2007). Dual role for argonautes in microRNA processing and posttranscriptional regulation of microRNA expression. Cell *131*, 1097-1108.

Direkze, N.C., Hodivala-Dilke, K., Jeffery, R., Hunt, T., Poulsom, R., Oukrif, D., Alison, M.R., and Wright, N.A. (2004). Bone marrow contribution to tumor-associated myofibroblasts and fibroblasts. Cancer Res *64*, 8492-8495.

Doedens, A.L., Stockmann, C., Rubinstein, M.P., Liao, D., Zhang, N., DeNardo, D.G., Coussens, L.M., Karin, M., Goldrath, A.W., and Johnson, R.S. (2010). Macrophage expression of hypoxia-inducible factor-1 alpha suppresses T-cell function and promotes tumor progression. Cancer Res *70*, 7465-7475.

Doench, J.G., and Sharp, P.A. (2004). Specificity of microRNA target selection in translational repression. Genes Dev *18*, 504-511.

Dontu, G., Abdallah, W.M., Foley, J.M., Jackson, K.W., Clarke, M.F., Kawamura, M.J., and Wicha, M.S. (2003). In vitro propagation and transcriptional profiling of human mammary stem/progenitor cells. Genes Dev *17*, 1253-1270.

Dotto, G.P., Weinberg, R.A., and Ariza, A. (1988). Malignant transformation of mouse primary keratinocytes by Harvey sarcoma virus and its modulation by surrounding normal cells. Proc Natl Acad Sci U S A *85*, 6389-6393.

Dvorak, H.F. (1986). Tumors: wounds that do not heal. Similarities between tumor stroma generation and wound healing. N Engl J Med *315*, 1650-1659.

Easton, D.F., Ford, D., and Bishop, D.T. (1995). Breast and ovarian cancer incidence in BRCA1-mutation carriers. Breast Cancer Linkage Consortium. Am J Hum Genet *56*, 265-271.

Elenbaas, B., Spirio, L., Koerner, F., Fleming, M.D., Zimonjic, D.B., Donaher, J.L., Popescu, N.C., Hahn, W.C., and Weinberg, R.A. (2001). Human breast cancer cells generated by oncogenic transformation of primary mammary epithelial cells. Genes Dev *15*, 50-65.

Elenbaas, B., and Weinberg, R.A. (2001). Heterotypic signaling between epithelial tumor cells and fibroblasts in carcinoma formation. Exp Cell Res *264*, 169-184.

Eng, C., Leone, G., Orloff, M.S., and Ostrowski, M.C. (2009). Genomic alterations in tumor stroma. Cancer Res *69*, 6759-6764.

Enkelmann, A., Heinzelmann, J., von Eggeling, F., Walter, M., Berndt, A., Wunderlich, H., and Junker, K. (2011). Specific protein and miRNA patterns characterise tumour-associated fibroblasts in bladder cancer. J Cancer Res Clin Oncol *137*, 751-759.

Erez, N., Truitt, M., Olson, P., Arron, S.T., and Hanahan, D. (2010). Cancer-Associated Fibroblasts Are Activated in Incipient Neoplasia to Orchestrate Tumor-Promoting Inflammation in an NF-kappaB-Dependent Manner. Cancer Cell *17*, 135-147.

Fackenthal, J.D., and Olopade, O.I. (2007). Breast cancer risk associated with BRCA1 and BRCA2 in diverse populations. Nat Rev Cancer *7*, 937-948.

Farazi, T.A., Horlings, H.M., Ten Hoeve, J.J., Mihailovic, A., Halfwerk, H., Morozov, P., Brown, M., Hafner, M., Reyal, F., van Kouwenhove, M.*, et al.* (2011). MicroRNA Sequence and Expression Analysis in Breast Tumors by Deep Sequencing. Cancer Res *71*, 4443-4453.

Farmer, P., Bonnefoi, H., Anderle, P., Cameron, D., Wirapati, P., Becette, V., Andre, S., Piccart, M., Campone, M., Brain, E.*, et al.* (2009). A stroma-related gene signature predicts resistance to neoadjuvant chemotherapy in breast cancer. Nat Med *15*, 68-74.

Fazi, F., and Nervi, C. (2008). MicroRNA: basic mechanisms and transcriptional regulatory networks for cell fate determination. Cardiovasc Res *79*, 553-561.

Febbraio, M.A., Rose-John, S., and Pedersen, B.K. (2010). Is interleukin-6 receptor blockade the Holy Grail for inflammatory diseases? Clin Pharmacol Ther *87*, 396-398.

Fernandez, H.R., Kavi, H.H., Xie, W., and Birchler, J.A. (2005). Heterochromatin: on the ADAR radar? Curr Biol *15*, R132-134.

Fiegl, H., Millinger, S., Goebel, G., Muller-Holzner, E., Marth, C., Laird, P.W., and Widschwendter, M. (2006). Breast cancer DNA methylation profiles in cancer cells and tumor stroma: association with HER-2/neu status in primary breast cancer. Cancer Res *66*, 29-33.

Fillmore, C.M., Gupta, P.B., Rudnick, J.A., Caballero, S., Keller, P.J., Lander, E.S., and Kuperwasser, C. (2010). Estrogen expands breast cancer stem-like cells through paracrine FGF/Tbx3 signaling. Proc Natl Acad Sci U S A *107*, 21737-21742.

Fillmore, C.M., and Kuperwasser, C. (2008). Human breast cancer cell lines contain stem-like cells that self-renew, give rise to phenotypically diverse progeny and survive chemotherapy. Breast Cancer Res *10*, R25.

Finak, G., Bertos, N., Pepin, F., Sadekova, S., Souleimanova, M., Zhao, H., Chen, H., Omeroglu, G., Meterissian, S., Omeroglu, A.*, et al.* (2008). Stromal gene expression predicts clinical outcome in breast cancer. Nat Med *14*, 518-527.

Fries, K.M., Blieden, T., Looney, R.J., Sempowski, G.D., Silvera, M.R., Willis, R.A., and Phipps, R.P. (1994). Evidence of fibroblast heterogeneity and the role of fibroblast subpopulations in fibrosis. Clin Immunol Immunopathol *72*, 283-292.

Fujimoto, H., Sangai, T., Ishii, G., Ikehara, A., Nagashima, T., Miyazaki, M., and Ochiai, A. (2009). Stromal MCP-1 in mammary tumors induces tumor-associated macrophage infiltration and contributes to tumor progression. Int J Cancer *125*, 1276-1284.

Gabriely, G., Wurdinger, T., Kesari, S., Esau, C.C., Burchard, J., Linsley, P.S., and Krichevsky, A.M. (2008). MicroRNA 21 promotes glioma invasion by targeting matrix metalloproteinase regulators. Mol Cell Biol *28*, 5369-5380.

Gabrilovich, D.I., and Nagaraj, S. (2009). Myeloid-derived suppressor cells as regulators of the immune system. Nat Rev Immunol *9*, 162-174.

Gangaraju, V.K., and Lin, H. (2009). MicroRNAs: key regulators of stem cells. Nat Rev Mol Cell Biol *10*, 116-125.

Garcia-Alvarez, J., Ramirez, R., Checa, M., Nuttall, R.K., Sampieri, C.L., Edwards, D.R., Selman, M., and Pardo, A. (2006). Tissue inhibitor of metalloproteinase-3 is up-regulated by transforming growth factor-beta1 in vitro and expressed in fibroblastic foci in vivo in idiopathic pulmonary fibrosis. Exp Lung Res *32*, 201-214.

Greten, F.R., Eckmann, L., Greten, T.F., Park, J.M., Li, Z.W., Egan, L.J., Kagnoff, M.F., and Karin, M. (2004). IKKbeta links inflammation and tumorigenesis in a mouse model of colitis-associated cancer. Cell *118*, 285-296.

Grivennikov, S., Karin, E., Terzic, J., Mucida, D., Yu, G.Y., Vallabhapurapu, S., Scheller, J., Rose-John, S., Cheroutre, H., Eckmann, L.*, et al.* (2009). IL-6 and Stat3 are required for survival of intestinal epithelial cells and development of colitis-associated cancer. Cancer Cell *15*, 103-113.

H. George Burkitt, P.R.W., Barbara Young, John W. Heath (1993). Wheater's Functional Histology (Edinburgh, Churchill Livingstone).

Habig, J.W., Dale, T., and Bass, B.L. (2007). miRNA editing--we should have inosine this coming. Mol Cell *25*, 792-793.

Hata, A., and Davis, B.N. (2009). Control of microRNA biogenesis by TGFbeta signaling pathway-A novel role of Smads in the nucleus. Cytokine Growth Factor Rev *20*, 517-521.

Heo, I., Joo, C., Kim, Y.K., Ha, M., Yoon, M.J., Cho, J., Yeom, K.H., Han, J., and Kim, V.N. (2009). TUT4 in concert with Lin28 suppresses microRNA biogenesis through pre-microRNA uridylation. Cell *138*, 696-708.

Herschkowitz, J.I., Simin, K., Weigman, V.J., Mikaelian, I., Usary, J., Hu, Z., Rasmussen, K.E., Jones, L.P., Assefnia, S., Chandrasekharan, S.*, et al.* (2007). Identification of conserved gene expression features between murine mammary carcinoma models and human breast tumors. Genome Biol *8*, R76.

Houghton, J., and Wang, T.C. (2005). Helicobacter pylori and gastric cancer: a new paradigm for inflammation-associated epithelial cancers. Gastroenterology *128*, 1567-1578.

Hu, M., Peluffo, G., Chen, H., Gelman, R., Schnitt, S., and Polyak, K. (2009). Role of COX-2 in epithelial-stromal cell interactions and progression of ductal carcinoma in situ of the breast. Proc Natl Acad Sci U S A *106*, 3372-3377.

Hu, M., Yao, J., Cai, L., Bachman, K.E., van den Brule, F., Velculescu, V., and Polyak, K. (2005). Distinct epigenetic changes in the stromal cells of breast cancers. Nat Genet *37*, 899-905.

Hu, M., Yao, J., Carroll, D.K., Weremowicz, S., Chen, H., Carrasco, D., Richardson, A., Violette, S., Nikolskaya, T., Nikolsky, Y.*, et al.* (2008). Regulation of in situ to invasive breast carcinoma transition. Cancer Cell *13*, 394-406.

Huang, M., Li, Y., Zhang, H., and Nan, F. (2010). Breast cancer stromal fibroblasts promote the generation of CD44+CD24- cells through SDF-1/CXCR4 interaction. J Exp Clin Cancer Res *29*, 80.

Hwang, R.F., Moore, T., Arumugam, T., Ramachandran, V., Amos, K.D., Rivera, A., Ji, B., Evans, D.B., and Logsdon, C.D. (2008). Cancer-associated stromal fibroblasts promote pancreatic tumor progression. Cancer Res *68*, 918-926.

Iliopoulos, D., Hirsch, H.A., and Struhl, K. (2009). An epigenetic switch involving NF-kappaB, Lin28, Let-7 MicroRNA, and IL6 links inflammation to cell transformation. Cell *139*, 693-706.

Iliopoulos, D., Hirsch, H.A., Wang, G., and Struhl, K. (2011). Inducible formation of breast cancer stem cells and their dynamic equilibrium with non-stem cancer cells via IL6 secretion. Proc Natl Acad Sci U S A *108*, 1397-1402.

Iliopoulos, D., Jaeger, S.A., Hirsch, H.A., Bulyk, M.L., and Struhl, K. (2010a). STAT3 activation of miR-21 and miR-181b-1 via PTEN and CYLD are part of the epigenetic switch linking inflammation to cancer. Mol Cell *39*, 493-506.

Iliopoulos, D., Lindahl-Allen, M., Polytarchou, C., Hirsch, H.A., Tsichlis, P.N., and Struhl, K. (2010b). Loss of miR-200 inhibition of Suz12 leads to polycomb-mediated repression required for the formation and maintenance of cancer stem cells. Mol Cell *39*, 761-772.

Iorio, M.V., Ferracin, M., Liu, C.G., Veronese, A., Spizzo, R., Sabbioni, S., Magri, E., Pedriali, M., Fabbri, M., Campiglio, M.*, et al.* (2005). MicroRNA gene expression deregulation in human breast cancer. Cancer Res *65*, 7065-7070.

Iyer, V., Klebba, I., Arendt, L.M., McCready, J., and Kuperwasser, C. (2011). Manuscript in preparation. (Boston, Tufts University School of Medicine).

Jacoby, R.F., Seibert, K., Cole, C.E., Kelloff, G., and Lubet, R.A. (2000). The cyclooxygenase-2 inhibitor celecoxib is a potent preventive and therapeutic agent in the min mouse model of adenomatous polyposis. Cancer Res *60*, 5040-5044.

Jazbutyte, V., and Thum, T. (2010). MicroRNA-21: from cancer to cardiovascular disease. Curr Drug Targets *11*, 926-935.

Jelaska, A., Strehlow, D., and Korn, J.H. (1999). Fibroblast heterogeneity in physiological conditions and fibrotic disease. Springer Semin Immunopathol *21*, 385-395.

Jemal, A., Siegel, R., Ward, E., Hao, Y., Xu, J., and Thun, M.J. (2009). Cancer statistics, 2009. CA Cancer J Clin *59*, 225-249.

Jemal, A., Siegel, R., Ward, E., Murray, T., Xu, J., and Thun, M.J. (2007). Cancer statistics, 2007. CA Cancer J Clin *57*, 43-66.

Ji, R., Cheng, Y., Yue, J., Yang, J., Liu, X., Chen, H., Dean, D.B., and Zhang, C. (2007). MicroRNA expression signature and antisense-mediated depletion reveal an essential role of MicroRNA in vascular neointimal lesion formation. Circ Res *100*, 1579-1588.

Jiang, L., Gonda, T.A., Gamble, M.V., Salas, M., Seshan, V., Tu, S., Twaddell, W.S., Hegyi, P., Lazar, G., Steele, I.*, et al.* (2008). Global hypomethylation of genomic DNA in cancer-associated myofibroblasts. Cancer Res *68*, 9900-9908.

Kalluri, R., and Zeisberg, M. (2006). Fibroblasts in cancer. Nat Rev Cancer *6*, 392-401.

Katoh, H., Hosono, K., Ito, Y., Suzuki, T., Ogawa, Y., Kubo, H., Kamata, H., Mishima, T., Tamaki, H., Sakagami, H.*, et al.* (2010). COX-2 and prostaglandin

EP3/EP4 signaling regulate the tumor stromal proangiogenic microenvironment via CXCL12-CXCR4 chemokine systems. Am J Pathol *176*, 1469-1483.

Kawahara, Y., Zinshteyn, B., Chendrimada, T.P., Shiekhattar, R., and Nishikura, K. (2007a). RNA editing of the microRNA-151 precursor blocks cleavage by the Dicer-TRBP complex. EMBO Rep *8*, 763-769.

Kawahara, Y., Zinshteyn, B., Sethupathy, P., Iizasa, H., Hatzigeorgiou, A.G., and Nishikura, K. (2007b). Redirection of silencing targets by adenosine-to-inosine editing of miRNAs. Science *315*, 1137-1140.

Keller, P.J., Lin, A.F., Arendt, L.M., Klebba, I., Jones, A.D., Rudnick, J.A., Dimeo, T.A., Gilmore, H., Jefferson, D.M., Graham, R.A.*, et al.* (2010). Mapping the cellular and molecular heterogeneity of normal and malignant breast tissues and cultured cell lines. Breast Cancer Res *12*, R87.

Kim, K.K., Kugler, M.C., Wolters, P.J., Robillard, L., Galvez, M.G., Brumwell, A.N., Sheppard, D., and Chapman, H.A. (2006). Alveolar epithelial cell mesenchymal transition develops in vivo during pulmonary fibrosis and is regulated by the extracellular matrix. Proc Natl Acad Sci U S A *103*, 13180-13185.

Kisseleva, T., Uchinami, H., Feirt, N., Quintana-Bustamante, O., Segovia, J.C., Schwabe, R.F., and Brenner, D.A. (2006). Bone marrow-derived fibrocytes participate in pathogenesis of liver fibrosis. J Hepatol *45*, 429-438.

Ko, S.D., Page, R.C., and Narayanan, A.S. (1977). Fibroblast heterogeneity and prostaglandin regulation of subpopulations. Proc Natl Acad Sci U S A *74*, 3429-3432.

Kojima, Y., Acar, A., Eaton, E.N., Mellody, K.T., Scheel, C., Ben-Porath, I., Onder, T.T., Wang, Z.C., Richardson, A.L., Weinberg, R.A.*, et al.* (2010). Autocrine TGF-beta and stromal cell-derived factor-1 (SDF-1) signaling drives the evolution of tumor-promoting mammary stromal myofibroblasts. Proc Natl Acad Sci U S A *107*, 20009-20014.

Kordon, E.C., and Smith, G.H. (1998). An entire functional mammary gland may comprise the progeny from a single cell. Development *125*, 1921-1930.

Korn, J.H., Torres, D., and Downie, E. (1984). Clonal heterogeneity in the fibroblast response to mononuclear cell derived mediators. Arthritis Rheum *27*, 174-179.

Krenning, G., Zeisberg, E.M., and Kalluri, R. (2010). The origin of fibroblasts and mechanism of cardiac fibrosis. J Cell Physiol *225*, 631-637.

Kuperwasser, C., Chavarria, T., Wu, M., Magrane, G., Gray, J.W., Carey, L., Richardson, A., and Weinberg, R.A. (2004). Reconstruction of functionally normal and malignant human breast tissues in mice. Proc Natl Acad Sci U S A *101*, 4966-4971.

Labarge, M.A., Petersen, O.W., and Bissell, M.J. (2007). Of microenvironments and mammary stem cells. Stem Cell Rev *3*, 137-146.

Lagna, G., Ku, M.M., Nguyen, P.H., Neuman, N.A., Davis, B.N., and Hata, A. (2007). Control of phenotypic plasticity of smooth muscle cells by bone morphogenetic protein signaling through the myocardin-related transcription factors. J Biol Chem *282*, 37244-37255.

LeBeau, A.M., Brennen, W.N., Aggarwal, S., and Denmeade, S.R. (2009). Targeting the cancer stroma with a fibroblast activation protein-activated promelittin protoxin. Mol Cancer Ther *8*, 1378-1386.

Leung, A.K., and Sharp, P.A. (2006). Function and localization of microRNAs in mammalian cells. Cold Spring Harb Symp Quant Biol *71*, 29-38.

Levental, K.R., Yu, H., Kass, L., Lakins, J.N., Egeblad, M., Erler, J.T., Fong, S.F., Csiszar, K., Giaccia, A., Weninger, W.*, et al.* (2009). Matrix crosslinking forces tumor progression by enhancing integrin signaling. Cell *139*, 891-906.

Li, C.L., Yang, W.Z., Chen, Y.P., and Yuan, H.S. (2008). Structural and functional insights into human Tudor-SN, a key component linking RNA interference and editing. Nucleic Acids Res *36*, 3579-3589.

Liao, D., Luo, Y., Markowitz, D., Xiang, R., and Reisfeld, R.A. (2009). Cancer associated fibroblasts promote tumor growth and metastasis by modulating the tumor immune microenvironment in a 4T1 murine breast cancer model. PLoS One *4*, e7965.

Lim, E., Vaillant, F., Wu, D., Forrest, N.C., Pal, B., Hart, A.H., Asselin-Labat, M.L., Gyorki, D.E., Ward, T., Partanen, A.*, et al.* (2009). Aberrant luminal progenitors as the candidate target population for basal tumor development in BRCA1 mutation carriers. Nat Med *15*, 907-913.

Lin, E.Y., Li, J.F., Gnatovskiy, L., Deng, Y., Zhu, L., Grzesik, D.A., Qian, H., Xue, X.N., and Pollard, J.W. (2006). Macrophages regulate the angiogenic switch in a mouse model of breast cancer. Cancer Res *66*, 11238-11246.

Liu, G., Friggeri, A., Yang, Y., Milosevic, J., Ding, Q., Thannickal, V.J., Kaminski, N., and Abraham, E. (2010). miR-21 mediates fibrogenic activation of pulmonary fibroblasts and lung fibrosis. J Exp Med *207*, 1589-1597.

Loeffler, M., Kruger, J.A., Niethammer, A.G., and Reisfeld, R.A. (2006). Targeting tumor-associated fibroblasts improves cancer chemotherapy by increasing intratumoral drug uptake. J Clin Invest *116*, 1955-1962.

Lu, Z., Liu, M., Stribinskis, V., Klinge, C.M., Ramos, K.S., Colburn, N.H., and Li, Y. (2008). MicroRNA-21 promotes cell transformation by targeting the programmed cell death 4 gene. Oncogene *27*, 4373-4379.

Ma, X.J., Dahiya, S., Richardson, E., Erlander, M., and Sgroi, D.C. (2009). Gene expression profiling of the tumor microenvironment during breast cancer progression. Breast Cancer Res *11*, R7.

Mack, C.P. (2011). Signaling mechanisms that regulate smooth muscle cell differentiation. Arterioscler Thromb Vasc Biol *31*, 1495-1505.

Mailleux, A.A., Spencer-Dene, B., Dillon, C., Ndiaye, D., Savona-Baron, C., Itoh, N., Kato, S., Dickson, C., Thiery, J.P., and Bellusci, S. (2002). Role of FGF10/FGFR2b signaling during mammary gland development in the mouse embryo. Development *129*, 53-60.

Mallepell, S., Krust, A., Chambon, P., and Brisken, C. (2006). Paracrine signaling through the epithelial estrogen receptor alpha is required for proliferation and morphogenesis in the mammary gland. Proc Natl Acad Sci U S A *103*, 2196-2201.

Marlow, R., Strickland, P., Lee, J.S., Wu, X., Pebenito, M., Binnewies, M., Le, E.K., Moran, A., Macias, H., Cardiff, R.D.*, et al.* (2008). SLITs suppress tumor

growth in vivo by silencing Sdf1/Cxcr4 within breast epithelium. Cancer Res *68*, 7819-7827.

Marotta, L.L., Almendro, V., Marusyk, A., Shipitsin, M., Schemme, J., Walker, S.R., Bloushtain-Qimron, N., Kim, J.J., Choudhury, S.A., Maruyama, R.*, et al.* (2011). The JAK2/STAT3 signaling pathway is required for growth of CD44+CD24- stem cell-like breast cancer cells in human tumors. J Clin Invest *121*.

McCready, J., Iyer, V., and Kuperwasser, C. (2011). Manuscript in preparation. (Boston, Tufts University School of Medicine).

McDaniel, S.M., Rumer, K.K., Biroc, S.L., Metz, R.P., Singh, M., Porter, W., and Schedin, P. (2006). Remodeling of the mammary microenvironment after lactation promotes breast tumor cell metastasis. Am J Pathol *168*, 608-620.

Medina, D. (2004). Stromal fibroblasts influence human mammary epithelial cell morphogenesis. Proc Natl Acad Sci U S A *101*, 4723-4724.

Meric, J.B., Rottey, S., Olaussen, K., Soria, J.C., Khayat, D., Rixe, O., and Spano, J.P. (2006). Cyclooxygenase-2 as a target for anticancer drug development. Crit Rev Oncol Hematol *59*, 51-64.

Micke, P., and Ostman, A. (2005). Exploring the tumour environment: cancer-associated fibroblasts as targets in cancer therapy. Expert Opin Ther Targets *9*, 1217-1233.

Millikan, R.C., Newman, B., Tse, C.K., Moorman, P.G., Conway, K., Dressler, L.G., Smith, L.V., Labbok, M.H., Geradts, J., Bensen, J.T.*, et al.* (2008). Epidemiology of basal-like breast cancer. Breast Cancer Res Treat *109*, 123-139.

Mintz, B., and Illmensee, K. (1975). Normal genetically mosaic mice produced from malignant teratocarcinoma cells. Proc Natl Acad Sci U S A *72*, 3585-3589.

Mishra, P.J., Mishra, P.J., Humeniuk, R., Medina, D.J., Alexe, G., Mesirov, J.P., Ganesan, S., Glod, J.W., and Banerjee, D. (2008). Carcinoma-associated fibroblast-like differentiation of human mesenchymal stem cells. Cancer Res *68*, 4331-4339.

Molyneux, G., Regan, J., and Smalley, M.J. (2007). Mammary stem cells and breast cancer. Cell Mol Life Sci *64*, 3248-3260.

Mori, L., Bellini, A., Stacey, M.A., Schmidt, M., and Mattoli, S. (2005). Fibrocytes contribute to the myofibroblast population in wounded skin and originate from the bone marrow. Exp Cell Res *304*, 81-90.

Musumeci, M., Coppola, V., Addario, A., Patrizii, M., Maugeri-Sacca, M., Memeo, L., Colarossi, C., Francescangeli, F., Biffoni, M., Collura, D.*, et al.* (2011). Control of tumor and microenvironment cross-talk by miR-15a and miR-16 in prostate cancer. Oncogene.

Nguyen, D.H., Oketch-Rabah, H.A., Illa-Bochaca, I., Geyer, F.C., Reis-Filho, J.S., Mao, J.H., Ravani, S.A., Zavadil, J., Borowsky, A.D., Jerry, D.J.*, et al.* (2011). Radiation Acts on the Microenvironment to Affect Breast Carcinogenesis by Distinct Mechanisms that Decrease Cancer Latency and Affect Tumor Type. Cancer Cell *19*, 640-651.

Nishikura, K. (2006). Editor meets silencer: crosstalk between RNA editing and RNA interference. Nat Rev Mol Cell Biol *7*, 919-931.

Nishikura, K. (2010). Functions and regulation of RNA editing by ADAR deaminases. Annu Rev Biochem *79*, 321-349.

North, T.E., Goessling, W., Walkley, C.R., Lengerke, C., Kopani, K.R., Lord, A.M., Weber, G.J., Bowman, T.V., Jang, I.H., Grosser, T.*, et al.* (2007). Prostaglandin E2 regulates vertebrate haematopoietic stem cell homeostasis. Nature *447*, 1007-1011.

Okayasu, I., Ohkusa, T., Kajiura, K., Kanno, J., and Sakamoto, S. (1996). Promotion of colorectal neoplasia in experimental murine ulcerative colitis. Gut *39*, 87-92.

Olumi, A.F., Grossfeld, G.D., Hayward, S.W., Carroll, P.R., Tlsty, T.D., and Cunha, G.R. (1999). Carcinoma-associated fibroblasts direct tumor progression of initiated human prostatic epithelium. Cancer Res *59*, 5002-5011.

Orimo, A., Gupta, P.B., Sgroi, D.C., Arenzana-Seisdedos, F., Delaunay, T., Naeem, R., Carey, V.J., Richardson, A.L., and Weinberg, R.A. (2005). Stromal

fibroblasts present in invasive human breast carcinomas promote tumor growth and angiogenesis through elevated SDF-1/CXCL12 secretion. Cell *121*, 335-348.

Orimo, A., and Weinberg, R.A. (2006). Stromal fibroblasts in cancer: a novel tumor-promoting cell type. Cell Cycle *5*, 1597-1601.

Orlandi, A., Bochaton-Piallat, M.L., Gabbiani, G., and Spagnoli, L.G. (2006). Aging, smooth muscle cells and vascular pathobiology: implications for atherosclerosis. Atherosclerosis *188*, 221-230.

Ostermann, E., Garin-Chesa, P., Heider, K.H., Kalat, M., Lamche, H., Puri, C., Kerjaschki, D., Rettig, W.J., and Adolf, G.R. (2008). Effective immunoconjugate therapy in cancer models targeting a serine protease of tumor fibroblasts. Clin Cancer Res *14*, 4584-4592.

Ostrand-Rosenberg, S., and Sinha, P. (2009). Myeloid-derived suppressor cells: linking inflammation and cancer. J Immunol *182*, 4499-4506.

Pan, X., Wang, Z.X., and Wang, R. (2011). MicroRNA-21: a novel therapeutic target in human cancer. Cancer Biol Ther *10*, 1224-1232.

Papagiannakopoulos, T., and Kosik, K.S. (2008). MicroRNAs: regulators of oncogenesis and stemness. BMC Med *6*, 15.

Park, E.J., Lee, J.H., Yu, G.Y., He, G., Ali, S.R., Holzer, R.G., Osterreicher, C.H., Takahashi, H., and Karin, M. (2010). Dietary and genetic obesity promote liver inflammation and tumorigenesis by enhancing IL-6 and TNF expression. Cell *140*, 197-208.

Patrick, D.M., Montgomery, R.L., Qi, X., Obad, S., Kauppinen, S., Hill, J.A., van Rooij, E., and Olson, E.N. (2010). Stress-dependent cardiac remodeling occurs in the absence of microRNA-21 in mice. J Clin Invest *120*, 3912-3916.

Petersen, O.W., Nielsen, H.L., Gudjonsson, T., Villadsen, R., Rank, F., Niebuhr, E., Bissell, M.J., and Ronnov-Jessen, L. (2003). Epithelial to mesenchymal transition in human breast cancer can provide a nonmalignant stroma. Am J Pathol *162*, 391-402.

Peyrin-Biroulet, L. (2010). Anti-TNF therapy in inflammatory bowel diseases: a huge review. Minerva Gastroenterol Dietol *56*, 233-243.

Phillips, R.J., Burdick, M.D., Hong, K., Lutz, M.A., Murray, L.A., Xue, Y.Y., Belperio, J.A., Keane, M.P., and Strieter, R.M. (2004). Circulating fibrocytes traffic to the lungs in response to CXCL12 and mediate fibrosis. J Clin Invest *114*, 438-446.

Ponti, D., Costa, A., Zaffaroni, N., Pratesi, G., Petrangolini, G., Coradini, D., Pilotti, S., Pierotti, M.A., and Daidone, M.G. (2005). Isolation and in vitro propagation of tumorigenic breast cancer cells with stem/progenitor cell properties. Cancer Res *65*, 5506-5511.

Prat, A., and Perou, C.M. (2011). Deconstructing the molecular portraits of breast cancer. Mol Oncol *5*, 5-23.

Proia, D.A., and Kuperwasser, C. (2005). Stroma: tumor agonist or antagonist. Cell Cycle *4*, 1022-1025.

Proia, D.A., and Kuperwasser, C. (2006). Reconstruction of human mammary tissues in a mouse model. Nat Protoc *1*, 206-214.

Proia, T.A., Keller, P.J., Gupta, P.B., Klebba, I., Jones, A.D., Sedic, M., Gilmore, H., Tung, N., Naber, S.P., Schnitt, S.*, et al.* (2011). Genetic predisposition directs breast cancer phenotype by dictating progenitor cell fate. Cell Stem Cell *8*, 149-163.

Qi, H.H., Ongusaha, P.P., Myllyharju, J., Cheng, D., Pakkanen, O., Shi, Y., Lee, S.W., Peng, J., and Shi, Y. (2008). Prolyl 4-hydroxylation regulates Argonaute 2 stability. Nature *455*, 421-424.

Qian, B., Katsaros, D., Lu, L., Preti, M., Durando, A., Arisio, R., Mu, L., and Yu, H. (2008). High miR-21 expression in breast cancer associated with poor disease-free survival in early stage disease and high TGF-beta1. Breast Cancer Res Treat.

Quante, M., Tu, S.P., Tomita, H., Gonda, T., Wang, S.S., Takashi, S., Baik, G.H., Shibata, W., Diprete, B., Betz, K.S.*, et al.* (2011). Bone marrow-derived myofibroblasts contribute to the mesenchymal stem cell niche and promote tumor growth. Cancer Cell *19*, 257-272.

Radisky, D., Hagios, C., and Bissell, M.J. (2001). Tumors are unique organs defined by abnormal signaling and context. Semin Cancer Biol *11*, 87-95.

Radisky, D.C., Kenny, P.A., and Bissell, M.J. (2007). Fibrosis and cancer: do myofibroblasts come also from epithelial cells via EMT? J Cell Biochem *101*, 830-839.

Radisky, E.S., and Radisky, D.C. (2007). Stromal induction of breast cancer: inflammation and invasion. Rev Endocr Metab Disord *8*, 279-287.

Rajewsky, N., and Socci, N.D. (2004). Computational identification of microRNA targets. Dev Biol *267*, 529-535.

Rehmsmeier, M., Steffen, P., Hochsmann, M., and Giegerich, R. (2004). Fast and effective prediction of microRNA/target duplexes. RNA *10*, 1507-1517.

Ricciotti, E., and Fitzgerald, G.A. (2010). Prostaglandins and inflammation. Arterioscler Thromb Vasc Biol *31*, 986-1000.

Richert, M.M., Schwertfeger, K.L., Ryder, J.W., and Anderson, S.M. (2000). An atlas of mouse mammary gland development. J Mammary Gland Biol Neoplasia *5*, 227-241.

Robb, G.B., and Rana, T.M. (2007). RNA helicase A interacts with RISC in human cells and functions in RISC loading. Mol Cell *26*, 523-537.

Robinson, G.W. (2007). Cooperation of signalling pathways in embryonic mammary gland development. Nat Rev Genet *8*, 963-972.

Ronnov-Jessen, L., and Petersen, O.W. (1993). Induction of alpha-smooth muscle actin by transforming growth factor-beta 1 in quiescent human breast gland fibroblasts. Implications for myofibroblast generation in breast neoplasia. Lab Invest *68*, 696-707.

Ronnov-Jessen, L., Petersen, O.W., Koteliansky, V.E., and Bissell, M.J. (1995). The origin of the myofibroblasts in breast cancer. Recapitulation of tumor environment in culture unravels diversity and implicates converted fibroblasts and recruited smooth muscle cells. J Clin Invest *95*, 859-873.

Ronnov-Jessen, L., van Deurs, B., Celis, J.E., and Petersen, O.W. (1990). Smooth muscle differentiation in cultured human breast gland stromal cells. Lab Invest *63*, 532-543.

Runo, J.R., and Loyd, J.E. (2003). Primary pulmonary hypertension. Lancet *361*, 1533-1544.

Russo, J., and Russo, I.H. (2004). Development of the human breast. Maturitas *49*, 2-15.

Saetrom, O., Snove, O., Jr., and Saetrom, P. (2005). Weighted sequence motifs as an improved seeding step in microRNA target prediction algorithms. RNA *11*, 995-1003.

Sansone, P., Storci, G., Tavolari, S., Guarnieri, T., Giovannini, C., Taffurelli, M., Ceccarelli, C., Santini, D., Paterini, P., Marcu, K.B.*, et al.* (2007). IL-6 triggers malignant features in mammospheres from human ductal breast carcinoma and normal mammary gland. J Clin Invest *117*, 3988-4002.

Scadden, A.D. (2005). The RISC subunit Tudor-SN binds to hyper-edited double-stranded RNA and promotes its cleavage. Nat Struct Mol Biol *12*, 489-496.

Scadden, A.D., and Smith, C.W. (2001). RNAi is antagonized by A-->I hyper-editing. EMBO Rep *2*, 1107-1111.

Schedin, P. (2006). Pregnancy-associated breast cancer and metastasis. Nat Rev Cancer *6*, 281-291.

Schmidt, M., Sun, G., Stacey, M.A., Mori, L., and Mattoli, S. (2003). Identification of circulating fibrocytes as precursors of bronchial myofibroblasts in asthma. J Immunol *171*, 380-389.

Selaru, F.M., Olaru, A.V., Kan, T., David, S., Cheng, Y., Mori, Y., Yang, J., Paun, B., Jin, Z., Agarwal, R.*, et al.* (2009). MicroRNA-21 is overexpressed in human cholangiocarcinoma and regulates programmed cell death 4 and tissue inhibitor of metalloproteinase 3. Hepatology *49*, 1595-1601.

Shackleton, M., Vaillant, F., Simpson, K.J., Stingl, J., Smyth, G.K., Asselin-Labat, M.L., Wu, L., Lindeman, G.J., and Visvader, J.E. (2006). Generation of a functional mammary gland from a single stem cell. Nature *439*, 84-88.

Sheedy, F.J., Palsson-McDermott, E., Hennessy, E.J., Martin, C., O'Leary, J.J., Ruan, Q., Johnson, D.S., Chen, Y., and O'Neill, L.A. (2010). Negative regulation of TLR4 via targeting of the proinflammatory tumor suppressor PDCD4 by the microRNA miR-21. Nat Immunol *11*, 141-147.

Sheffield, L.G., and Welsch, C.W. (1988). Transplantation of human breast epithelia to mammary-gland-free fat-pads of athymic nude mice: influence of mammotrophic hormones on growth of breast epithelia. Int J Cancer *41*, 713-719.

Shimoda, M., Mellody, K.T., and Orimo, A. (2010). Carcinoma-associated fibroblasts are a rate-limiting determinant for tumour progression. Semin Cell Dev Biol *21*, 19-25.

Sica, A., and Bronte, V. (2007). Altered macrophage differentiation and immune dysfunction in tumor development. J Clin Invest *117*, 1155-1166.

Silzle, T., Randolph, G.J., Kreutz, M., and Kunz-Schughart, L.A. (2004). The fibroblast: sentinel cell and local immune modulator in tumor tissue. Int J Cancer *108*, 173-180.

Singh, A., Purohit, A., Ghilchik, M.W., and Reed, M.J. (1999). The regulation of aromatase activity in breast fibroblasts: the role of interleukin-6 and prostaglandin E2. Endocr Relat Cancer *6*, 139-147.

Sinha, P., Clements, V.K., Fulton, A.M., and Ostrand-Rosenberg, S. (2007). Prostaglandin E2 promotes tumor progression by inducing myeloid-derived suppressor cells. Cancer Res *67*, 4507-4513.

Sleeman, K.E., Kendrick, H., Robertson, D., Isacke, C.M., Ashworth, A., and Smalley, M.J. (2007). Dissociation of estrogen receptor expression and in vivo stem cell activity in the mammary gland. J Cell Biol *176*, 19-26.

Smith, G.H. (1996). Experimental mammary epithelial morphogenesis in an in vivo model: evidence for distinct cellular progenitors of the ductal and lobular phenotype. Breast Cancer Res Treat *39*, 21-31.

Song, B., Wang, C., Liu, J., Wang, X., Lv, L., Wei, L., Xie, L., Zheng, Y., and Song, X. (2010). MicroRNA-21 regulates breast cancer invasion partly by targeting tissue inhibitor of metalloproteinase 3 expression. J Exp Clin Cancer Res *29*, 29.

Sorlie, T. (2004). Molecular portraits of breast cancer: tumour subtypes as distinct disease entities. Eur J Cancer *40*, 2667-2675.

Sotgia, F., Del Galdo, F., Casimiro, M.C., Bonuccelli, G., Mercier, I., Whitaker-Menezes, D., Daumer, K.M., Zhou, J., Wang, C., Katiyar, S.*, et al.* (2009). Caveolin-1-/- null mammary stromal fibroblasts share characteristics with human breast cancer-associated fibroblasts. Am J Pathol *174*, 746-761.

Sousa, A.M., Liu, T., Guevara, O., Stevens, J., Fanburg, B.L., Gaestel, M., Toksoz, D., and Kayyali, U.S. (2007). Smooth muscle alpha-actin expression and myofibroblast differentiation by TGFbeta are dependent upon MK2. J Cell Biochem *100*, 1581-1592.

Spaeth, E.L., Dembinski, J.L., Sasser, A.K., Watson, K., Klopp, A., Hall, B., Andreeff, M., and Marini, F. (2009). Mesenchymal stem cell transition to tumor-associated fibroblasts contributes to fibrovascular network expansion and tumor progression. PLoS ONE *4*, e4992.

Stoker, A.W., Hatier, C., and Bissell, M.J. (1990). The embryonic environment strongly attenuates v-src oncogenesis in mesenchymal and epithelial tissues, but not in endothelia. J Cell Biol *111*, 217-228.

Sugimoto, H., Mundel, T.M., Kieran, M.W., and Kalluri, R. (2006). Identification of fibroblast heterogeneity in the tumor microenvironment. Cancer Biol Ther *5*, 1640-1646.

Tan, W., Zhang, W., Strasner, A., Grivennikov, S., Cheng, J.Q., Hoffman, R.M., and Karin, M. (2011). Tumour-infiltrating regulatory T cells stimulate mammary cancer metastasis through RANKL-RANK signalling. Nature *470*, 548-553.

Thum, T., Gross, C., Fiedler, J., Fischer, T., Kissler, S., Bussen, M., Galuppo, P., Just, S., Rottbauer, W., Frantz, S.*, et al.* (2008). MicroRNA-21 contributes to myocardial disease by stimulating MAP kinase signalling in fibroblasts. Nature *456*, 980-984.

Tiscornia, G., and Izpisua Belmonte, J.C. (2010). MicroRNAs in embryonic stem cell function and fate. Genes Dev *24*, 2732-2741.

Tlsty, T.D., and Coussens, L.M. (2006). Tumor stroma and regulation of cancer development. Annu Rev Pathol *1*, 119-150.

Tomasek, J.J., Vaughan, M.B., Kropp, B.P., Gabbiani, G., Martin, M.D., Haaksma, C.J., and Hinz, B. (2006). Contraction of myofibroblasts in granulation tissue is dependent on Rho/Rho kinase/myosin light chain phosphatase activity. Wound Repair Regen *14*, 313-320.

Trimboli, A.J., Cantemir-Stone, C.Z., Li, F., Wallace, J.A., Merchant, A., Creasap, N., Thompson, J.C., Caserta, E., Wang, H., Chong, J.L.*, et al.* (2009). Pten in stromal fibroblasts suppresses mammary epithelial tumours. Nature *461*, 1084-1091.

Trimmer, C., Sotgia, F., Whitaker-Menezes, D., Balliet, R.M., Eaton, G., Martinez-Outschoorn, U.E., Pavlides, S., Howell, A., Iozzo, R.V., Pestell, R.G.*, et al.* (2011). Caveolin-1 and mitochondrial SOD2 (MnSOD) function as tumor suppressors in the stromal microenvironment: a new genetically tractable model for human cancer associated fibroblasts. Cancer Biol Ther *11*, 383-394.

Tu, S., Bhagat, G., Cui, G., Takaishi, S., Kurt-Jones, E.A., Rickman, B., Betz, K.S., Penz-Oesterreicher, M., Bjorkdahl, O., Fox, J.G.*, et al.* (2008). Overexpression of interleukin-1beta induces gastric inflammation and cancer and mobilizes myeloid-derived suppressor cells in mice. Cancer Cell *14*, 408-419.

Ulrich, C.M., Bigler, J., and Potter, J.D. (2006). Non-steroidal anti-inflammatory drugs for cancer prevention: promise, perils and pharmacogenetics. Nat Rev Cancer *6*, 130-140.

Vane, J.R., Mitchell, J.A., Appleton, I., Tomlinson, A., Bishop-Bailey, D., Croxtall, J., and Willoughby, D.A. (1994). Inducible isoforms of cyclooxygenase and nitric-oxide synthase in inflammation. Proc Natl Acad Sci U S A *91*, 2046-2050.

Vargo-Gogola, T., and Rosen, J.M. (2007). Modelling breast cancer: one size does not fit all. Nat Rev Cancer *7*, 659-672.

Vaughan, M.B., Howard, E.W., and Tomasek, J.J. (2000). Transforming growth factor-beta1 promotes the morphological and functional differentiation of the myofibroblast. Exp Cell Res *257*, 180-189.

Villadsen, R., Fridriksdottir, A.J., Ronnov-Jessen, L., Gudjonsson, T., Rank, F., LaBarge, M.A., Bissell, M.J., and Petersen, O.W. (2007). Evidence for a stem cell hierarchy in the adult human breast. J Cell Biol *177*, 87-101.

Volinia, S., Calin, G.A., Liu, C.G., Ambs, S., Cimmino, A., Petrocca, F., Visone, R., Iorio, M., Roldo, C., Ferracin, M.*, et al.* (2006). A microRNA expression signature of human solid tumors defines cancer gene targets. Proc Natl Acad Sci U S A *103*, 2257-2261.

Wagner, K.U., Boulanger, C.A., Henry, M.D., Sgagias, M., Hennighausen, L., and Smith, G.H. (2002). An adjunct mammary epithelial cell population in parous females: its role in functional adaptation and tissue renewal. Development *129*, 1377-1386.

Wang, Q., Zhang, Z., Blackwell, K., and Carmichael, G.G. (2005). Vigilins bind to promiscuously A-to-I-edited RNAs and are involved in the formation of heterochromatin. Curr Biol *15*, 384-391.

Weaver, V.M., Petersen, O.W., Wang, F., Larabell, C.A., Briand, P., Damsky, C., and Bissell, M.J. (1997). Reversion of the malignant phenotype of human breast cells in three-dimensional culture and in vivo by integrin blocking antibodies. J Cell Biol *137*, 231-245.

Webber, J., Steadman, R., Mason, M.D., Tabi, Z., and Clayton, A. (2010). Cancer exosomes trigger fibroblast to myofibroblast differentiation. Cancer Res *70*, 9621-9630.

Winslow, M.M., Pan, M., Starbuck, M., Gallo, E.M., Deng, L., Karsenty, G., and Crabtree, G.R. (2006). Calcineurin/NFAT signaling in osteoblasts regulates bone mass. Dev Cell *10*, 771-782.

Wiseman, B.S., and Werb, Z. (2002). Stromal effects on mammary gland development and breast cancer. Science *296*, 1046-1049.

Witkiewicz, A.K., Dasgupta, A., Sotgia, F., Mercier, I., Pestell, R.G., Sabel, M., Kleer, C.G., Brody, J.R., and Lisanti, M.P. (2009). An absence of stromal

caveolin-1 expression predicts early tumor recurrence and poor clinical outcome in human breast cancers. Am J Pathol *174*, 2023-2034.

Wixler, V., Hirner, S., Muller, J.M., Gullotti, L., Will, C., Kirfel, J., Gunther, T., Schneider, H., Bosserhoff, A., Schorle, H.*, et al.* (2007). Deficiency in the LIM-only protein Fhl2 impairs skin wound healing. J Cell Biol *177*, 163-172.

Worthley, D.L., Ruszkiewicz, A., Davies, R., Moore, S., Nivison-Smith, I., Bik To, L., Browett, P., Western, R., Durrant, S., So, J.*, et al.* (2009). Human gastrointestinal neoplasia-associated myofibroblasts can develop from bone marrow-derived cells following allogeneic stem cell transplantation. Stem Cells *27*, 1463-1468.

Wu, M., Jung, L., Cooper, A.B., Fleet, C., Chen, L., Breault, L., Clark, K., Cai, Z., Vincent, S., Bottega, S.*, et al.* (2009). Dissecting genetic requirements of human breast tumorigenesis in a tissue transgenic model of human breast cancer in mice. Proc Natl Acad Sci U S A *106*, 7022-7027.

Yang, L., Huang, J., Ren, X., Gorska, A.E., Chytil, A., Aakre, M., Carbone, D.P., Matrisian, L.M., Richmond, A., Lin, P.C.*, et al.* (2008). Abrogation of TGF beta signaling in mammary carcinomas recruits Gr-1+CD11b+ myeloid cells that promote metastasis. Cancer Cell *13*, 23-35.

Yang, W., Chendrimada, T.P., Wang, Q., Higuchi, M., Seeburg, P.H., Shiekhattar, R., and Nishikura, K. (2006). Modulation of microRNA processing and expression through RNA editing by ADAR deaminases. Nat Struct Mol Biol *13*, 13-21.

Yao, Q., Cao, S., Li, C., Mengesha, A., Kong, B., and Wei, M. (2011). Micro-RNA-21 regulates TGF-beta-induced myofibroblast differentiation by targeting PDCD4 in tumor-stroma interaction. Int J Cancer *128*, 1783-1792.

Zeisberg, E.M., Potenta, S., Xie, L., Zeisberg, M., and Kalluri, R. (2007). Discovery of endothelial to mesenchymal transition as a source for carcinoma-associated fibroblasts. Cancer Res *67*, 10123-10128.

Zhang, J.G., Wang, J.J., Zhao, F., Liu, Q., Jiang, K., and Yang, G.H. (2010). MicroRNA-21 (miR-21) represses tumor suppressor PTEN and promotes growth and invasion in non-small cell lung cancer (NSCLC). Clin Chim Acta *411*, 846-852.

CHAPTER VII:

Appendix